



TRANSLATE

Research Report

Prepared for Met Éireann
by
University of Galway and ICHEC, the Irish
Centre for High-End Computing
and
University College Cork and
MaREI, the SFI Research Centre
for Energy, Climate and Marine

Authors: Enda O'Brien, Paraic Ryan,
Paul Holloway, Jingyu Wang,
Parvaneh Nowbakht, Christopher Phillips,
James Fitton, Barry O'Dwyer, Paul Nolan.



Rialtas na hÉireann
Government of Ireland

© Met Éireann, 2024

Met Éireann's Weather and Climate Research Programme



TRANSLATE Research Report

DISCLAIMER:

Publishers, editors, reviewers and authors do not accept any legal responsibility for errors, omissions or claims, nor do they provide any warranty, express or implied, with respect to information published in Met Éireann publications. All or part of this publication may be reproduced without further permission, provided the source is acknowledged.

Published by Met Éireann

a division of the Department of Housing, Local Government and Heritage

ISBN: 978-1-917198-00-4

Price: Free

April 2024

Online version

Met Éireann

65/67 Glasnevin Hill, Dublin, D09 Y921, Ireland

Tel: +353-1-8064200

Email: researchfunding@met.ie

Website: www.met.ie

This report should be cited as: O'Brien, E., Ryan, P., Holloway, P., Wang, J., Nowbakht, P., Phillips, C., Fitton, J., O'Dwyer, B. and Nolan, P. (2024) TRANSLATE Research Report. Prepared for Met Éireann by University of Galway, Irish Centre for High-End Computing, University College Cork, and MaREI, the SFI Research Centre for Energy, Climate, and Marine. ISBN: 978-1-917198-00-4.

© Met Éireann, 2024
Met Éireann's Weather and Climate
Research Programme



TRANSLATE

Research Report

Prepared for Met Éireann
by
University of Galway and
The Irish Centre for High-End Computing and
University College Cork and
MaREI, the SFI Research Centre for Energy,
Climate and Marine

**Authors: Enda O'Brien, Paraic Ryan,
Paul Holloway, Jingyu Wang,
Parvaneh Nowbakht, Christopher Phillips,
James Fitton, Barry O'Dwyer, Paul Nolan**

ACKNOWLEDGEMENTS

This report is published as part of Met Éireann's Weather and Climate Research Programme, funded and administered by Met Éireann, a division of the Department of Housing, Local Government and Heritage.

The authors would like to acknowledge the contribution to this research made by:

The Irish Centre for High-End Computing (ICHEC) for the provision of high-resolution national climate projection datasets and computational facilities, **Senior Geologist Billy O'Keeffe from Transport Infrastructure Ireland (TII) and Consultant Engineer Puspita Das from Arup, for technical support relating to Irish road drainage systems**, as well as Seanie Griffin and Catriona Duffy of Met Éireann for their help with data validation.

The members of the project steering committee for their valuable input and contributions, namely Brian Batt & Kevin McCormick – DECC, Conor Quinlan – EPA, David Dodd – Local Authorities, Frank McGovern – EPA, Glen Nolan - Marine Institute Ireland, Peter Thorne – Maynooth University, Jane Strachan - UK Met Office, Sajj Varghese - Met Éireann, Keith Lambkin (Chair) - Met Éireann, Claire Scannell - Met Éireann, as well as past members Jan Rajczak of MeteoSwiss, Bart van den Hurk of Deltares, and Chris Hewitt of the UK Met Office.

The authors would like to acknowledge and thank Catherine Gillman for her administrative assistance in the publication of the report.

The authors are grateful to Met Éireann for funding the project.

► Details of Project Partners

Dr Enda O'Brien

Irish Centre for High-End Computing (ICHEC)
University of Galway
Ireland
Email: enda.obrien@ichec.ie

Dr Paraic Ryan

Department of Civil and Environmental
Engineering
University College Cork
Cork
Ireland
Tel.: +353 21 4903862
E-mail: paraic.ryan@ucc.ie

Dr Paul Holloway

Department of Geography, Environmental
Research Institute
University College Cork
Cork
Ireland
Email: paul.holloway@ucc.ie

Dr Jingyu Wang

Department of Civil and Environmental
Engineering
University College Cork
Cork
Ireland
Email: jingyuwang@ucc.ie

Dr Paul Nolan

Irish Centre for High-End Computing (ICHEC)
University of Galway
Grand Canal Quay
Dublin 2
Ireland
Email: paul.nolan@ichec.ie

Parvaneh Nowbakht

Department of Geography, Environmental
Research Institute
University College Cork
Cork
Ireland
Email: parvaneh.nowbakht@ucc.ie

Dr James Fitton

Formally MaREI-SFI Research Centre for Energy,
Climate and Marine
University College Cork
Cork
Ireland

Dr Barry O'Dwyer

Formally MaREI-SFI Research Centre for Energy,
Climate and Marine
University College Cork
Cork
Ireland

Dr Christopher Phillips

MaREI-SFI Research Centre for Energy,
Climate and Marine
University College Cork
Cork
Ireland

► Table of Contents

Details of Project Partners	ii	PART B: Climate Services and Risk-based Decisions Support	37
1. Introduction	7	7. Introduction to Part B	38
PART A: Standardised Climate Projections for Ireland	10	8. Climate Services Co-Creation	40
2. Introduction to Part A	11	9. Climate Risk	44
3. Producing Standardised Climate Projections	13	10. GIS Semi-Quantitative Risk Assessment Framework	47
3.1 Integrating two different RCM ensembles	14	11. Geo-Spatial Semi-Quantitative Risk Case Study	53
3.2 Historical Observations	14	12. Fully-Quantitative Risk Based Decision Support	61
3.3 Managing Uncertainty	14	12.1 Step-by-Step Guide	62
3.4 Scenario-Based Climate Ensembles	14	12.2 Illustrative Case-study	67
3.5 Climate Sensitivity Decomposition	15	13. Part B Discussion and Conclusions	79
3.6 Global Warming Level or Temperature Threshold-Based Climate Ensembles	16	References	82
4. Combining European and National Climate Projections	19		
5. Sample projection results	21		
5.1 Climate Means	22		
5.2 Projected Frequency Distribution	27		
5.3 Projected Global Warming Level Climate Summaries over Ireland	29		
5.4 ETCCDI Extreme Index Calculation	31		
6. Part A Discussion and Conclusions	36		



Executive Summary

Climate change poses a significant risk to Ireland. The impacts of climate change will potentially affect all aspects of Ireland's society. It is therefore important that decision makers, planners and policy makers have access to both local, robust, and standardised climate information and appropriate risk-based adaptation decision-support tools. Following the publication of the National Adaptation Framework, (2018), and the requirement for government sectors to produce Sectoral Adaptation Plans, there was an unprecedented requirement for accessible, and sometimes technical, national climate information. Following a review of the statutory Sectoral Adaptation Plan, the Climate Change Advisory Council recommended that Ireland would benefit from the development of a common set of climate projections that capture the range of change in future climate projections for use in adaptation, infrastructure and investment planning to 2050.

The TRANSLATE project (<https://www.met.ie/science/TRANSLATE>) was established by Met Éireann in 2021 to produce standardised climate projections and services for Ireland addressing this climate information gap. TRANSLATE represents a step-change in future climate information for Ireland. It examines both national and international climate projections of relevance to Ireland, enhances them and tailors them to the local Irish context. The result is a standardised, accessible, easy to use high resolution national resource with associated risk-based decision support tools to help Irish society speak a common climate language.

Developed in partnership with University of Galway – Irish Centre for High End Computing (ICHEC), and University College Cork – SFI Research Centre for Energy, Climate and Marine (MaREI), TRANSLATE moves beyond the generic average future temperature and precipitation information often associated with regional climate

projections. It uses this information to create user and sector relevant climate indices that can be effectively and directly integrated into adaptation planning such as sectoral adaptation plans, as well as risk frameworks. TRANSLATE has produced an accessible risk framework which gives decision makers insight into changing future risk. It is envisaged that the results from TRANSLATE will help to inform national policy, further our understanding of the impacts of climate change at a local scale in Ireland and as a result, help inform effective adaptation pathways.

Part A of this report outlines the principles and methods used to generate the climate change projections and presents selected results to the end of the 21st century. Part B of the report outlines the development of risk-based climate services which utilise, and build upon, the standardised projections dataset. Further details of both can be found in complementary publications by O'Brien and Nolan (2023) and in Wang et al., (2024).





Key Results:

The development of the standardised national climate projections (part A) was guided by international examples of best practice and informed by similar projects undertaken by other geographically small countries, including the UK, the Netherlands and Switzerland. The climate projections presented in this report for Ireland are in broad agreement with previous national projections as well as European and Global climate projections over this region adding confidence to the results.

The results are presented in this report under both emission scenarios (RCPs, radiative concentrative pathways – RCP2.6, RCP4.5 and RCP8.5 representing early, mid and late action respectively) and global warming scenarios i.e., what Ireland could look like if global average temperatures exceed certain temperature thresholds. In the case of TRANSLATE these thresholds are when global average temperatures exceed 1.5°C, 2°C, 2.5°C, 3°C and 4°C. It should be noted that Ireland currently sits at 1.1°C of global warming.

These new standardised climate projections for Ireland have been bias corrected – a correction applied based on historical observations to remove systematic model errors, and as such both percentage change in climate compared to the past, as well as more accurate climate values of the future can be presented. The level of confidence (uncertainty) in these projections are also discussed.

Temperature Projections

Future temperature increases are projected to be relatively uniform: in other words, the coldest, average, and warmest days are all expected to warm by similar amounts, although nighttime temperatures warm slightly more than daytime ones, in line with observations and broader modelling experience. Temperatures are projected to increase in proportion to the forcing (as represented by the RCP2.6, 4.5 and 8.5 emission scenarios) or increasing global warming levels. While both maximum and minimum temperatures are projected to increase across all seasons, summer is projected to have the highest increase in average maximum temperatures



(with an increase of 0.5°C to 3.5°C) and Autumn is projected to have the highest increase in average minimum temperatures (with an increase of 1.1°C to 4.4°C) depending on the emission scenario or global warming threshold. Temperatures increase nationwide in proportion to the forcing from each future emission scenario and the temperature changes show a gradient across the country, with changes increasing from west to east. The increased temperatures are primarily driven by increases in greenhouse gas emissions.

Precipitation Projections

Future annual rainfall is projected to increase overall. During winter, rainfall is projected to increase across all future scenarios examined. There is a high level of variability on the size of this increase with a range of between 4% and 38% change from the historical baseline depending on the emission scenario or global warming level. For summer, beyond 2°C of global warming there is a trend towards decreasing rainfall which becomes amplified for the higher global warming thresholds. Up to 2°C of global warming however there is no clear trend and a very large variability in rainfall where year-to-year fluctuations can easily produce wet years (or seasons) that are 4 times wetter than dry ones.

Part A – Technical Summary

Two separate ensembles of dynamically downscaled CMIP5, (coupled model intercomparison project), projections were analysed. Each ensemble was processed separately, with the raw model output detrended, bias-corrected (given systematic model errors from the historical period), and further downscaled to produce a compact set of future climate projections. These two ensembles produce very consistent results, increasing confidence in both, and in the methods used. Future projected fields show plenty of detail (depending on local geography), but the change maps relative to the base period are much smoother, reflecting the global climate change signal. Future forcing uncertainty is represented by 3 different emission scenarios, while model response uncertainty is represented by sub-ensembles corresponding to

different climate sensitivities. The resulting matrix of distinct climate ensembles is complemented by ensembles of temperature threshold-based projections, drawn from the same underlying simulations.

The final standardised product consists of over 30 separate projected “climates” of 4 main variables, namely daily minimum, mean and maximum temperature, and daily precipitation. The output includes a wide range of standard climate charts, a set of data files at daily resolution over a full annual cycle for different statistics of interest (means, standard deviations, percentiles, occurrence frequencies), and at the lowest level, 30-year time series of detrended and bias-corrected variables at daily resolution for each model ensemble member. These time series may be queried in various ways, e.g., for any new climate index that may be required, and represent a rich resource for further open-ended research.

Part B – Technical Summary

TRANSLATE also integrated the standardised climate projections for Ireland into a range of risk-based climate services, as outlined in part B of the report. These climate services were developed through a co-creation process, which highlighted hazard indicators and vulnerability/exposure metrics that were important to sectoral, local authority, and industry stakeholders. Subsequently, we utilised open-source software to automate the production of a range of hazard indicators (e.g., number of weather warning days) identified by the sectors from the part A climate projections. GIS, (geographical information system), information and automated code was also developed for a number of vulnerability and exposure metrics, using publicly available data. All of this information is available from Met Éireann. A six step semi-quantitative risk analysis framework was also developed, with an accompanying step-by-step guide that incorporates the TRANSLATE projections and includes computer code to support migration to the emerging hexagon analytical grid format. The use of this framework is illustrated through a case-study example, which examines the potential impact of climate change on school closures and missed education days.

While the semi-quantitative risk analysis approach is shown to be very useful for highlighting potential climate risk hot spots nationally, it is limited when attempting to implement effective climate adaptation action. Consequently, as part of the TRANSLATE climate service offering, a fully quantitative risk-based decision support guide was also developed and is presented in part B of this report. Again, this approach is illustrated through a comprehensive case-study which was conducted in collaboration with Transport Infrastructure Ireland (TII). This case study quantifies the impacts of projected climate change on national road drainage systems. It also examines the effectiveness of a climate adaptation strategy for these systems. It was found that climate change impacts on probability of road flooding under intense rainfall are projected to increase beyond the current acceptable limits set by TII (0% probability for 5-year intense rainfall event). The analysis also indicated that a proactive climate adaptation strategy adopted by TII in 2015 may require adjustment, with a need to increase climate resilience of the pipe network, and the potential to make savings through adopting a less conservative adaptation approach for attenuation ponds. This showcases the strength of risk-based decision support in informing effective climate adaptation actions.



1

Introduction

Within government and private-sector institutions, and among the general public, there is growing awareness of the risks of future climate change – due partly to climate model predictions, and partly to increasingly robust observational evidence of recent and current climate change (The Royal Society, UK; National Academy of Sciences, USA, 2020). Consequently, there is increasing demand for reliable climate projections and associated climate services to aid in the development of appropriate impact, adaptation and mitigation policies and measures. Each of the 31 local authority administrations in Ireland has their own Climate Change Adaptation Plans. The main hazards of concern for these and other public-sector bodies are heavy rainfall and associated flooding, heatwaves, drought and storm/high wind events. Climate change will potentially exacerbate the frequency and intensity of existing hazards, as well as introduce new problems. Irish local authorities, sectors and industry stakeholders need to understand how climate change will affect their activities and, in many cases, will need to implement appropriate adaptation actions to reduce increases in future risks.

In response, the TRANSLATE project (<https://www.met.ie/science/TRANSLATE>) was established by Met Éireann in 2021 to produce a standardised set of climate projections for Ireland. The TRANSLATE project also included a first iteration of climate services built around these standardised climate projections. The first set of climate projections and climate services are now complete. They are freely available from Met Éireann with common climate projection maps and data available for download from Climate Ireland (<https://www.climateireland.ie/data-explorer/>). A technical description of the methods used to produce the standardised projections, along with some representative results, is provided by O'Brien and Nolan (2023, henceforth referred to as OB&N). Since both this report and OB&N describe the TRANSLATE project, they inevitably overlap to some extent. However, Part A of this report focuses more on the projections project output and applications, and readers are referred to OB&N for more technical details.

The standardised climate projections work (described in Part A herein) was informed and guided by similar projects undertaken by other geographically small countries, such as UKCP18 in the UK (Murphy et al., 2018; Lowe et al., 2018), KNMI'14 in the Netherlands (van den Hurk et al., 2014; Lenderink et al., 2015) and CH2018 in Switzerland (CH2018, 2018). In the case of Norway, Nilsen et al. (2022) highlight the utility and value of such projections by showing how they are disseminated and used to develop a 'chain' of climate services. Given the very different

approaches used even by those few countries mentioned above, it is clear that the generation of standardised national climate projections and climate services does not have a 'one-size-fits-all' solution. In the end, TRANSLATE climate projections work took the best available model output resources and statistical post-processing methods and distilled them into a set of climate projections for Ireland that try to accommodate the competing demands for detail and compactness, and try to strike an honest balance between confidence and uncertainty. The following sections in Part A describe how we did this.

While information on how the climate is projected to change is vital, local authorities, sectors and industry stakeholder also need to be supported in a) understanding how these changes might impact upon them, and b) deciding what climate adaptation action they should take to reduce any projected future increases in climate impacts. The IPCC has highlighted that climate risk assessment is the most appropriate tool for achieving this (IPCC, 2021). In this context, Part B of this report presents the development and implementation of risk-based decision support climate services for Ireland. This work incorporates the standardised climate projections developed in Part A and, through a co-creation process, established semi-quantitative and fully-quantitative risk frameworks, data and step-by-step guides. Importantly, these step-by-step guides are illustrated through two case studies. The semi-quantitative case study investigates the

potential impact of climate change on school closures and missed education days, producing maps of projected changes in risk. The fully-quantitative case study examines the projected impacts of climate change on national road drainage systems through close collaboration with Transport Infrastructure Ireland (TII) and industry partners. These two case studies not only illustrate implementation of the step-by-step guides but, importantly, also show the relative merits of the two approaches. The semi-quantitative analysis is shown to be a key first step in understanding and highlighting potential climate change risks and hotspots; however, it is normally not suitable for informing climate adaptation decision making. The fully-quantitative risk-based decision support, on the other hand, can provide detailed insight into the values of projected future risks and figures on the effectiveness and cost-benefit of proposed climate adaptation strategies.



PART
A:

Standardised Climate Projections for Ireland

A scenic landscape at sunset with sheep grazing in a field, overlaid with a large number 2 and geometric teal shapes. The background shows a sunset over a body of water with rolling hills and sheep grazing in a field. The foreground is dominated by a large, light blue number '2' and a teal geometric pattern of overlapping triangles and lines.

2

Introduction to Part A

Climate projections for a country the size of Ireland typically depend on a chain of simulations that starts with ensembles of global climate models (GCMs) on relatively coarse grids. Since only a handful of grid-points in GCMs are located over Ireland, these models are downscaled to smaller domains with finer grids by ensembles of regional climate models (RCMs), each nested within one or more of the GCMs. These RCMs (and GCMs) make the best projections that can be obtained using the laws of physics alone. However, they can be supplemented with statistical information (i.e., bias corrections and further downscaling adjustments) from past observations. The final climate projections thus consist of the most accurate blend of physics and statistics that we can objectively and systematically achieve. We can have confidence, then, in offering them as a ‘standard’.

The following sections provide an overview of how the TRANSLATE standardised climate projections over Ireland were produced. The TRANSLATE projections themselves are freely available from Met Éireann. They may be accessed at three different levels. The first level consists of a set of maps and related charts that show a range of statistics (means, standard deviations, percentiles and occurrence frequencies) of each of the 4 main variables (daily minimum, mean and maximum temperature and daily precipitation) for each projected climate. The second level consists of a set of NetCDF data files containing the distillation of the 30-year time series from each climate sub-ensemble into more integrated or representative annual cycles, frequency histograms and climate index counts. The third level consists of the 30-year (or 20-year, in the case of temperature “threshold” or global warming level climates) time series of daily values for each variable from each model simulation, i.e., each member of the underlying ensemble, also in NetCDF format. These time series are detrended and bias-corrected, as described in OB&N, but in the case of the EURO-CORDEX ensemble at least, remain on their native grid in order to reduce data storage. These continuous multi-year time series files may be revisited and queried to produce any new statistic or climate index that may be desired – as indeed is done routinely in Part B (e.g., see section 10 below). These files provide a lot of versatility and flexibility to

TRANSLATE and permit open-ended research into the information they contain. The standardised climate projections for Ireland produced by Part A of the TRANSLATE project are also used as input to the climate services and risk-based decision-making component of TRANSLATE, as described in Part B of this report. This includes the development of automated code, which can be used to generate hazard metrics of interest from the climate projection NetCDF files.



3

**Producing
Standardised
Climate
Projections**

3.1 Integrating two different RCM ensembles

In practice, the RCM input used by TRANSLATE came from two separate ensembles that each dynamically downscaled a common set of CMIP5 global simulations. All the RCMs in those two ensembles had at least 12km grid resolution over Ireland: one ensemble was from Nolan and Flanagan (2020) on a 4km grid; the other was from the EURO-CORDEX project (www.euro-cordex.net/) on a 12km grid. (More recent CMIP6 global simulations dynamically downscaled by RCMs are only starting to become available now – see https://wcrp-cordex.github.io/simulation-status/CORDEX_CMIP6_status.html – and, once complete, will be used in future versions of TRANSLATE). After systematic post-processing by TRANSLATE, the climates projected by both those ensembles separately, for any given scenario or time-period, are remarkably similar. Thus, the Nolan and Flanagan (2020) and EURO-CORDEX ensemble projections tend to cross-validate each other, increasing confidence in both and in the methods used by TRANSLATE, as may be seen in Fig. 4 below.

3.2 Historical Observations

High-resolution (approximately 1km grid spacing) gridded observations of daily mean, minimum and maximum surface air temperature (at 2m height) for the Republic of Ireland and daily precipitation over all Ireland were provided by Met Éireann, spanning the reference historical period 1976-2005. The production of these datasets is described by Walsh (2016, 2017), while the time period available has expanded from 1981-2010 to span 1961-2014. The temperature fields were supplemented by temperature observations at 5km grid spacing over Northern Ireland from the UK Met Office's CEDA archive (Hollis et al., 2018).

Those 30-year, high-resolution gridded observations of daily minimum, maximum and mean air surface temperature and daily precipitation were used to validate the corresponding variables in RCM output for the same historical period (1976-2005), and to facilitate statistical downscaling and bias-correction of all future projections, as described below.

3.3 Managing Uncertainty

The uncertainty inherent in all model projections of the future arises from three sources, namely forcing uncertainty, response uncertainty and model internal (unforced) variability (Hawkins and Sutton, 2009; Lehner et al., 2020).

The TRANSLATE projections accommodate future *forcing uncertainty* by considering 3 future emission scenarios (or representative concentration pathways, or RCPs in CMIP5 terminology). The future low-, medium- and high-emission scenarios we used are commonly referred to as RCP2.6, RCP4.5 and RCP8.5, respectively.

Climate response uncertainty is captured by classifying the full model ensemble into 3 different sensitivity sub-ensembles, based on each model's future projections of mean temperature change over Ireland.

Internal model uncertainty derives from natural low-frequency variability within each simulation and is reduced by multi-year averaging and by using ensembles rather than single-simulation instances. This is achieved by condensing future time evolution into 3 future periods (2021-2050, 2041-2070 and 2071-2100).

For each RCP scenario, and each model sensitivity level, a representative stable climate is then obtained for each 30-year time period by detrending it, applying objective bias-correction (i.e., quantile-delta mapping, as per Canonn et al., 2015) and statistically downscaling it to the most detailed grid available (i.e., the observational grid, at least for the variables considered so far). As detailed in OB&N, these processes generate reconstructed 30-year time series for each individual simulation.

Of course, these uncertainties all factor into the assessment of risk and they are incorporated into the quantitative risk-based framework and case study described in Part B, Section 12 of this report.

3.4 Scenario-Based Climate Ensembles

TRANSLATE has incorporated each of these 3 different sources of uncertainty by decomposing future climate projections into a matrix of discrete climates along 3 different dimensions (i.e., forcing,

response sensitivity and time period). This matrix or ‘Rubik’s Cube’ structure is shown schematically in Fig. 1. It is worth emphasising that each of the 27 distinct ‘climates’ that make up the ‘cube’ consists of an ensemble of 30 years of daily values for each of 4 variables (daily minimum, mean and maximum of surface air temperature and daily precipitation). Hence, a lot of data is processed to generate the means, standard deviations and percentiles of each variable for each day through the annual cycle, as well as occurrence frequency histograms on a seasonal and annual basis, and representative climate indices on an annual basis. All these data have been used to reduce future uncertainty as much as possible, while simultaneously accommodating it in order to delineate the climatic ranges that may occur for any given forcing scenario.

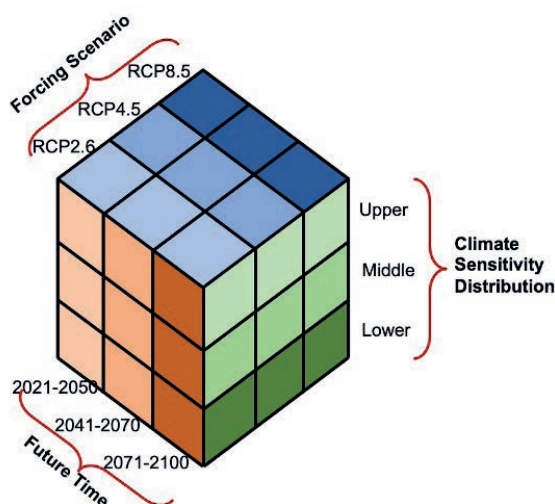


Figure 1. Schematic of how future climate uncertainties can be accommodated in a limited set of possible climates, adapted from Fig. 10.9 of CH2018 (CH2018 report, 2018). Each sub-cube shown corresponds to an ensemble of long-term climate simulations. Different RCP emission scenarios represent forcing uncertainty, while the climate sensitivity axis represents response uncertainty.

3.5 Climate Sensitivity Decomposition

For any given RCP forcing scenario and for any future time period, the decomposition of the ‘climate sensitivity’ axis in Fig. 1 was done to

accommodate model response uncertainty by classifying each global CMIP5 model into low-, middle- or high-sensitivity sub-ensembles. Sensitivity was defined by the mean temperature change over Ireland for three different future scenarios and time periods relative to 1976-2005, using the RCM ensemble-mean for each of the six underlying GCMs. This Ireland-mean temperature change was chosen by TRANSLATE as more relevant to Ireland than the global Equilibrium Climate Sensitivity (ECS) metric, where ECS is the equilibrium global-mean surface temperature change that occurs in each model in response to instantaneous doubling of CO₂ concentrations.

Fig. 2 shows the mean surface temperature changes over Ireland from the RCM ensemble means from 3 different future scenarios and time periods, all relative to 1976-2005. Fig. 2a is for the EURO-CORDEX ensemble; Fig. 2b is for the Nolan and Flanagan (2020) ensemble. For all 3 metrics in both ensembles, the HadGEM2-ES model is clearly the most sensitive, while the MPI-ESM-LR model is the least sensitive. The difference in the projected mean temperature changes over Ireland under RCP8.5 by the end of the century between the most (HadGEM2-ES) and the least (MPI-ESM-LR) sensitive models is almost 1.7°C (3.63° vs. 1.94°C) in the Nolan and Flanagan (2020) ensemble.

The sensitivity over Ireland of the other global CMIP5 models (those in the 4 middle rows of Figs. 2a and 2b) is somewhere in between, but more mixed. However, if all these models are combined as the ‘mid-range’ ensemble on the climate sensitivity axis of Fig. 1, then the ordering among them does not matter. Figs. 2a and 2b are both consistent in showing HadGEM2-ES to be the most sensitive model when downscaled over Ireland; MPI-ESM-LR is the least sensitive, while the others are all somewhere in-between.

Decomposition along the climate sensitivity axis of Fig. 1 is then relatively straightforward: all RCMs nested in the HadGEM2-ES global model make up the ‘high-sensitivity’ ensemble; all RCMs nested in the MPI-ESM-LR model make up the ‘low-sensitivity’ ensemble; and all RCMs nested in any of the other GCMs constitute the ‘medium-sensitivity’ ensemble. Note that this leads to approximately 70% of all simulations being placed in the mid-

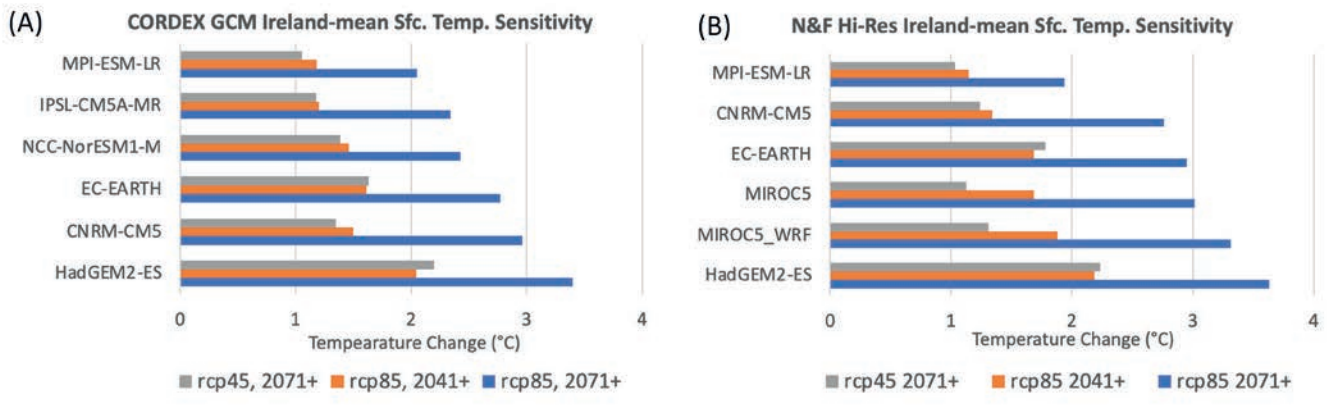


Figure 2. CMIP5 global models used by TRANSLATE, ranked by the mean surface temperature change over Ireland from the RCM ensemble-mean under the RCP8.5 scenario for the period 2071-2100 (blue bars). (A) is from the EURO-CORDEX ensemble; (B) from the Nolan and Flanagan (2020) ensemble. The orange bars in each chart show the ensemble- and area-mean temperature change under RCP8.5 for 2041-2070, while the grey bars show the same temperature change metric under RCP4.5 for 2071-2100. Changes are relative to 1976-2005.

sensitivity ensembles of Fig. 1, and about 15% in each of the low- and high-sensitivity ensembles. Thus, the three sensitivity ensembles shown in Fig. 1 should not be considered equally likely, but as a rudimentary histogram of model uncertainty.

Further statistical post-processing leads to a condensed reference set of climate data and spatial maps representing annual, seasonal, monthly or even daily statistics for a range of variables (prognostic and diagnostic, such as derived indices) at different future time periods under different external forcing scenarios, and/or global warming 'thresholds'. The reference set typically encompasses alternative climates from both the lower and higher climate sensitivity ranges, as determined by the spread of the underlying ensembles. Moreover, the climate represented by each sensitivity-based sub-ensemble tries to preserve the characteristics and frequency of extreme events, or probabilistic outliers.

3.6 Global Warming Level or Temperature Threshold-based Climate Ensembles

TRANSLATE supplemented the range of 27 'scenario'-based climates with a set of 5 temperature 'threshold'-based climates, i.e., climates based on the 20-year time periods centred on the year when each global climate model crossed specific Global Warming Level (GWL) thresholds. The GWLs considered were 1.5, 2.0, 2.5, 3.0 and 4.0°C above pre-industrial levels. Note that global mean temperatures were used to identify the model years to use for each GWL, in contrast to the Ireland-only temperatures that were used to classify the models into different sensitivity categories.

A template for constructing such threshold-based climate scenarios is provided by Vautard et al. (2014) and Fig. 3 shows a sample case of how it was done for TRANSLATE. In practice, and as shown in Table 1, global temperature crosses

at least the 1.5°C threshold under almost all RCP scenarios, while the 2.5°C threshold is crossed in all the RCP8.5 simulations and most of the RCP4.5 ones. However, the only simulations that reached the 4.0°C threshold were those run under RCP8.5. Given that each GCM is downscaled by several different RCMs, the number of ensemble members contributing to each GWL climate ranges from 66 (or more) at the 1.5°C threshold down to 28 at the 4.0°C level.

The appeal of these GWL climates is that, in principle, they are independent of forcing

scenario or future timeperiod; they simply show what the climate in Ireland would be like in a world that is warmer than the pre-industrial past by specific amounts. The main assumption behind them is that the path to any given warming level does not matter as much as simply reaching that warming level. This assumption is largely supported by the common global warming levels reached by different scenarios (SSP45 and SSP85) as shown, e.g., in Figs. 7-9 of Guo et al (2023).

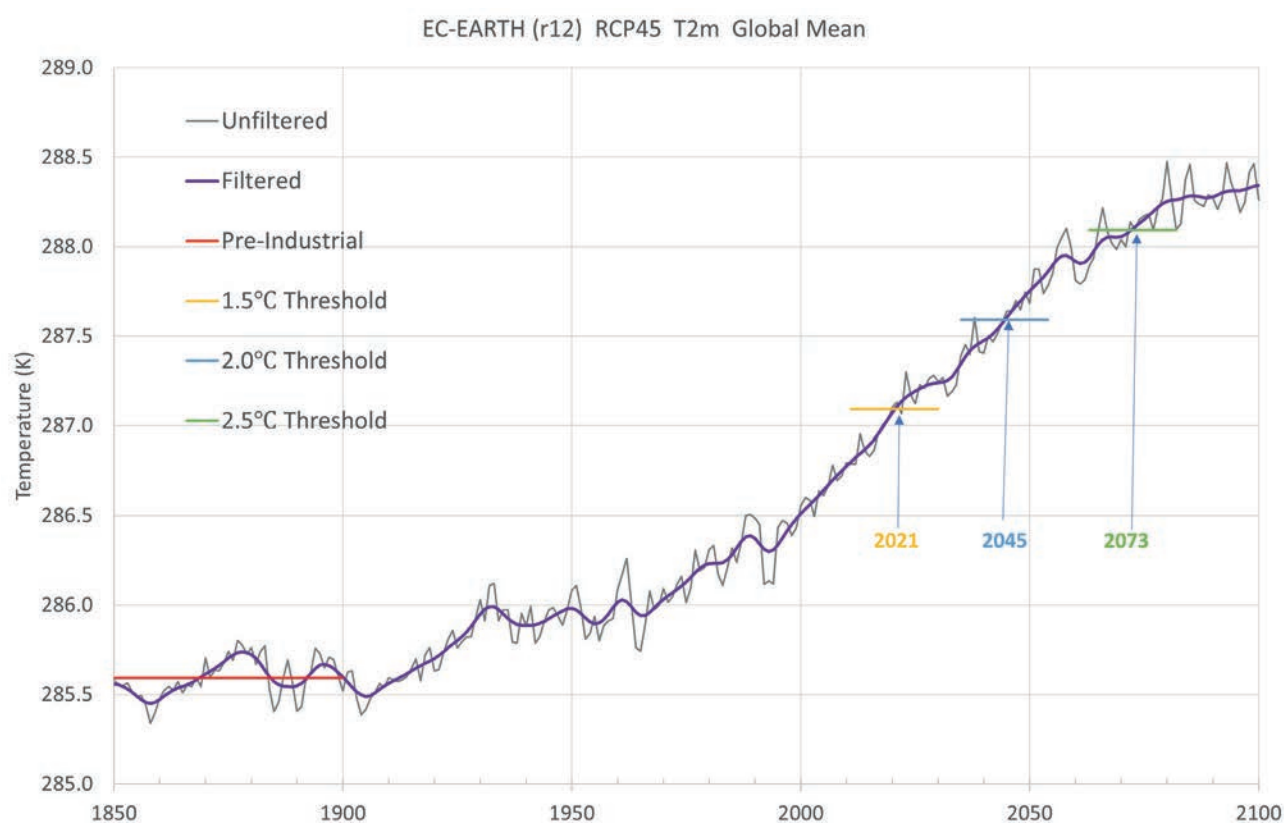


Figure 3. A specific example, using the r12i1p1 run of the ICHEC-EC-EARTH model under RCP4.5, of how the threshold-crossing dates are determined, in this case for each of the 1.5°, 2.0° and 2.5°C temperature increases, relative to the pre-industrial period 1850-1900. The annual-mean of the global-mean surface air temperature is calculated for each year (grey unfiltered time series) and then smoothed using 11 repeated applications of a triangular '1-2-1' filter (purple filtered time series). The mean of the filtered time series is computed for the pre-industrial period (red horizontal line) and the dates when the filtered time series reaches the different thresholds above that pre-industrial mean are noted (i.e., 2021, 2045 and 2073 in this case). The 20 (unfiltered) years surrounding these dates (yellow, blue and green horizontal lines) are then taken as a member of the ensemble representing each threshold or GWL climate.

Table 1. The year when the (filtered) global-mean surface air temperature of each CMIP-5 global model first crossed each of the 5 global warming levels (above pre-industrial values) for each of the 3 emission scenarios used (RCP2.6, RCP4.5, RCP8.5). Data gaps mean that either a simulation did not reach the threshold, or that such a simulation was not available (e.g., IPSL-LR output was only available for the RCP2.6 scenario, while IPSL_MR was only available for RCP4.5 and RCP8.5 scenarios).

CMIP-5 Model	1.5°C			2.0°C			2.5°C			3 deg			4 deg
	rnp26	rnp45	rnp85	rnp26	rnp45	rnp85	rnp26	rnp45	rnp85	rnp26	rnp45	rnp85	rnp85
CNRM	2042	2037	2030		2058	2045		2085	2057			2067	2088
EC-EARTH r1		2023	2021		2047	2037		2077	2052			2062	2083
EC-EARTH r2	2027	2021	2017		2045	2035		2073	2049			2061	2082
IPSL-LR	2012			2036									
IPSL-MR		2017	2015		2031	2031		2056	2042		2077	2051	2068
MPI-ESM-LR r1	2024	2025	2014		2043	2037		2094	2050			2062	2083
MPI-ESM-LR r2	2017	2021	2020		2039	2034		2073	2045			2059	2081
HadG E M2-ES r1	2022	2030	2023	2049	2040	2035		2059	2048			2056	2073
NCC-NorESM1-M		2038	2033		2071	2049			2062			2072	2096
MICROC5-r1	2051	2039	2033		2069	2051			2060			2072	2083



4

**Combining
European
and National
Climate
Projections**

The Nolan and Flanagan (2020) high-resolution ensemble had 4-6 members, while the coarser EURO-CORDEX ensemble had approximately 19-29 members, depending on the scenario and the variable of interest. Although each ensemble is based on many of the same GCMs, they both use very different RCMs. Hence, it is worth comparing projections from each ensemble separately before combining them into a single final product. Moreover, once they are detrended, bias-corrected and downscaled to the same high-resolution observational grid, the question arises as to how much weight should be given to each individual simulation when combining them into a single integrated ensemble? In practice, the final projections for all the fields we have compared from both sets of ensembles are so similar as to be climatically identical. For simplicity, then, the two sets of ensembles were combined into a single final set by giving equal weight to each ensemble member, regardless of its origin.

An example is shown in Fig. 4, for the 99th percentile of daily precipitation amounts during autumn (September-November), from the middle-sensitivity ensemble under RCP4.5 for the period 2071-2100. Since autumn tends to be the wettest season in Ireland, these charts indicate what the wettest days during the wettest season would be like under that scenario. The top row (Fig. 4a-c) shows the fields from the Nolan and Flanagan (2020) ensemble, the EURO-CORDEX ensemble and the combined ensemble, respectively. The differences between the fields in Figs. 4a and 4b are very small and difficult to see, so it

is not surprising that their combination in Fig. 4c looks much the same again. The bottom row (Fig. 4d-f) shows the ratios of the top row fields to the corresponding observed field from 1976-2005; here, the differences between the Nolan and Flanagan (2020) ensemble (Fig. 4d) and the EURO-CORDEX ensemble (Fig. 4e) are more apparent, though still small. Their combination in Fig. 4f shows a relatively simple pattern of rainy autumn days becoming wetter over most of the country by slightly more than 10% relative to the end of the 20th century.

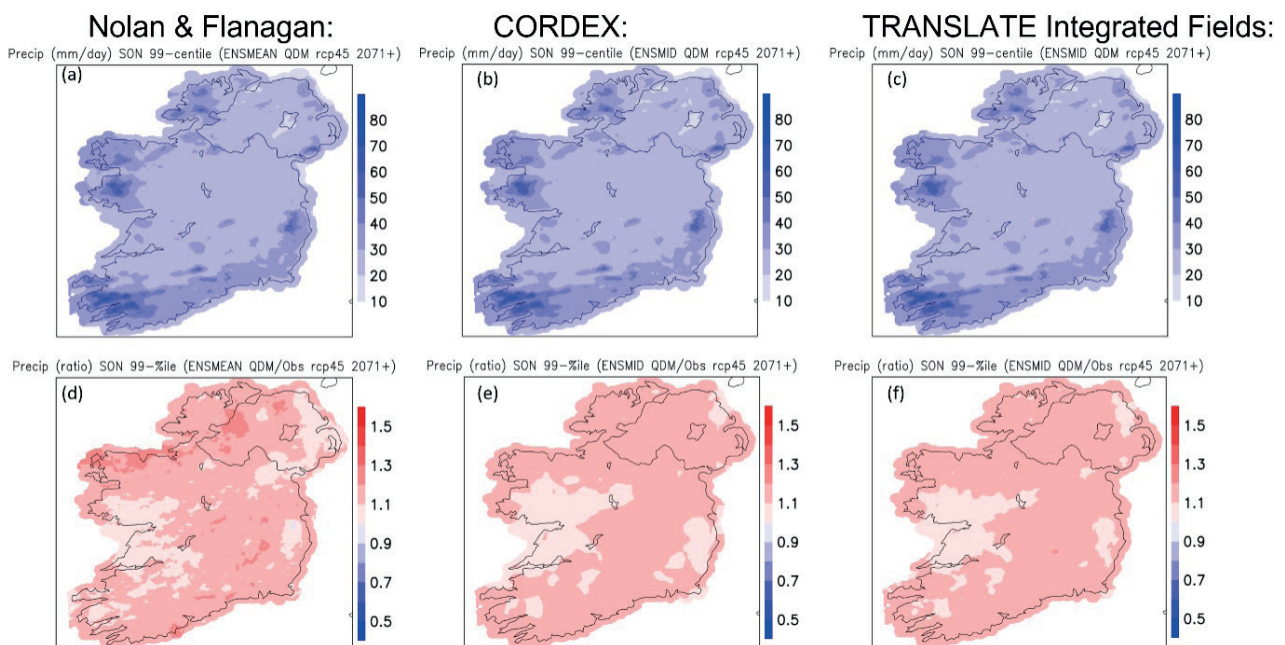


Figure 4. Panels a-c show the 99th percentile of daily precipitation amounts projected for the September-November season, by the mid-sensitivity ensembles under the RCP4.5 scenario for the period 2071-2100. (a) shows the field from the Nolan and Flanagan (2020) ensemble; (b) from the EURO-CORDEX ensemble, while (c) is from the combination of the two, with equal weight assigned to each ensemble member. Panels d-f show ratios of the fields in a-c relative to the corresponding observed field from 1976-2005.



5

**Sample
Projection
Results**

5.1 Climate Means

The projected end-century annual mean temperature fields under the three different emission scenarios and three different sensitivity ensembles are shown in Fig. 5. Each map shows a lot of spatial detail, most of which corresponds to local elevations. All the main mountain ranges in Ireland can be easily identified. In each map, temperatures tend to be slightly cooler in the midlands and north, and slightly warmer around the coasts and towards the south, much as they are today. There is also a clear gradient across the nine maps shown, with temperatures increasing from left to right as the climate sensitivity increases, and from top to bottom as the emission scenarios increase from RCP2.6 to RCP8.5. Note that ‘absolute value’ maps like this that have been bias-corrected are typically more credible than raw RCP output, which can have misleading biases.

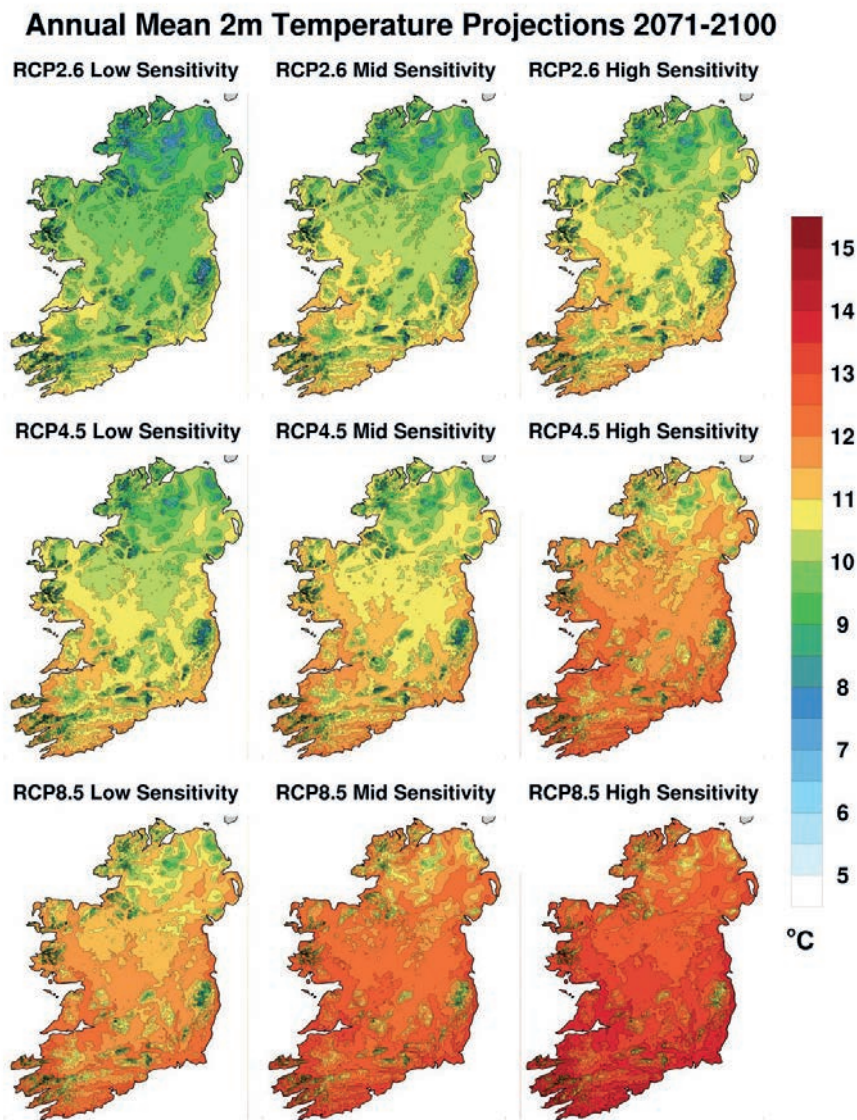


Figure 5. Projected annual mean surface temperature fields (°C) for the 2071-2100 period under the three different forcing scenarios and for the three different sensitivity ensembles.

The differences between each map in Fig. 5 and the annual mean temperature during the reference period 1976-2005 are shown in Fig. 6. Projected temperature changes relative to the reference period are all relatively uniform and smooth, with just a slight increasing gradient from west to east in each map. This gradient is likely due to the moderating influence of the Gulf Stream extension in the Atlantic acting most strongly on that part of Ireland closest to it. The inter-map differences are larger, with temperature

changes increasing between maps from left to right as climate sensitivity increases, and from top to bottom as the emissions forcing increases. Of course, annual mean temperature is precisely the field that was used to define climate sensitivity, so the gradient from left to right in Fig. 6 is predetermined by that choice. Even so, it is apparent in Fig. 6 that projected climates are more sensitive to the changes in RCP scenario than to the differences between the model responses (as measured by their climate sensitivity).

Annual 2m Temperature Change 2071-2100 w.r.t 1976-2005

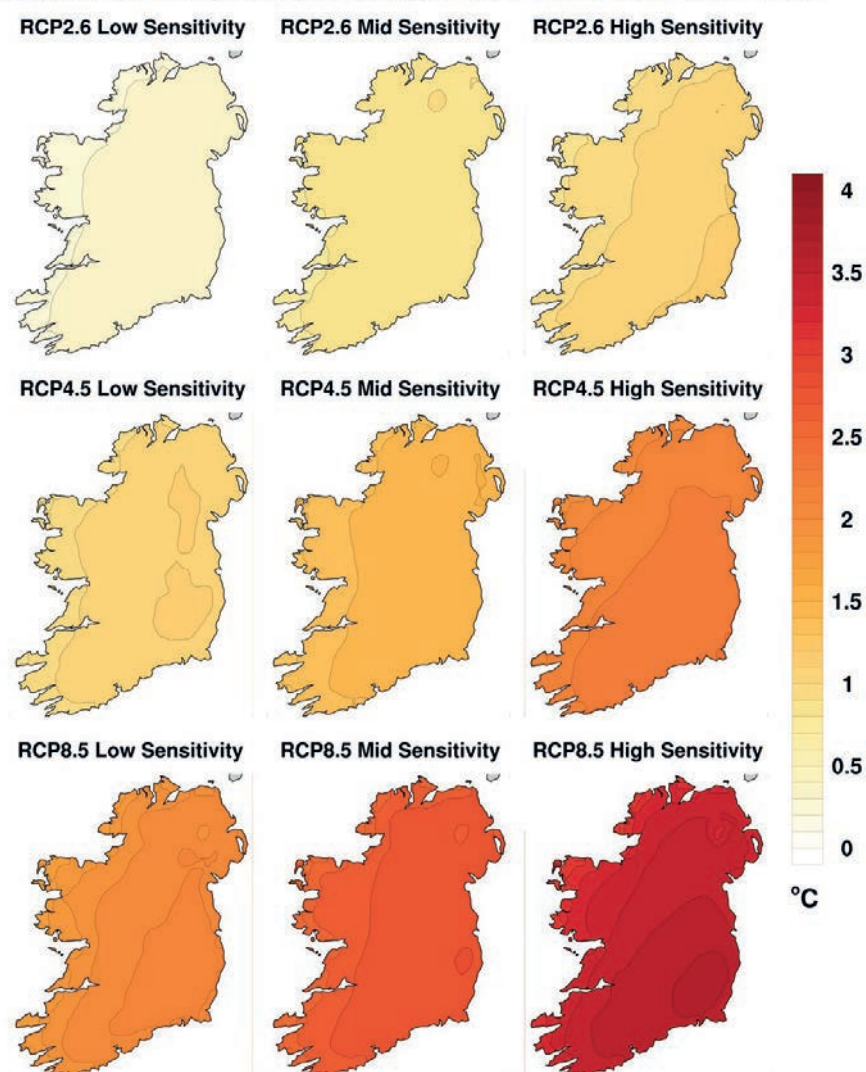


Figure 6. Differences between projected annual mean temperatures from the end-century period 2071-2100 and the reference period 1976-2005, under the forcing scenarios RCP2.6, RCP4.5 and RCP8.5, and the three different sensitivity ensembles.

The cross-section through Fig. 1 for the annual mean of daily precipitation during the late-century 2071-2100 is shown in Fig. 7. There is very little difference between any of the maps in Fig. 7: they all show higher precipitation (up to 8mm day⁻¹) over the higher elevations and along the western seaboard, with lowest values (2-3mm day⁻¹) over the midlands and eastern regions.

However, the differences between the 9 maps in Fig. 7 become more apparent when shown in Fig. 8 as percentage changes relative to observations during the reference period 1976-2005. Fig. 8 shows that any precipitation increases tend to be largest (in percentage terms) in the midlands and east.

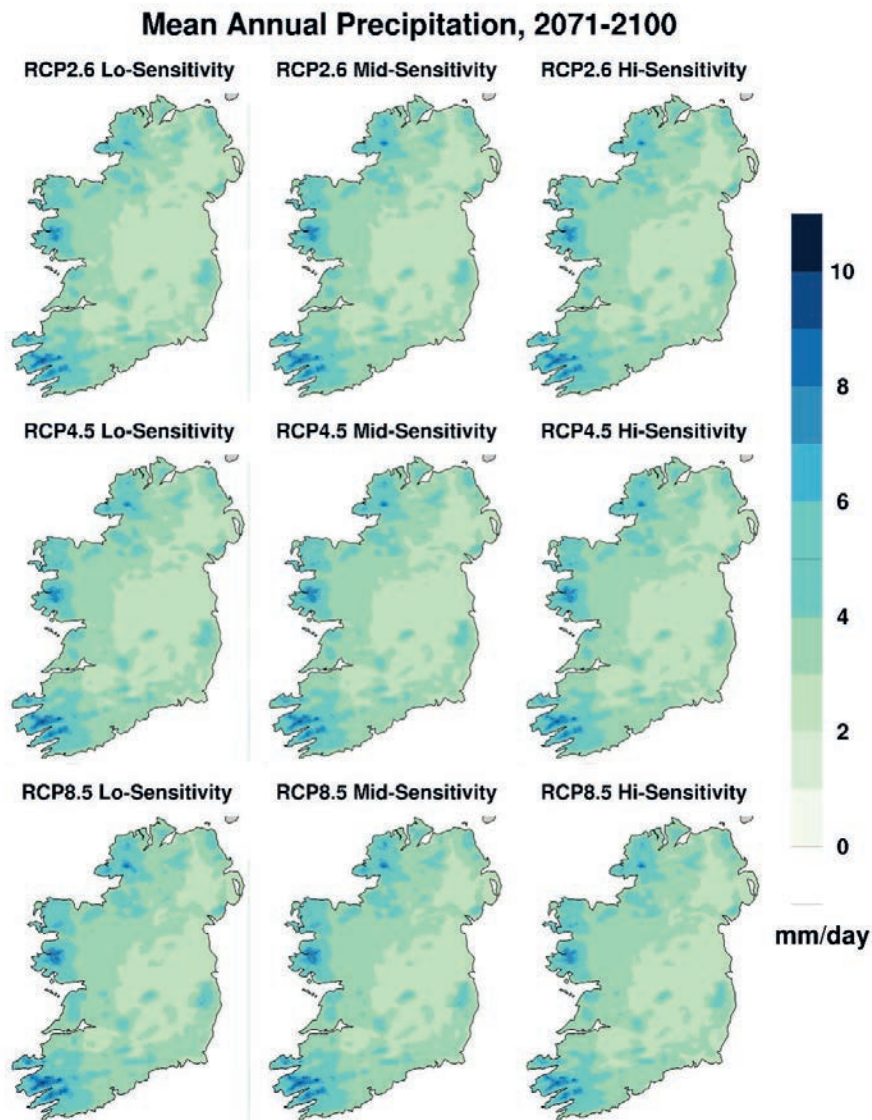


Figure 7. Projected annual mean daily precipitation fields (mm day⁻¹) for the 2071-2100 period under the three different forcing scenarios and for the three different sensitivity ensembles.

Even the annual mean precipitation changes shown in Fig. 8 mask significantly different behaviour between the summer and winter seasons. Fig. 9 shows projected precipitation changes during the end-century period as in Fig. 8, but for the summer months June-August, while Fig. 10 shows the corresponding change maps for the winter months December- February. Figs. 8-10 all use the same contour intervals and the same

colour palette. The clear message is that summers are projected to become drier, while winters are projected to be wetter. Those patterns are amplified as the emission scenarios increase from RCP2.6 through RCP4.5 to RCP8.5. In contrast, the (temperature-based) climate sensitivity dimension does not show much variation, or any clear pattern.

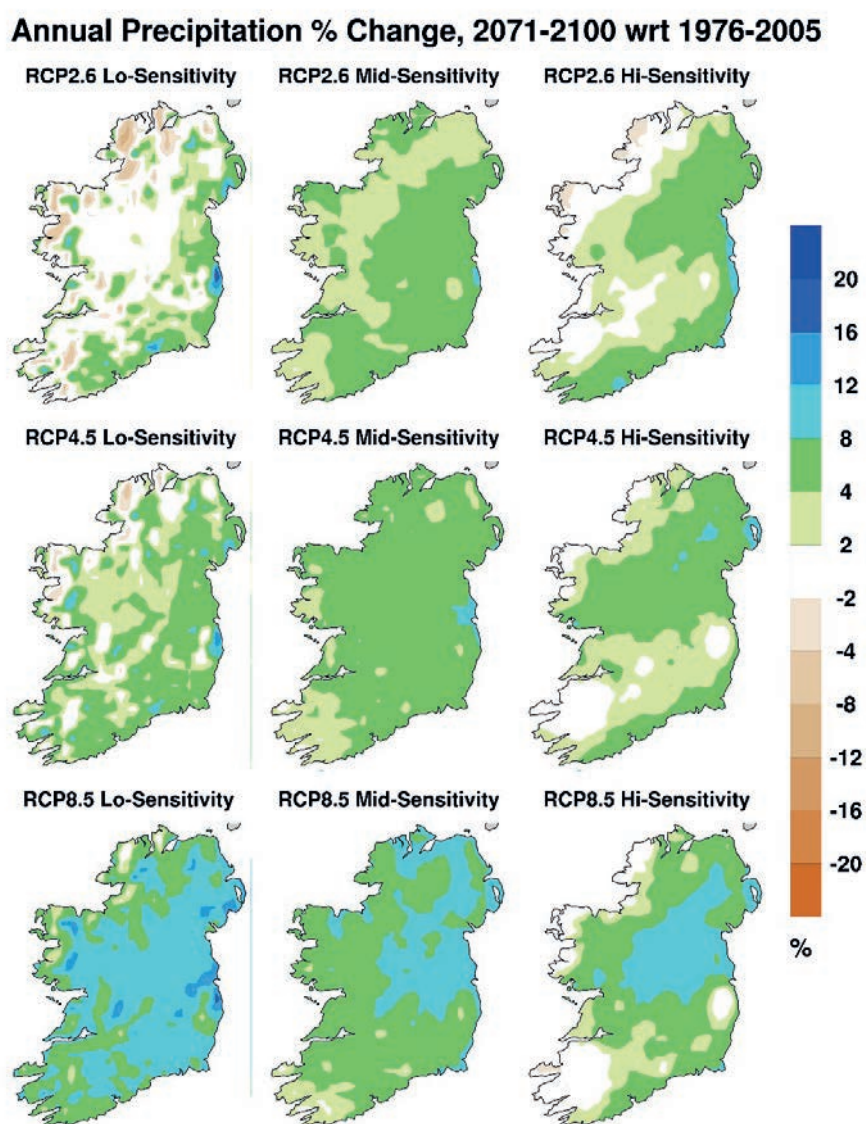


Figure 8. Differences between projected annual mean daily precipitation from the end-century period 2071-2100 and the reference period 1976-2005, under the forcing scenarios RCP2.6, RCP4.5 and RCP8.5, and the three different sensitivity ensembles.

Summer Precipitation % Change, 2071-2100 wrt 1976-2005

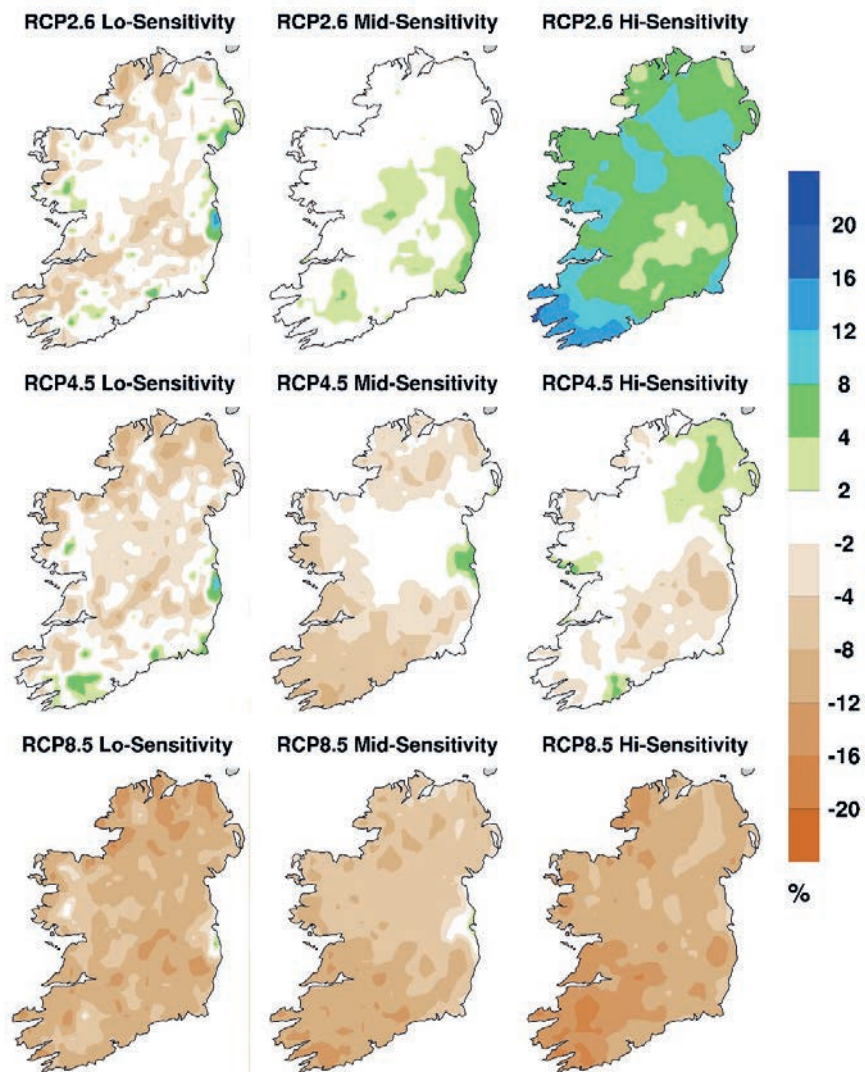


Figure 9. Percentage change in end-century projected daily precipitation, as in Fig. 8, but for the summer months June-August.

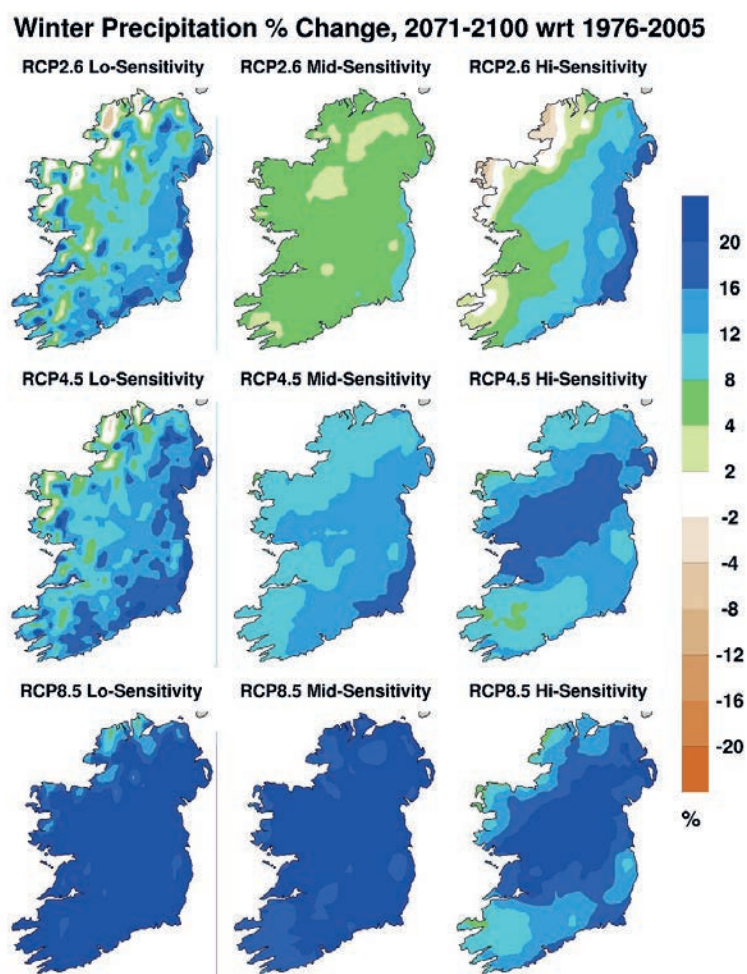


Figure 10. Percentage change in end-century projected daily precipitation, as in Fig. 8, but for the winter months December-February.

5.2 Projected Frequency Distributions

Frequency histograms were computed for each of the four main variables (T_{mean} , T_{min} , T_{max} and precipitation) and for each 30-year climate instance (or ensemble member) of each projected climate. Temperature frequencies were binned in 1°C increments from -10°C to 35°C , while precipitation frequencies were binned in increments of 2mm day^{-1} up to 80mm day^{-1} .

Fig. 11a shows annual and seasonal T_{min} histograms for 2071-2100 under RCP4.5 from the mid-sensitivity ensemble (solid curves) and for the observed reference period 1976-2005 (dashed curves), with local (grid-point) frequencies averaged over both the ensemble and the island of Ireland. The shading around each solid curve spans the range from minimum to maximum within the ensemble. The simplest interpretation of Fig. 11a is that all the

frequency curves retain much the same shape over time, but are shifted about 2°C to the right from the reference period to the end of the 21st century. The most dramatic changes thus occur near the tails. For example, winter season T_{min} values of -5°C occurred with a frequency of about 0.02 (i.e., once every 50 winter-time days) during the reference period, as shown by the dashed blue curve in Fig. 11a, but the frequency of similar cold nights by 2071-2100 under this scenario is projected to drop by a factor of 5 to about 0.004 (i.e., once every 250 winter days, only every 3 years or so). At the other extreme, summer nights with T_{min} values around 17°C are projected to occur up to 10 times more frequently than in the past. 'Tropical nights', with T_{min} not falling below 20°C , did not occur at all during the reference period but are projected to occur with a small but finite frequency in the future under this scenario.

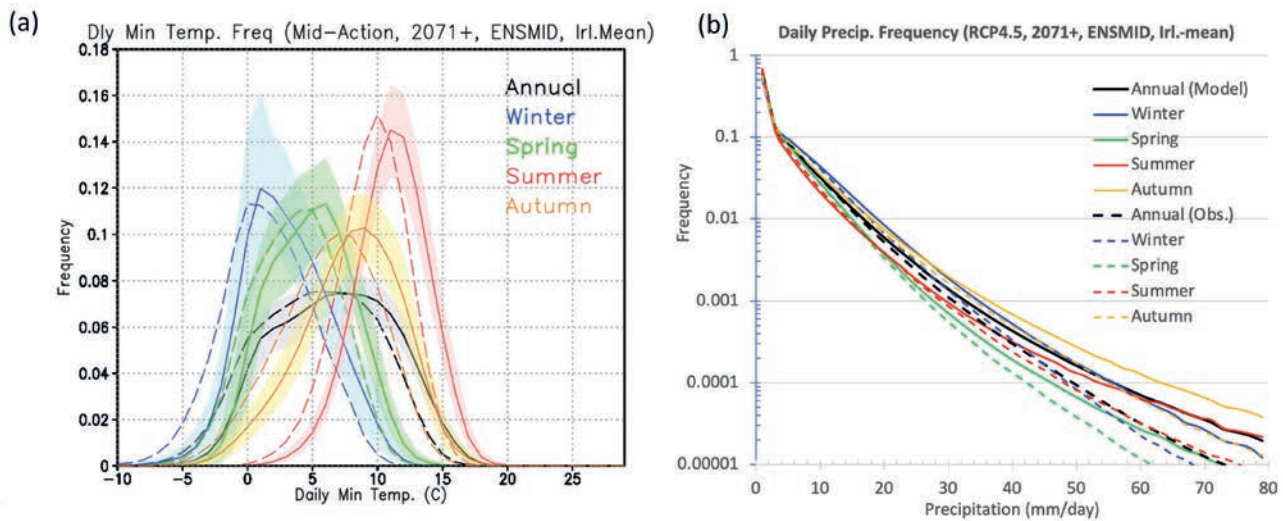


Figure 11. (a): Frequency distribution of projected daily minimum temperature (T_{min}) under the RCP45 (mid-range) forcing scenario for end-of-century 2071-2100 from the mid-sensitivity ensemble, averaged over all Ireland, for each season and the annual cycle (solid curves). Shaded areas around each projected curve span the range from minimum to maximum value within the ensemble. The corresponding observed T_{min} values from the reference period 1976-2005 are shown as dashed curves. The temperature ‘bins’ are 1°C wide; a frequency of 0.1 means that temperatures within that 1°C bin occur once every 10 days on average. **(b):** As in (a) except for daily precipitation, with frequency on a logarithmic scale, and for precipitation bins 2mm day^{-1} wide. No shading is shown as in (a) to avoid confusing the plot but, as the frequency decreases to 0.0001 (i.e., once in 10,000 days), the range of daily precipitation spans up to 50mm day^{-1} from ensemble minimum to ensemble maximum.

Precipitation is distributed differently to temperature, and so the precipitation frequency histograms in Fig. 11b have a logarithmic y-axis. As in Fig. 11a, the biggest differences between the past and projected future precipitation distributions are at the high-rainfall, low-frequency tails. Thus, the wettest days are projected to get wetter in all seasons, as well as for the year as a whole (all the solid curves at the tail of Fig. 11b are to the right of the corresponding dashed curves). Springtime rainfall events of 60mm day^{-1} that had a nominal occurrence frequency of 0.00001 (or a return period of 100,000 days) in the past (green dashed curve) are projected to occur about 3 times more often by the end of the century under this scenario (green solid curve).

The low frequencies of extreme events in Fig. 11b are referred to as ‘nominal’ above because, in reality, they are relatively high-frequency localised events whose frequency value is reduced by the all-Ireland averaging. The curves in Fig. 11 result from computing local frequencies and ensemble averaging first, and then doing all-Ireland averaging, instead of the other way round. This ordering does not really matter in the

case of temperature (Fig. 11a), since temperature anomalies tend to span wide areas. However, in the case of precipitation (Fig. 11b), it has the effect of expanding the sample size by several orders of magnitude before averaging it down again. Instead of approximately 20 ensemble members each with a single 30-year time series of daily data from which to compute event frequency, each ensemble member has 30 years of such data for each of about 2,000 (EURO-CORDEX) grid-points, or 30 years for each of hundreds of effectively independent locales where intense precipitation can occur. This sample multiplier effect is how return periods of up to 100,000 days (approximately 275 years) can be plotted in Fig. 11b. Even so, it is notable that most curves in Fig. 11b have such smooth trajectories all the way down to the lowest frequencies and could reasonably be extrapolated further if desired. Plots like Fig. 11b that are restricted to individual grid-points or small regions of just a few points only extend smoothly to frequencies of 0.001 (return periods of 3 years or so) before becoming noisy and non-monotonic (i.e., reporting isolated very wet events at the extreme tails of the distributions).

5.3 Projected Global Warming Level Climate Summaries over Ireland

As was done for the scenario climates, the Global Warming Level (GWL) climates were first produced from the EURO-CORDEX and Nolan and Flanagan ensemble separately, and then combined into a synthesised ensemble mean set of statistics and maps based on the number of ensemble members in each set. Each ensemble member received the standard TRANSLATE treatment of de-trending, bias-correction and statistical downscaling (as explained previously and in OB&N). Some highly integrated results from the overall ensemble means are shown in Figs. 12 and 13.

Fig. 12 shows changes in daily minimum, mean and maximum temperatures (blue, green and red symbols, respectively) with respect to the 1976-

2005 reference period, for each of the 5 GWLs considered. The overall ensemble mean changes are joined by the solid curves; the ensemble minimum and maximum changes are joined by the dashed curves. The range between ensemble minimum and maximum is about 3°C for each variable at each GWL. Even for the 2.5°C GWL, some ensemble member (or members) project negative temperature changes over Ireland (relative to 1976-2005), although these are relative outliers, and the ensemble mean changes are about 1.5°C.

As shown in Supplementary Table 3 in OB&N, the estimated Ireland-mean temperature change from pre-industrial times to 1976-2005 was about 0.5°C. Thus, all the points in Fig. 12 could be raised by approximately 0.5°C to reflect the real Irish warming level corresponding to each GWL.

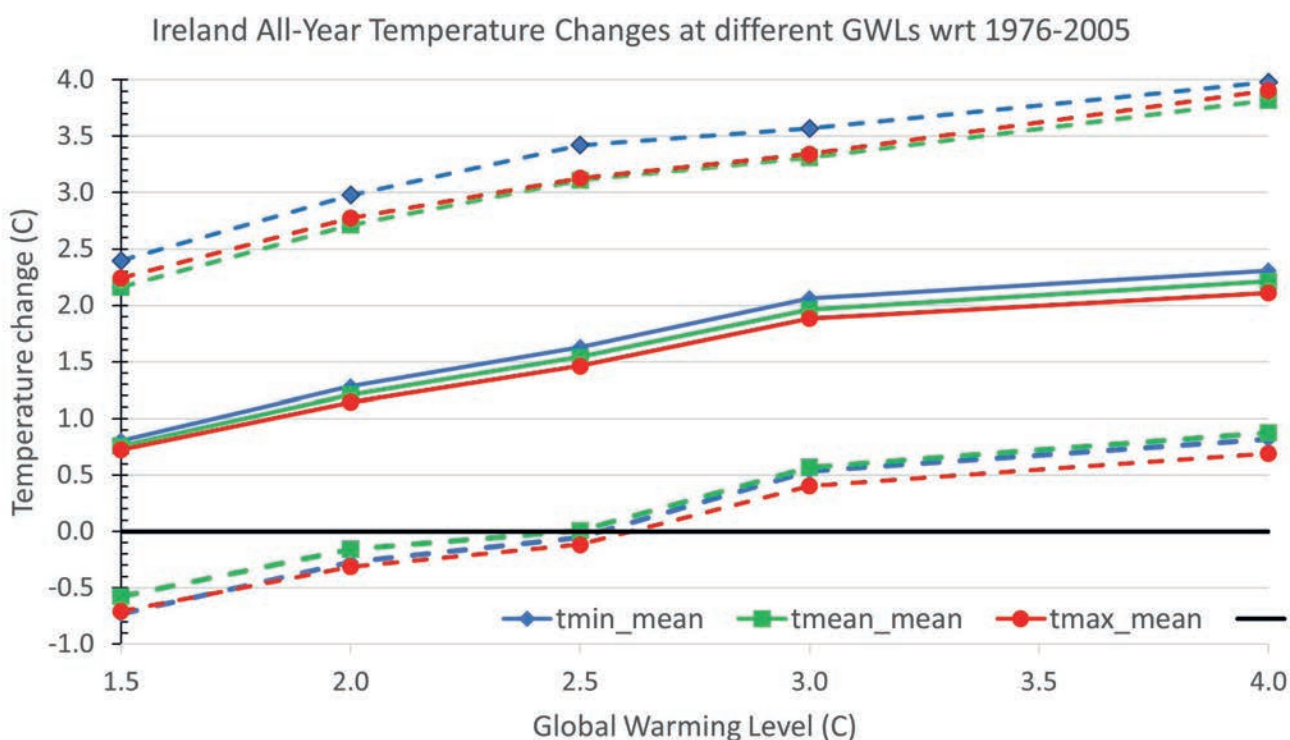


Figure 12. Ireland-mean temperature changes (with respect to 1976-2005) at each of 5 global warming levels, for daily minimum temperature (T_{min} , blue symbols); daily mean temperature (T_{mean} , green symbols); and daily maximum temperature (T_{max} , red symbols). Changes are expressed as temperature differences in °C. The symbols joined by the solid lines are overall ensemble means, while the symbols joined by the dashed lines are ensemble minima and maxima. Thus, the range between the lower dashed curves (ensemble minima) and upper dashed curves (ensemble maxima) represents the full range of possible changes projected by the ensemble.

Clearly, for each GWL, most ensemble members project Irish warming levels somewhat lower than the GWL, although some do project Irish warming levels that are higher. Overall, it seems that temperature changes over Ireland track the global changes reasonably well for changes up to 2.0°C, but then tend to progressively lag the global changes as warming levels increase. This is not particularly surprising, since most of the extra warming in a 4.0°C warmer world is projected to occur in polar and high-latitude regions (see, e.g., Fig. SPM.5a in IPCC 2021: Summary for Policymakers).

Another point to note in Fig. 12 is that the changes in daily minimum temperature (T_{min} , blue symbols) tend to be consistently larger than the changes in daily mean or maximum temperature (green and red symbols). This is also consistent with a classic signature of the greenhouse effect, which is that night-time temperatures are expected to increase more than daytime temperatures as greenhouse gas concentrations increase: see, e.g., Cox et

al. (2020), or Fig. 3.4 of the IPCC special report <https://www.ipcc.ch/sr15/chapter/chapter-3/>.

Fig. 13 is similar to Fig. 12 but compares the annual changes in daily precipitation (green symbols) with summer changes (red symbols) and winter changes (blue symbols) for each GWL. Changes are computed as ratios with respect to 1976-2005, so the thick horizontal black line at 1.0 on the y-axis separates projected increases above it from decreases below. Again, the ensemble-mean results are joined by the solid lines, while ensemble minima and maxima are joined by the dashed lines. According to the ensemble means, winters are projected to get increasingly wetter for larger GWLs, while summers are projected to get increasingly dryer. However, the projected mean changes mask a great deal of precipitation variability both within and between ensemble members – as may be seen by the factor of 4 or so between the ensemble minima and maxima in Fig. 13. The ensembles show somewhat greater variability (i.e., larger range between ensemble

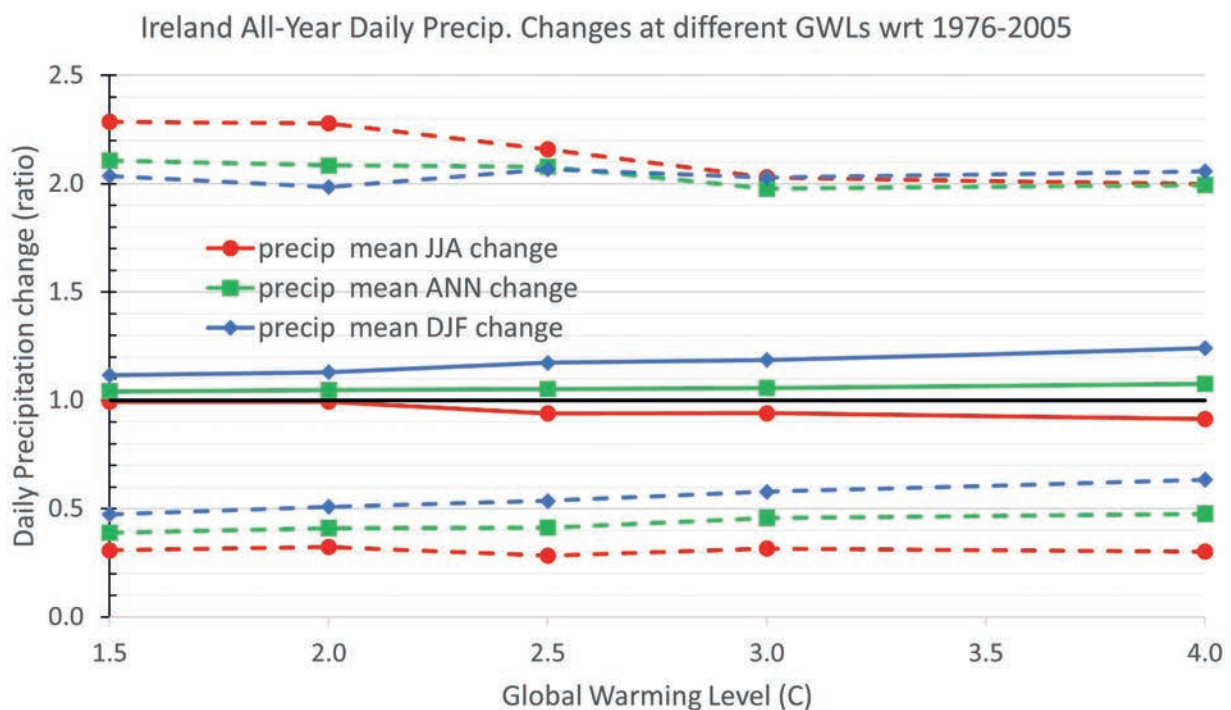


Figure 13. Ireland-mean daily precipitation rate changes (expressed as ratios with respect to 1976-2005) at each of 5 global warming levels, as in Fig. 1, but for winter (DJF, blue symbols), summer (JJA, red symbols) and annual year-round changes (green symbols). Symbols joined by solid lines are overall ensemble means, while symbols joined by dashed lines are ensemble minima and maxima.

minimum and maximum) during the summer months JJA than during the winter. The apparent reduction in ensemble range at the 3.0°C and 4.0°C GWLs should be treated with some caution since, as shown in Table 1 above, the ensembles at these GWLs have much fewer members than the lower GWLs have, and the reduction in range could be simply an artefact of reduced ensemble size. Pendergass et al. (2017) show that precipitation variability is more likely to increase in a warmer world.

5.4 ETCCDI extreme Index Calculation

A total of 27 standard climate indices are defined by the Expert Team on Climate Change Detection and Indices (ETCCDI¹). Most of the indices measure different aspects of climate extremes. They can all be easily computed from the (detrended and bias-corrected) 30-year time series files for each member of each ensemble shown in Fig. 1, or from the 20-year time series for each ensemble member of each temperature threshold climate. TRANSLATE saves each such (reconstructed) time series so that any ETCCDI index, or indeed other custom indices (e.g., 'growing season duration'), can be computed on demand.

By default, TRANSLATE computed 12 ETCCDI indices for each of the 27 scenario climates and each of the 5 GWL climates. The indices were first computed for each year of the 30-year daily time series for each individual model, averaged over those 30 years, then reported as the median over all ensemble members. Four of the selected indices are based on daily maximum temperature (TXx, TXn, SU and CSU), four on daily minimum temperature (TNn, TNx, FD and TR15) and four on precipitation (rx1day, rx5day, rr1 and r20mm). Several other indices were also computed on a more selective basis (e.g., just for the 3 scenario climates for mid- and end-century periods).

As an example, Fig. 14 shows the annual number of 'tropical nights', with minimum temperature > 15°C (or TR15) from the 1976-2005 reference period in the top-left panel, along with changes

to the annual TR15 counts at the 5 different GWLs in the remaining panels. The reference period had relatively few such warm nights – approximately 5 per year over most of the country. There is then a large monotonic increase in the number of such warm nights as GWLs rise. At the 4.0°C GWL, parts of the south of Ireland are projected to have over 40 more such warm nights per year, or over 8 times more than in the recent past. This reflects how projected changes at the tails of frequency distributions are typically much larger than changes to the means.

The standard ETCCDI tropical night index counts days with minimum temperatures above 20°C, but Ireland experienced no such days at all during the reference period. A few such days are projected for the future – typically one every 2 or 3 years – but while they will remain rare, they formally represent an 'infinite' increase relative to the past.

A second example (Fig. 15) is taken from the 'scenario' projections. As in Figs. 5-10, this is another cross-section through the matrix in Fig. 1 at the end-century period (2071-2100) and shows the changes in the RX1day index relative to 1976-2005, where RX1day is the amount of precipitation that falls on the wettest day of the year. The RX1day values used for the ratios shown in Fig. 15 are the 30-year mean values from each 30-year period and, in the case of the projected climate, the ensemble median of each 30-year mean as well. Thus, the fields in Fig. 15 show changes to the *expected* rainfall amounts on the wettest day of the year, and not changes to the *maximum possible* rainfall within a single day. The RX1day values are only expected to decrease in a few small (brown-shaded) areas under the RCP2.6 scenario, and are expected to increase under all other scenarios. Indeed, these wettest days of the year are expected to become up to 50% wetter over large areas of the country under the RCP8.5 scenario by the end of the century. These changes to RX1day (an 'extreme' index) may be compared with the much lower projected mean changes shown in Fig. 8 or Fig. 10. However, there are no clear-cut

¹ ETCCDI indices are listed at http://etccdi.pacificclimate.org/list_27_indices.shtml

regional patterns apparent in Fig. 15, reflecting the highly variable nature of this index – and indeed of precipitation in general.

Charts like Figs. 14 and 15 can also easily be generated for each of the other 11 (or more) indices that have been computed for each discrete TRANSLATE ‘climate’.

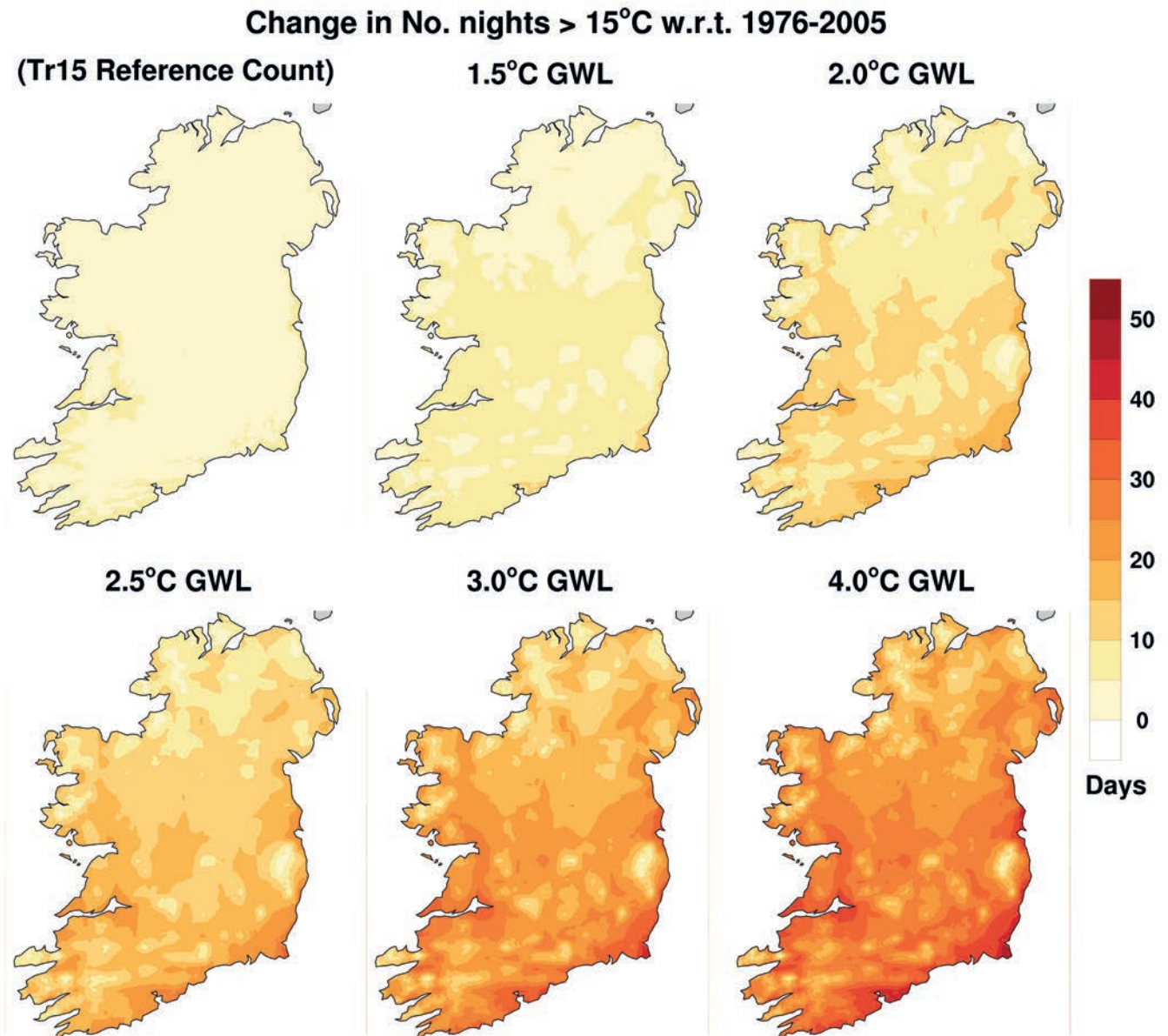


Figure 14. Annual number of nights with minimum temperature > 15°C from reference period 1976-2005 (top left), with annual changes in number of such nights relative to that period for 5 different GWLs on the remaining panels.

Rx1day: Max. Annual 1-day Precip.; Mid-Century wrt 1976-2005

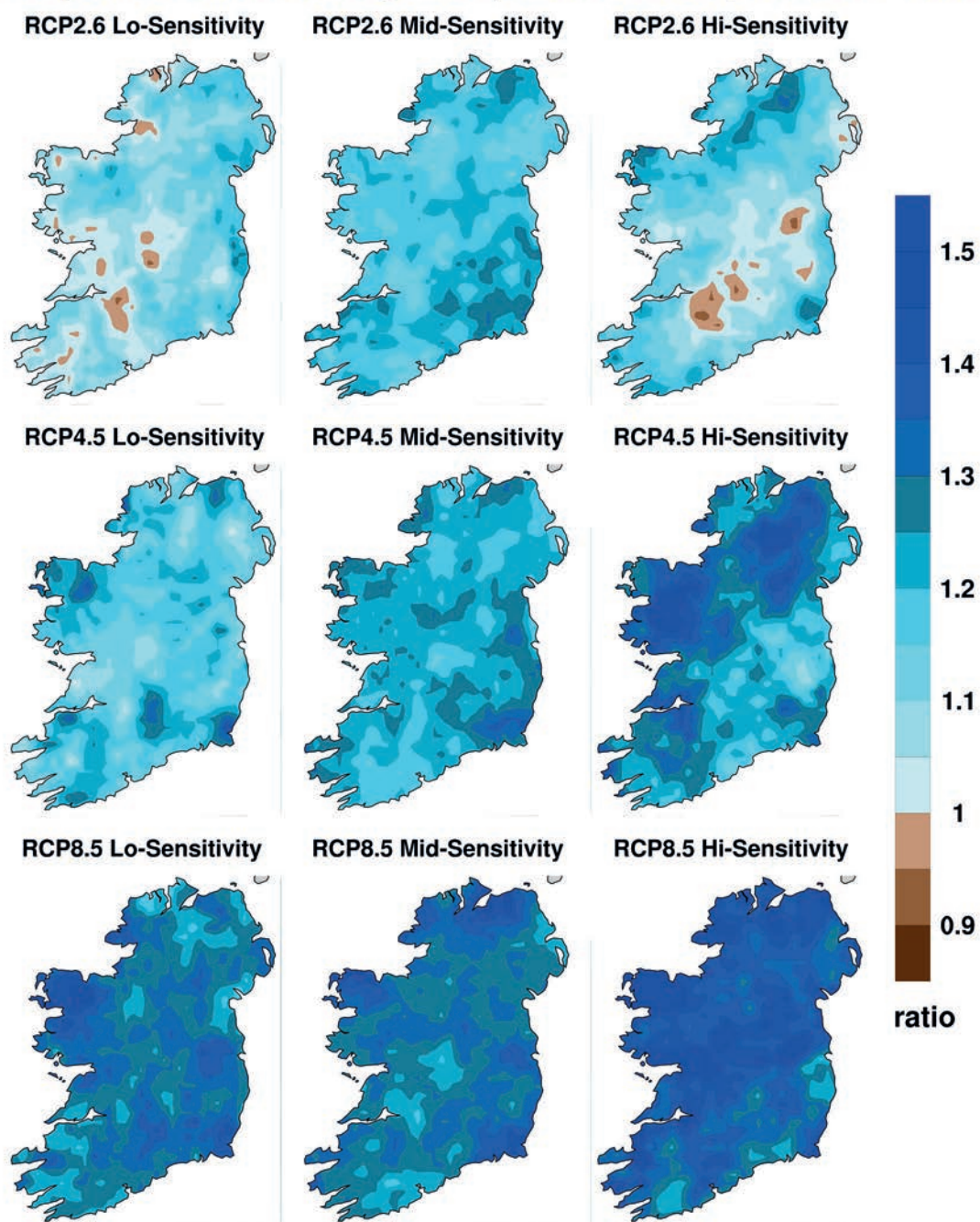


Figure 15. Changes to the expected annual maximum 1-day precipitation amount (RX1day index), shown as a ratio between the projected 2071-2100 period and the 1976-2005 reference period. As in Figs. 8-10, the panels here are a cross-section through Fig. 1, showing RX1day ratios for each of the forcing scenarios RCP2.6, RCP4.5 and RCP8.5 and the three different sensitivity ensembles.



6

**Part A
Discussion
and
Conclusions**

A paradox of various national standards for future climate projections (e.g., UKCP18, CH2018 and KNMI'14 in the UK, Switzerland and the Netherlands, respectively) is just how different they all are from each other, each reflecting different national circumstances. This is also true of more recent projections for Central America by Tamayo et al. (2022). Nevertheless, it is clear from those projects that any standard future projection for Ireland should be based on high-resolution dynamical downscaling of global CMIP models. They should include a range of forcing scenarios to accommodate future emissions uncertainty, and a range of climate sensitivity responses to accommodate model response uncertainty.

Ideally, future projections should be based on as large an ensemble as practically possible, with each ensemble member providing an independent climate instance of daily values of relevant variables for periods long enough to provide stable statistics (i.e., 20-30 years). Aggregated projections based on the modelled temperature crossing key thresholds are also worthwhile. The time series of each variable in each climate instance should be detrended, bias-corrected and statistically downscaled to the best possible grid-spacing to provide a stable climate reconstruction, which can then be queried for a wide range of statistics and climate indices. As shown in OB&N, statistical downscaling can add meaningful spatial information to climate projection fields that have coarser grids, just as dynamical downscaling by RCMs can provide

more spatial detail than the low-resolution GCMs that drive them. Nevertheless, downscaling does not fundamentally alter or feed back on the climate change signal that is passed down from the coarser model grid.

An initial set of standardised climate projections for Ireland has been produced by the TRANSLATE project, based on the dynamical downscaling work already done by Nolan and Flanagan (2020), and by the EURO-CORDEX project, using the principles and specific methods described above and in OB&N. The most commonly used TRANSLATE projections are publicly available at <https://www.climateireland.ie/data-explorer/>. The complete dataset is available on request from Met Éireann (email enquiries@met.ie).



The two underlying sets of downscaled ensembles are nested in the same global CMIP5 models but are very different in the RCMs they use and in their native grid spacing. Given their different grid spacings and ensemble sizes, their post-processing by TRANSLATE to provide detrended, bias-corrected and fully-downscaled output was done somewhat differently, as described in OB&N. Nevertheless, the final projected output fields from both sets of ensembles tend to look remarkably similar (Fig. 4). The future projected fields (e.g., Fig. 5) tend to include local details that reflect the main geographical features of Ireland, but the difference fields with respect to the reference 1976-2005 climate tend to be smooth and bland, reflecting the large-scale pattern of the underlying climate change signal (e.g., Fig. 6). The similarity in the final future projections between the Nolan and Flanagan (2020) fields and the EURO-CORDEX fields tends to serve as cross-validation between them, increasing confidence in the validity of both.

The next steps for TRANSLATE are to include more variables in our projections (especially wind, humidity and radiation) and to produce an updated TRANSLATE 2, based on regional downscaling of CMIP6 simulations. A multi-member, high-resolution ensemble based on CMIP6 models and analogous to the Nolan and Flanagan (2020) ensemble has been completed by Paul Nolan (Nolan, 2024) and has already been post-processed by TRANSLATE. CMIP6 simulations downscaled by RCMs over the EURO-CORDEX domain will be processed once they become available – see https://wcrp-cordex.github.io/simulation-status/CORDEX_CMIP6_status.html.

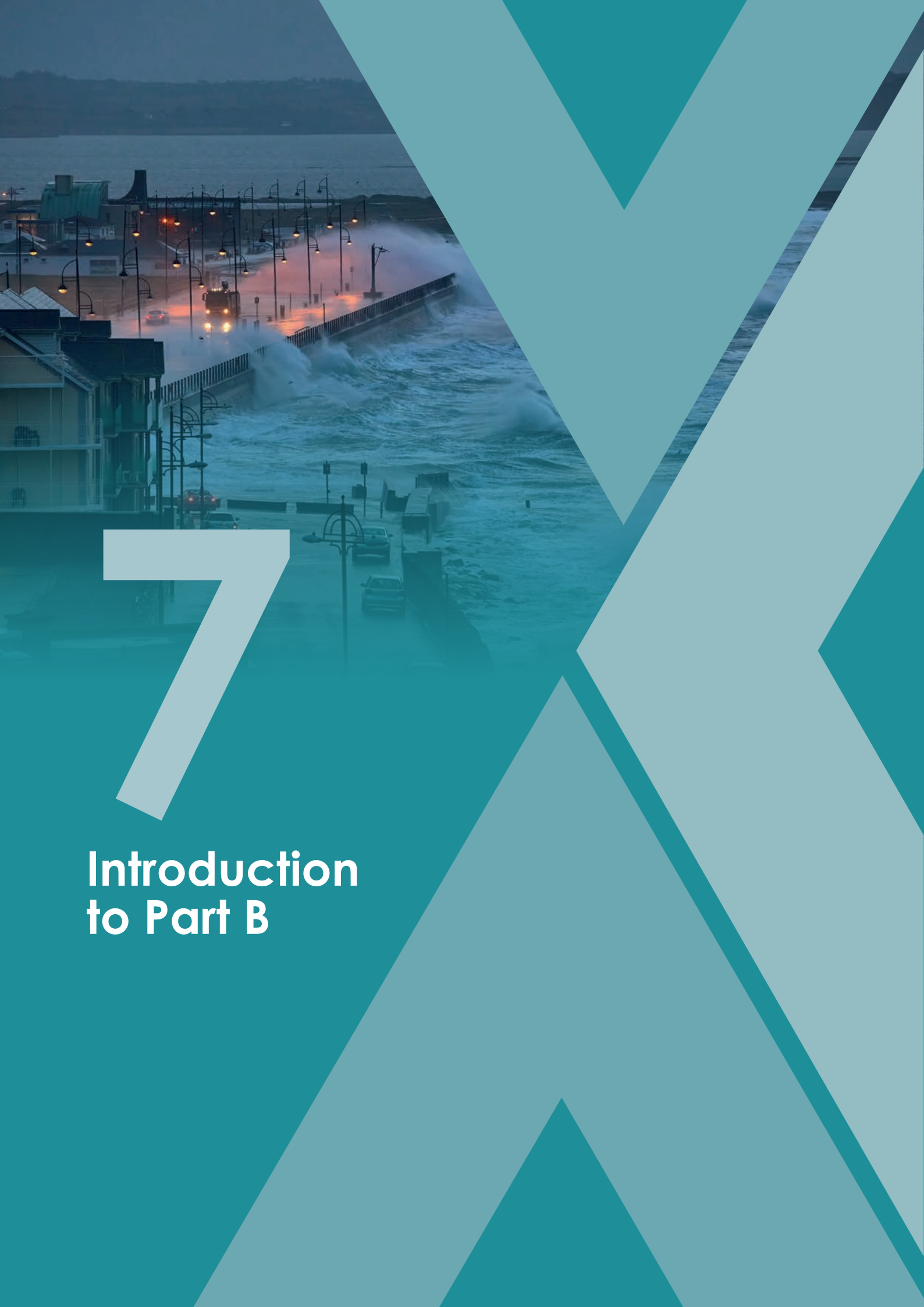
A TRANSLATE project to make future projections of extreme events based on ‘peak over threshold’ statistics is currently in progress, and other related initiatives are also planned.

Ultimately, our intent is to provide quantitative information that is as complete and accessible as is practically possible about likely future climates in Ireland to meet the needs of those whose job it is to plan and manage the national infrastructure and make national policy in other climate-related fields.



PART
B:

Climate Services and Risk-Based Decision Support



7

Introduction to Part B

The subsequent sections offer guidance on how to incorporate the standardised climate projections generated in TRANSLATE Part A into a variety of climate services. These services aim to help assess the future climate effects on different sectors in Ireland and aid in making risk-based adaptation decisions. This process involves acquiring relevant data; creating spatial data and hazard indicators; and constructing semi-quantitative and fully-quantitative risk-based frameworks and user guides based on the climate risk definition proposed by the IPCC 6th Assessment Report.

Additionally, it is crucial to showcase these frameworks through case studies developed in collaboration with industry partners. Specifically, two case studies are conducted to analyse the impacts of Ireland's changing climate. The first case study employs a high-level, semi-quantitative approach to assess the risks associated with missed education days caused by extreme weather events. The second case study employs a fully-quantitative approach to examine the impact of climate change on the national road drainage systems. This case study also examines the effectiveness of climate adaptation measures

implemented in 2015 in TII standards through modification of Ireland's drainage standards. The frameworks, prototype datasets and illustrative case studies developed in Part B of the TRANSLATE project serve as valuable resources and toolkits to address the needs of stakeholders and will help to facilitate effective and appropriate climate adaptation decision-making.





8

**Climate
Services
Co-Creation**

The primary aim of climate services is to better inform decision-makers at all levels, from small businesses, local professional organisations and public and city administrations (European Commission, 2015; Basseur and Gallardo, 2016). Climate services transform climate science data into information and products (e.g., projections, forecasts, risk assessment guides and tools) tailored to meet specific end-user and stakeholder decision-making requirements in relation to risk assessment and adaptation (European Commission, 2015; Bessembinder et al., 2019; Hewitt et al., 2020). The development of any climate service should involve collaboration between climate experts and stakeholders, aiming to advise and build capacity in relation to climate adaptation (European Commission, 2015; Bessembinder et al., 2019). Climate services are intended to enhance end-user knowledge and understanding of climate impacts to support climate-sensitive decisions (Hewitt et al., 2012; European Commission, 2015). End-users can be anyone with a need for high-quality climate information (Skelton et al., 2019), but the incorporation of a participatory component that focuses on collaboration with end-users during climate service development is important to ensure context relevance (Findlater, 2021).

Co-creation in the development of climate services improves the usability of climate projections, tailors information to the actual needs of users, communicates uncertainty more effectively and increases the application of this novel information (Christel et al., 2018). Despite this surge of interest in co-production, many climate services are developed considering only usefulness and usability, despite the wide array of considerations required for a truly co-created output. One of the primary objectives of TRANSLATE was, therefore, to identify,

document and prioritise sectoral requirements for standardised climate projections and customised climate risk products and analytical tools through a review of existing adaptation plans, relevant literature and stakeholder engagement. At a national level, extreme precipitation and heatwaves were the two most frequent climate services identified by the local authority sectoral adaptation plans, combined with thematic areas of water, transport, infrastructure and the built and natural environments (Fig. 16).

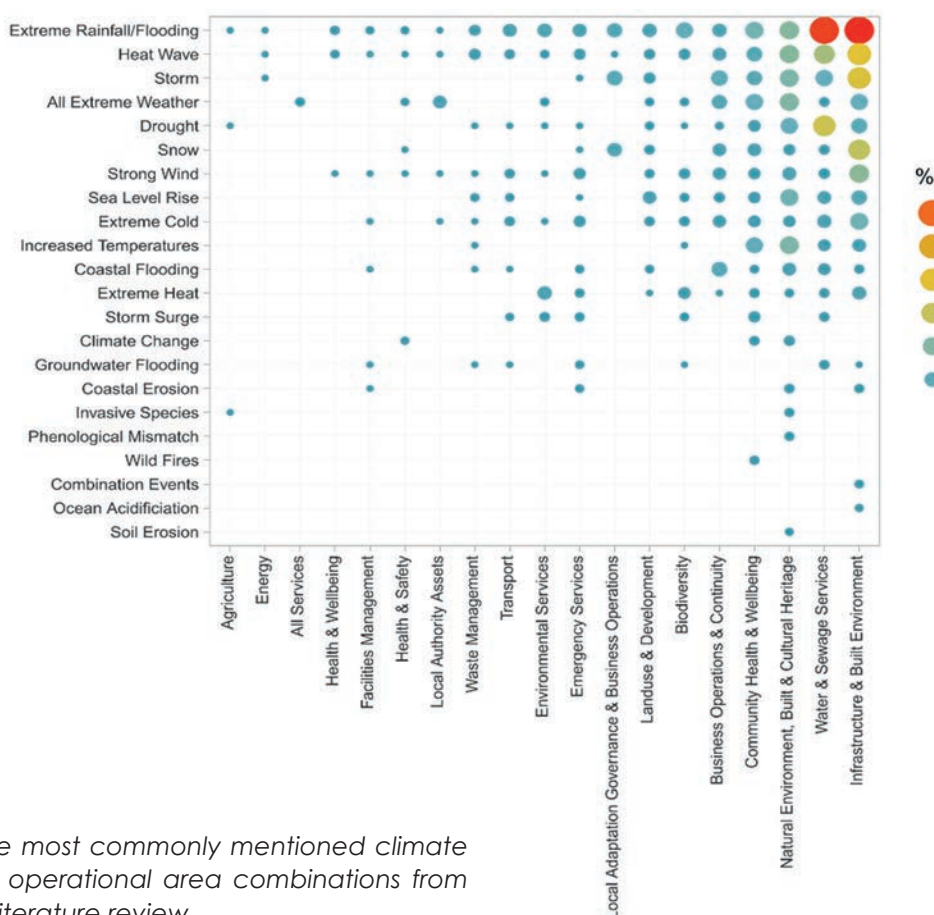




Figure 16. The most commonly mentioned climate hazards and operational area combinations from the sectoral literature review.

Similar patterns were observed at our national workshops that included over 60 participants across the sectors in November 2021 (on climate projections) and January 2022 (on climate services), with precipitation and temperature-related climate variables and hazards identified most frequently (See Table 2). With regards to sectoral risk, 34 hazard indicators were provided, with 31 of these linked to temperature and precipitation, which were the principal climate variables analysed in Part A of this report. A large proportion of stakeholder discussion centred on the importance of Met Éireann extreme weather warnings, as these provided quantitative thresholds the sectors used when working towards

adaptation planning and climate risk decision-making (i.e., school closures, changing hospital appointments, etc). Similarly, 105 metrics of exposure and vulnerability were identified by participants. Exposure metrics included properties; community infrastructure (hospitals, schools, childcare); transport infrastructure (underground pipes, airfields); heritage sites; assets; road networks; power (power plants, service lines); piers; harbours; vulnerable habitats; economic value of risk and agricultural features (soil type, land use, crop yield). Vulnerability metrics included population density and deprivation indices.

	Climate	Hazard indicator	Derived
	Atmospheric	Pressure	
		Ultraviolet radiation levels	
	Precipitation	Wet days	✓
		Very wet days	
		Met Éireann Yellow Warning days - rain	✓
		Met Éireann Orange Warning days - rain	✓
		Met Éireann Red Warning days - rain	✓
		Met Éireann Yellow Warning days - snow	
		Dry periods	✓
		Humidity	
		Met Éireann Drought - absolute drought	
		Met Éireann Drought - partial drought	
		Agricultural drought risk (SPI)	
		Agricultural drought risk (SPEI)	
		Potential soil moisture deficit	
		Potential evapotranspiration (PET)	


Climate	Hazard indicator	Derived	
	Temperature	Heat-stress days (maximum temperature, days over 30C)	✓
		Met Éireann Yellow Warning days - low temperature/ice	✓
		Met Éireann Orange Warning days - low temperature/ice	✓
		Met Éireann Red Warning days - low temperature/ice	✓
		Variability in temperature	
		Met Éireann Yellow Warning days - high temperatures	✓
		Met Éireann Orange Warning days - high temperatures	✓
		Met Éireann Red Warning days - high temperatures	✓
		Summer days	
		Heatwave index	✓
		Heating degree days	
		Met Éireann Drought - dry spells	
		Cooling degree days	
		Tropical nights	
		Growing degree days	✓
		Shade temperatures	
	Shade temperatures		
	Water	Sea level rise	
		Flood risk	
	Wind	Gust wind speed	

Table 2. List of climate categories and hazard indicators identified by the sectors

Finally, participants identified near future (2021-2050) climate projections as the most useful time periods, although all timeframes were identified as useful to the sectors for adaptation planning in response to climate risk. Challenges identified relating to climate adaptation were:

- 1) Obtaining data on climate impacts at an appropriate spatial resolution and a lack of accessible and reliable site-specific data.
- 2) Defining what climate projections mean for specific locations, communities and assets.
- 3) Selecting the appropriate scenario or adaptation strategy and an approach for understanding when risks will worsen.



9

**Climate
Risk**

The general concept of climate risk as outlined in the IPCC's 6th Assessment Report is shown in Fig. 17. This IPCC definition of risk is the potential for adverse consequences for human or ecological systems, recognising the diversity of values and objectives associated with such systems. In the context of climate change impacts, risks result from dynamic interactions between climate-related hazards with the exposure and vulnerability of the affected human, infrastructure or ecological system to the hazards. Hazards, exposure and vulnerability may each be subject to uncertainty in terms of magnitude and likelihood of occurrence, and each may change over time and space due to socio-economic changes and human decision-making (IPCC, 2021). Risks can arise from potential impacts of climate change, as well as human responses to climate change. Relevant adverse consequences include those on lives, livelihoods, health and well-being, economic, social and cultural assets and investments, infrastructure, ecosystems and species. Climate risk is thus represented as the interaction of hazard, vulnerability and exposure, and can be quantified using the following equation:

$$\text{Climate risk} = \text{Hazard} * \text{Vulnerability} * \text{Exposure} \quad \text{Eq.1}$$

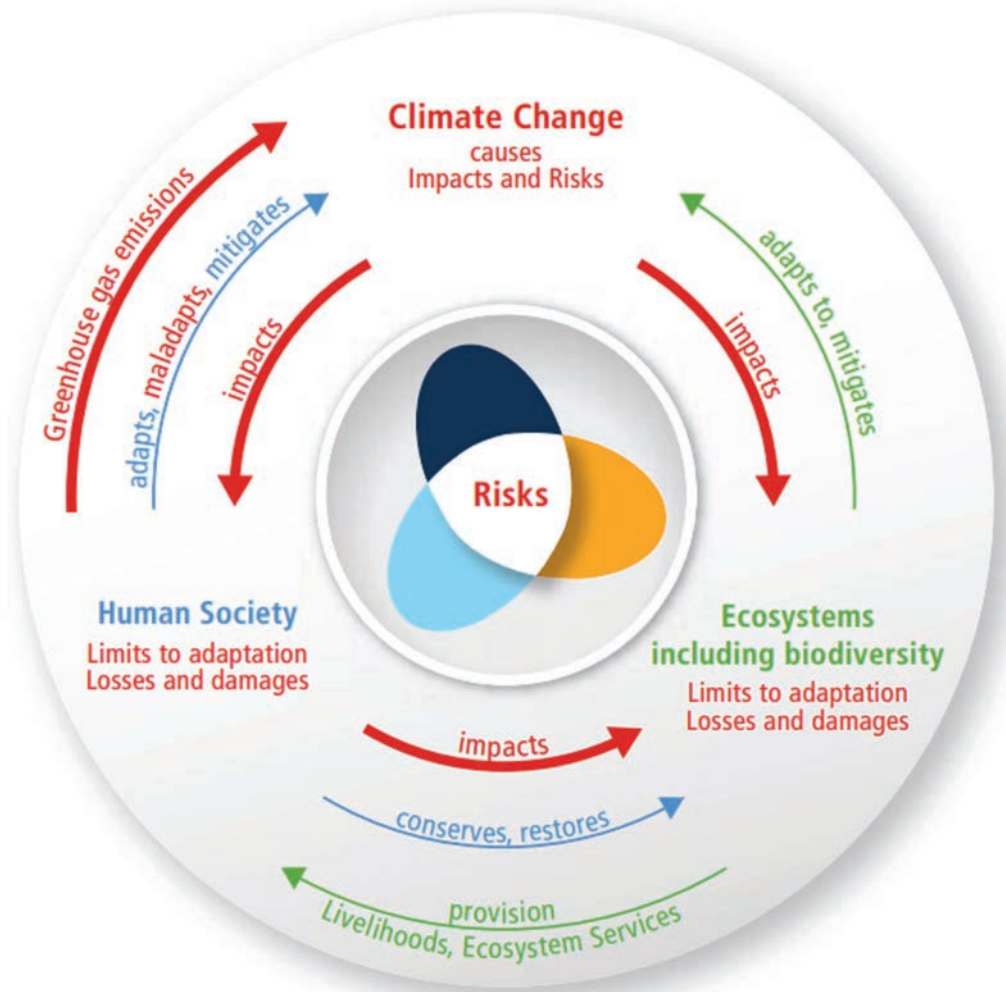
The definition of relevant concepts in the equation are listed as follows:

'Hazard': The potential occurrence of a natural or human-induced physical event or trend that may cause loss of life, injury or other health impacts, as well as damage and loss to property, infrastructure, livelihoods, service provision, ecosystems and environmental resources.

'Vulnerability': The propensity or predisposition to be adversely affected. Vulnerability encompasses a variety of concepts and elements including sensitivity or susceptibility to harm and lack of capacity to cope and adapt.

'Exposure': The presence of people, livelihoods, species or ecosystems; environmental functions, services and resources; infrastructure; or economic, social or cultural assets in places and settings that could be adversely affected. This component of risk is also referred to as 'consequences' in much of the traditional risk literature (Gallina et al., 2016; Zscheischler et al., 2018; Ryan et al., 2021).

The general framework proposed by the IPCC for climate risk assessment can be applied for semi-quantitative and fully-quantitative climate risk analysis across a range of sectors, as will be discussed in detail below and illustrated through case studies in the following sections of this report.



The risk propeller shows that risk emerges from the overlap of:

- Climate hazard(s)
 - Vulnerability
 - Exposure
- ...of human systems, ecosystems and their biodiversity

Figure 17. Concept of climate risks defined by IPCC (2021)



10

**GIS Semi-
Quantitative
Risk
Assessment
Framework**

The delivery of standardised climate projections in multiple formats that are easily integrated by multiple sectors into existing software fundamentally supports digital collaboration. This was supported by the January 2022 workshop, as most participants (45%) noted a preference for off-the-shelf desktop GIS data and software (ArcGIS, QGIS) for the delivery and utilisation of climate service products. To support climate-based, semi-quantitative risk assessments, we used the findings from Section 8 to build a 6-step GIS Semi-Quantitative Risk Assessment Framework (Fig. 18).

- Step 1 identifies and generates hazard indicators from the climate projections generated in Part A
- Step 2 identifies potential geospatial exposure and vulnerability metrics
- Step 3 builds the analytical grid that the risk analysis is undertaken at
- Step 4 aggregates the hazard, exposure and vulnerability data to this grid
- Step 5 indexes the aggregated hazard, exposure and vulnerability values, and then calculates indicative multi-hazard risk
- Step 6 calculates risk across various climate scenarios and timescales to provide insight into geospatial risk distribution and hotspots

that may impact risk in the relevant sector that one is operating in. Examples were provided in Section 9, with hazards related to climate change impacts including drought and temperature extremes. Therefore, individuals aiming to quantify risk in their sectors should identify appropriate indicators that can represent relevant hazards. Risk can be single hazard or multi-hazard. These hazard indicators typically differ from the climate indices developed by Part A, as ours focus on sector-specific definitions of hazard.

Software was developed to automatically produce the following hazard indicators identified by the sectors in Section 8 and derived from the standardised projections provided by Part A of TRANSLATE: Met Éireann weather warnings for high temperature, low temperature and heavy precipitation, heatwave index, growing degree days, maximum temperatures of daily maximum temperatures, days over a threshold of 30 degrees Celsius and hot spell frequency. The 14 hazard indicators generated for current and future projections (for all time-periods and RCP scenarios) as part of TRANSLATE are available. Examples are shown in Fig. 19. This is in addition to the WMO-standard ETCCDI indices produced by Part A.

Other hazard indicators or climate indices were produced in response to engagement with the biodiversity sector, and in particular the ECHOES project, for which frost days, precipitation days (<0.5mm and <0.05mm), total precipitation and temperature days (<5°C) were generated (Kenobi et al., 2023, <https://echoesproj.eu/>). This latter case study demonstrates the utility of the automated process, as different thresholds to test different sector-specific requirements can be used. End-users in each sector can thus specify their own thresholds and quickly generate their own hazard indicators or climate indices.

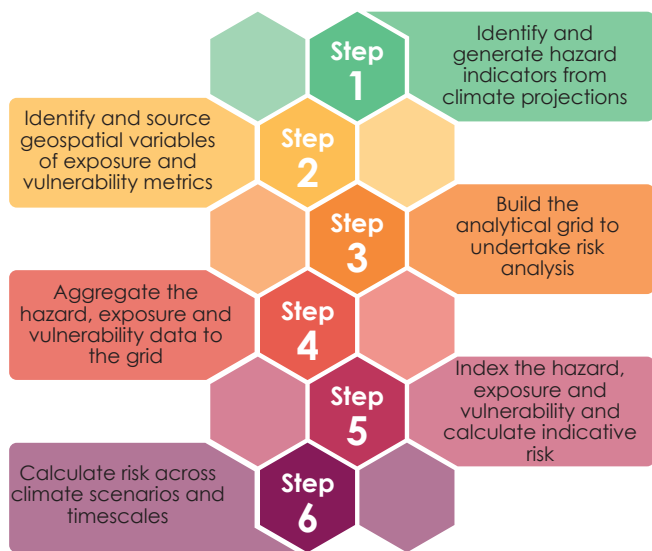


Figure 18. Framework of GIS decision support risk analysis

Step 1 – Identify and generate hazard indicators from climate projections

The first step is to identify potential climate hazards

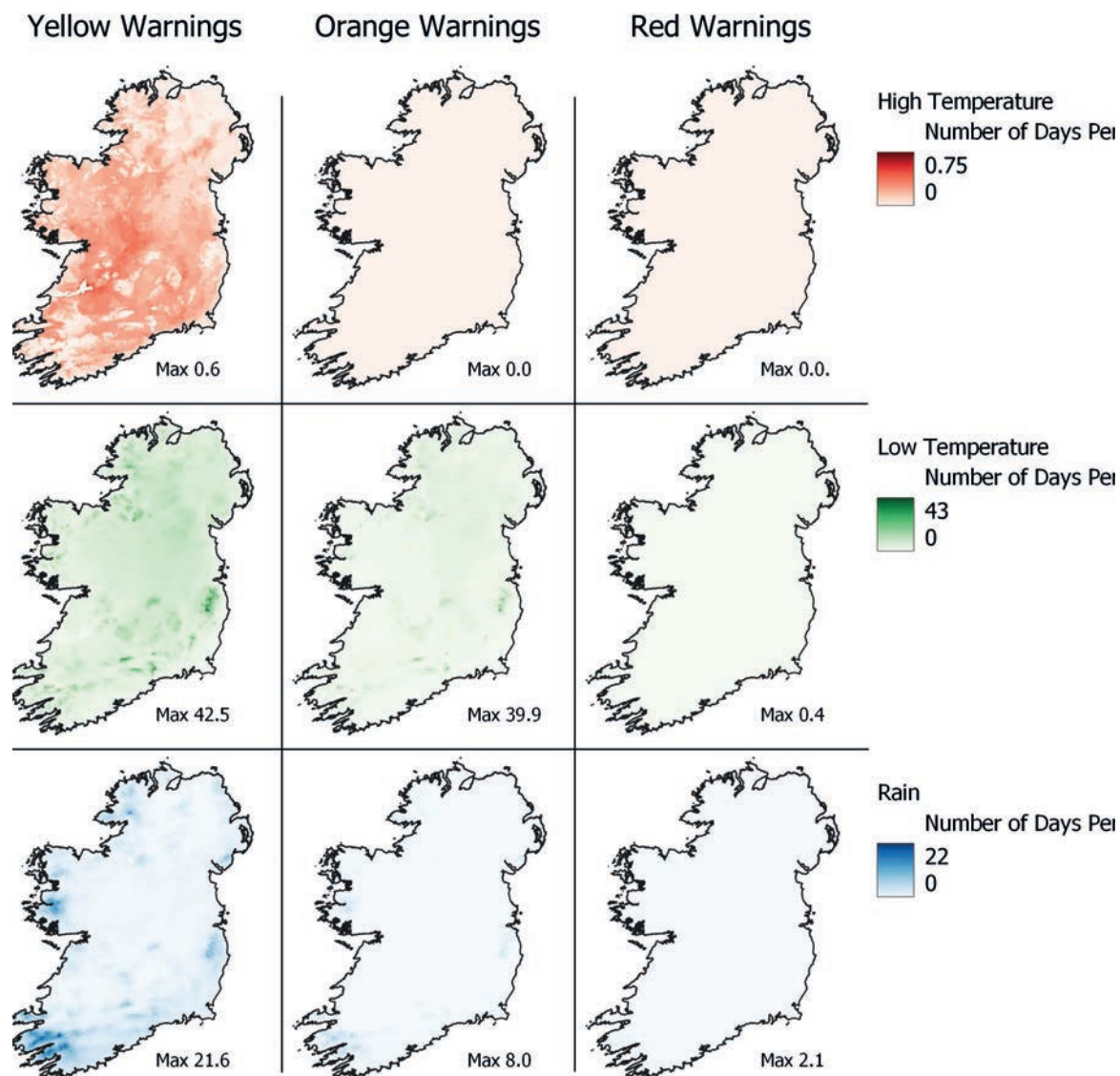


Figure 19. Number of weather warnings for high temperature, low temperature and precipitation from the historical observations (1976-2005)

Step 2 – Gather spatial data for exposure and vulnerability metrics

The second step is to identify and source geospatial variables for exposure and vulnerability metrics in the relevant sector. Again, examples were provided in Sections 8 and 9, with exposure and vulnerability related to climate change impacts including population density, deprivation and sectoral infrastructure. Therefore, individuals

aiming to quantify risk in their sectors should identify appropriate metrics that can represent exposure and vulnerability. Several national geospatial repositories exist, including the EPA Geoportal (<https://gis.epa.ie/>), the Central Statistics Office (CSO and <https://data.gov.ie/>) and Tailte Éireann, (data available through the National Mapping Agreement), where GIS data can be downloaded and integrated into the GIS software of choice. Similarly, many sectors

may have their own spatial data in the form of shapefiles, rasters and/or geopackages that are not in the public domain but can be utilised.

We assembled a database of spatial data sources that was generated within the broad themes of hazard, exposure and vulnerability. This included assets, background and supporting delineations (e.g., administration boundaries), the environment, additional hazards and socio-economic vulnerability.

Step 3 – Generate analytical grid to undertake risk assessment

The third step is to build the analytical grid on which to undertake the semi-quantitative risk assessment. Given the nature of spatial data models, GIS data is stored predominantly in two formats, vector and raster. Vector data uses a discrete object view of the world, such as points, lines and polygons (areas), while raster data uses a continuous representation where every grid in a region has a value. Climate data, and subsequently hazard indicators, are generated on a continuous surface, while spatial data representing exposure and vulnerability metrics are often captured on a discrete level (e.g., train station, road network, lake body). Therefore, to incorporate hazard, exposure and vulnerability into a single framework, the risk analysis must be undertaken at an aggregated scale.

This aggregated scale could be a square grid that has commonly been used in GIS research to date, or it could be undertaken on administrative boundaries such as electoral divisions. We propose the use of hexagons that have begun to become the new de facto standard in recent years, in part due to their low perimeter-to-area ratio that reduces sampling bias, their ability to represent hierarchical structures (i.e. cells can be subdivided into smaller hexagons) and their improved visualisation qualities that do not distract end-users as much as regular square grids (Holloway, 2023). The H3 grid (Sahr et al., 2003) is an open-source concept that covers the whole globe at multiple spatial scales. The project team developed software to automatically produce the hexagonal grid at multiple spatial scales and our subsequent work utilises such a grid, but users can utilise their own grid structure.

Step 4 – Aggregate hazard, exposure and vulnerability data to the analytical grid

Once the grid structure has been decided upon, we must aggregate the data to the grid units. There are multiple methods of achieving what is essentially a resampling, spatial join or interpolation exercise. A lot has been written on these topics, but we identify several important issues that arise for a GIS semi-quantitative risk assessment. These issues are 1) that data exists in diverse formats and types, making standardisation difficult, and 2) that processing data to the H3 grid at various grid scales may cause data distortion. Fig. 20 illustrates the issue of alignment between air temperature and the hexagonal grid. Our recommendations include:

1. It is best practice to choose grid scales as close as possible to the scale of the data that is to be gridded. This results in less data smoothing or data loss during the aggregation process.
2. The nearest neighbour approach is an effective method used at scales close to the scale of data being used and when categorical data is desired.
3. Statistical summaries should be applied to answer specific questions, but also when grid scales are coarser than the data scale.
4. Zonal statistics is the most effective method of aggregating hazard indicators (or other rasters) to the analytical grid. It allows the user to incorporate the values of several pixels within a raster layer with the help of a polygonal vector layer which defines the zones for calculations. This method ensures the highest retention of values as every pixel is considered in the calculation of the zonal statistics.

It is important to ensure consistency between methods. For example, if one uses a spatial join method for roads (as shown in Fig. 21), they should subsequently use a spatial join function for all subsequent vector layers of exposure and vulnerability. Software and user guides have been created to provide step-by-step instructions to undertake this process in both Python and QGIS

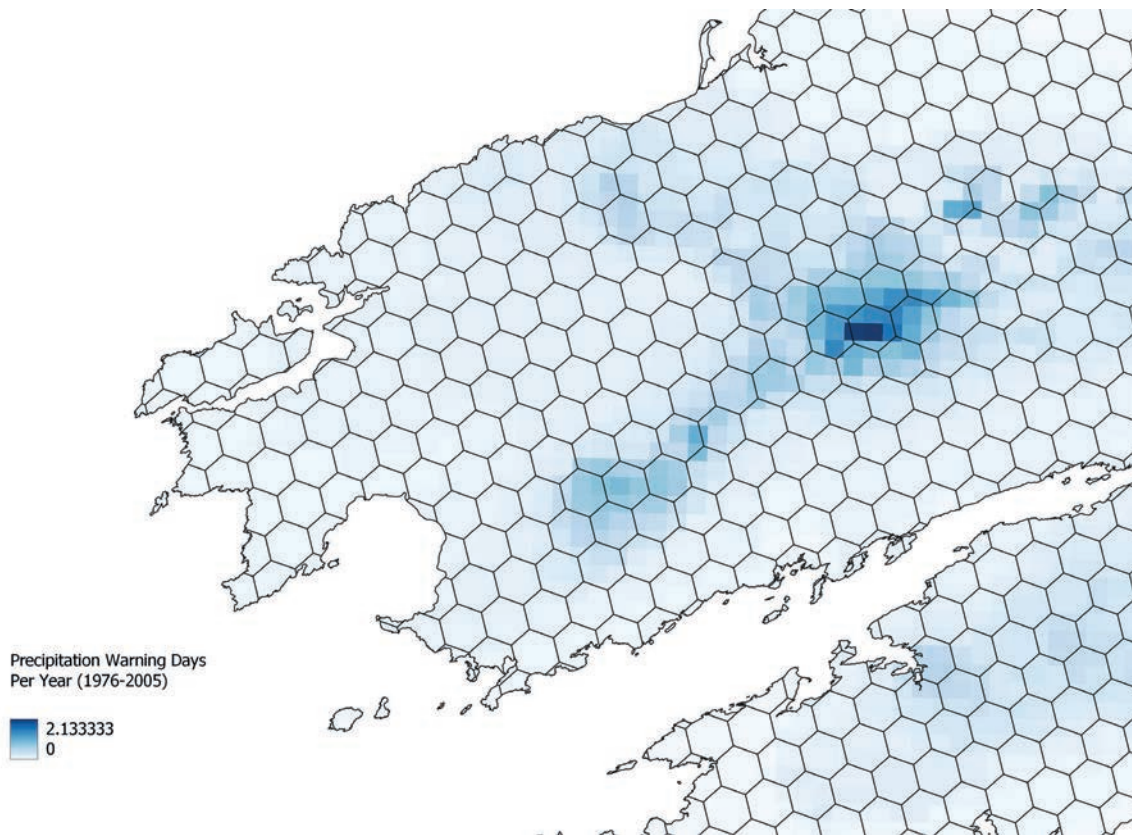


Figure 20. Vector layer (zones-hexagon grid cells) overlaying a raster layer (pixels). In this case, the raster layer represents average number of yellow warning precipitation days 1976-2005.

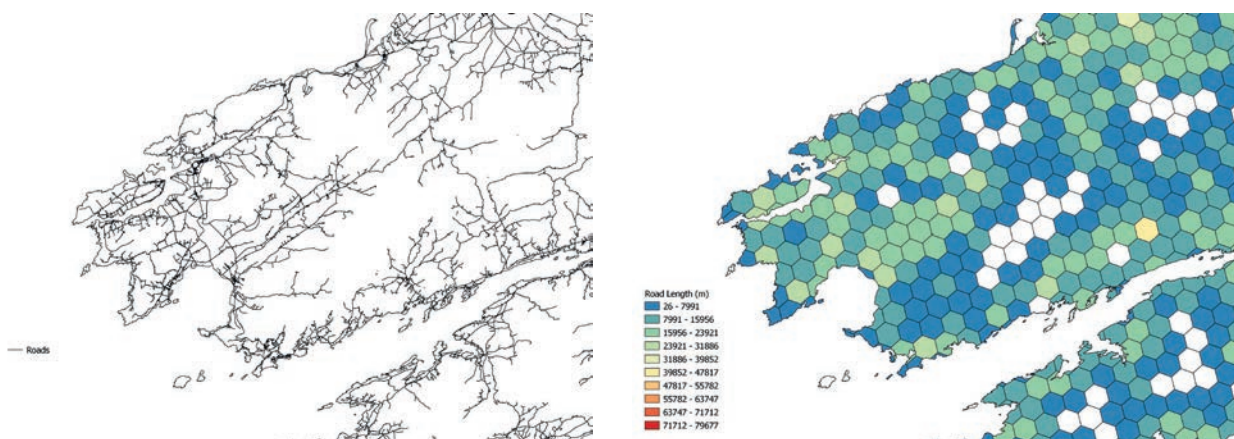


Figure 21. Example of a vector layer of lines representing roads in County Cork in the left panel, and the total length of roads in the hexagonal grids that overlay it, captured using a spatial join function. Road data is the Ordnance Survey Ireland (OSi) National 250k Map of Ireland road network (OSi 2016) licensed under Creative Commons Attribution 4.0

Step 5 – Index the hazard, exposure and vulnerability values and calculate risk

To represent the semi-quantitative risk on a geospatial level, a risk index must be calculated for each hexagonal grid unit. There are two predominant methods in GIS risk assessment. The first is to threshold the values based on subjective decisions, while the second is to scale the existing values from 0-1. Where clear delineations of an indicator or metric are observed in the sectors, or where multiple types of infrastructure etc. are considered in a single analysis, a subjective threshold may be suitable, but justifications would be needed as outputs could theoretically change based on user decisions on these thresholds. Where possible, we propose the index method that scales values between 0-1, following the method previously developed by project team members and published in Hawchar et al. (2020). This approach is in line with the IPCC climate risk approach, which would standardise climate risk in Ireland to a global approach. It is noted that, in some cases, such as the case study presented in Section 11, it will be necessary to specify a baseline vulnerability, exposure or hazard value (i.e. value > 0) to avoid illogical zero risk values. This is discussed further in the context of the Section 11 case study. Normalisation follows Eq. 2:

$$i = (x - x_{min}) / (x_{max} - x_{min}) \quad \text{Eq.2}$$

where i can represent normalised Hazard (H), Exposure (E), or Vulnerability (V).

To calculate risk, we apply the following formula:

$$\text{Risk} = \sum H * E * V \quad \text{Eq.3}$$

where \sum is the sum of total risk across each of the hazards. In other words, H*E*V is calculated separately for each of the three hazards, then summed to generate multi-hazard risk. Each grid then has a risk value that can be used to identify potential risk hotspots, which can be subsequently normalised further to capture the relative risk associated with the grid. For visualisation purposes, we have divided the indicative risk value by the maximum value across all future projections to create a scale of 0-1 for readability. User guides

have been created to provide step-by-step instructions to undertake this process in QGIS.

Step 6 – Calculate risk across climate scenarios and time scales

One of the most pertinent challenges for sectors identified in Section 8 is how to select the appropriate scenario or adaptation strategy, and how to understand when risks will worsen. The GIS Semi-Quantitative Risk Assessment Framework provides the opportunity to explore such challenges identified by the sectors. Steps 1-5 can be repeated with different climate projections at different timescales and RCP scenarios. User guides have been created to provide step-by-step instructions to undertake this process in QGIS. It is noted that while this semi-quantitative approach is useful in assessing potential risk hotspots and areas of concern, it is not generally suitable for informing effective climate adaptation action. Such actions tend to require investment, which can be considerable and cumulative over time. It is thus vital that, prior to such decisions, a fully-quantitative risk-based decision support approach is used to avoid making inappropriate adaptation decisions, or no decisions at all. This is discussed in detail in Section 12 of this report.



11

Geo-Spatial Semi-Quantitative Risk Case Study

The semi-quantitative risk analysis framework is demonstrated through a case study examining the possible impacts of climate change on school closures and resulting missed education days. Through this case study, the research team engaged in various meetings with educators and decision-makers across primary, secondary and tertiary education institutions to ascertain decisions that are made with regards to school closures.

Risk: Missed education days due to climate change

Rationale: School closures can impact education in a variety of ways. Engzell et al. (2021) found that an 8-week closure in Netherlands for Covid-19 resulted in a 3-percentile loss of education, while a growing body of research suggests that children who miss school because of a natural hazard may experience new or exacerbated academic difficulties (Esnard et al., 2018). With projected climate change potentially increasing climate hazards, quantifying the risk associated with missed education days is an important consideration. For the less-educated households, these losses grew to 60% for the same time period (Engzell et al., 2021), which suggests a need to study the vulnerable, with other studies (Burzynska and Contreras, 2020) corroborating socioeconomic deprivation as a disproportionate factor in long-term missed education. Given the implications of long-term (or even short-term) school closures on the educational attainment and well-being of children, as well as the increased possibility of non-completion rates increasing as students are forced to learn remotely, identifying high-risk areas that may need to investigate climate adaptation measures in the future is important (Holloway, 2023). Considering the above, and the public awareness of school closure impacts across government sectors and all levels of society, the examination of climate change impacts on lost education days offers an engaging and relatively simplistic case study for illustration of the semi-quantitative risk assessment framework developed as part of TRANSLATE.



Step 1 – Identify and generate hazard indicators from climate projections

Schools are closed by the state in Ireland in the event of extreme weather events, specifically Red Weather Warnings as issued by Met Éireann. For low temperature, this represents air minima of less than -10°C for three consecutive nights; for high temperature, this represents a maxima in excess of 30°C and a minima of 20°C for five days and nights; and for heavy precipitation, this represents greater than 80mm in 24 hours. Each hazard on its own may generate a school closure but,

based on the importance of extreme weather warning thresholds identified by the sectors during our co-creation workshops, we have opted to consider the thresholds for low temperature, high temperature and heavy precipitation in this case study (red warnings in Figs. 22-24). By incorporating all three hazards, we are capturing multi-hazard risk. Finally, as schools are closed during the summer, we extracted only the weather warnings from September to May, excluding June, July and August as these events should not impact school closures.

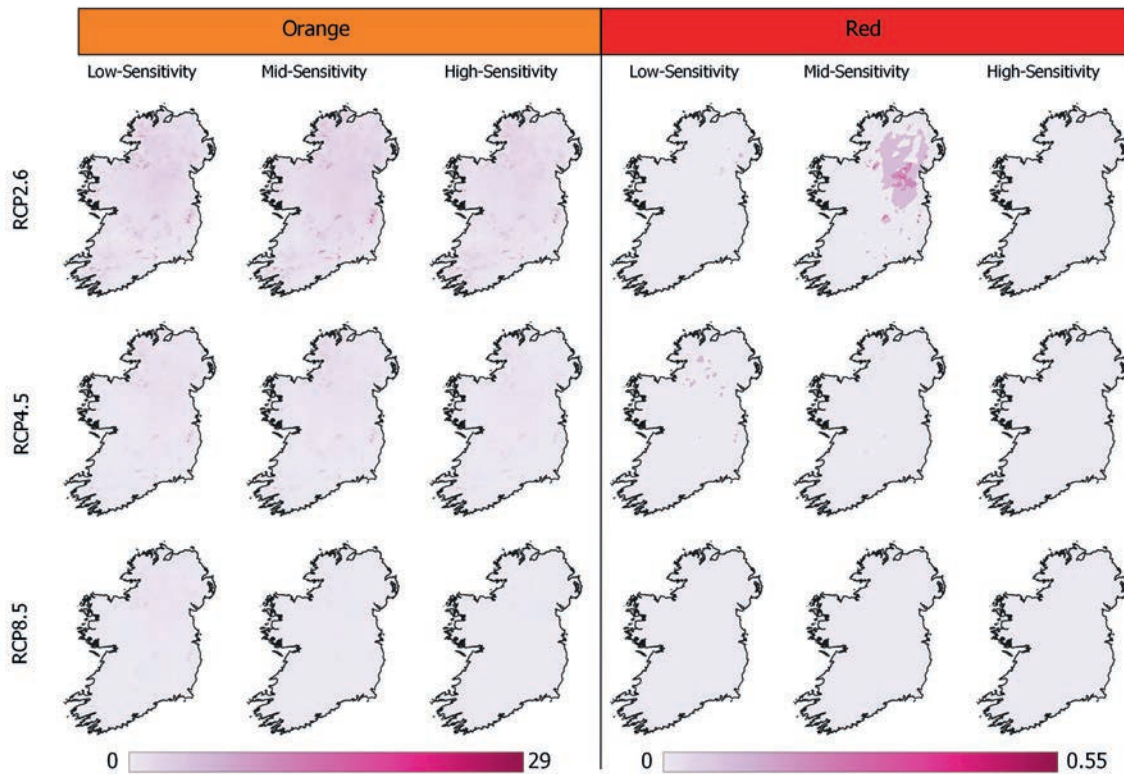


Figure 22. Projected orange and red weather warnings for low temperature across three RCP scenarios and three ensemble sensitivities

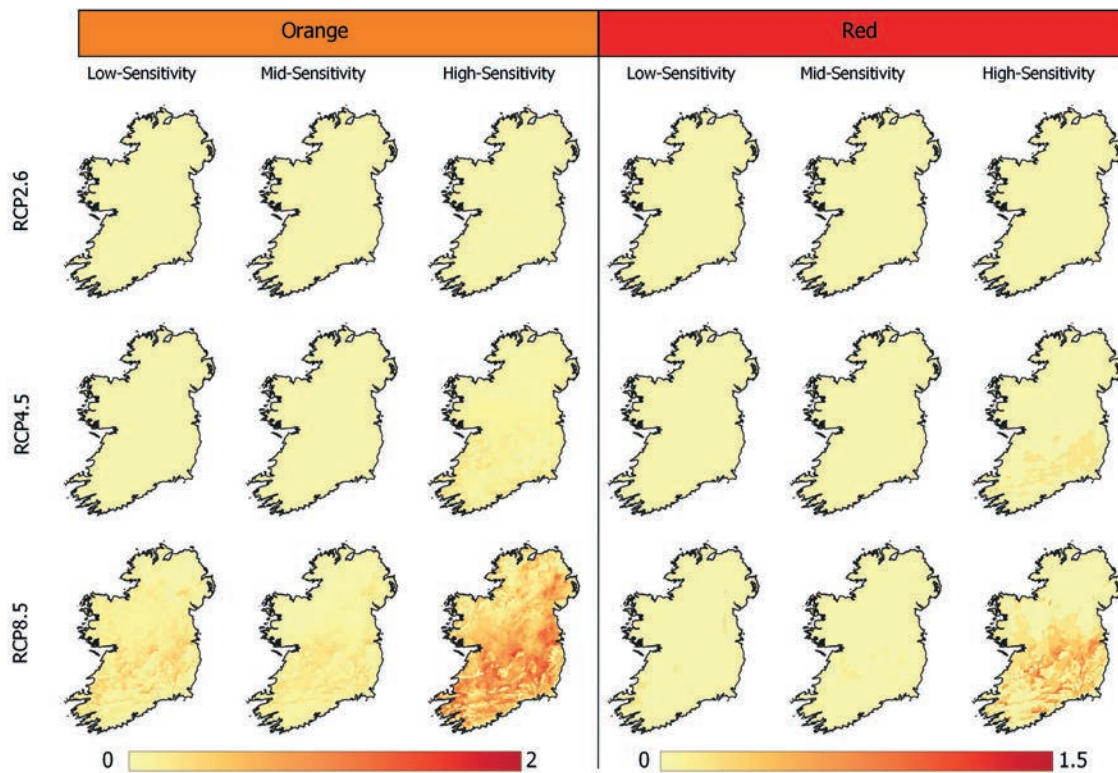


Figure 23. Projected orange and red weather warnings for high temperature across three RCP scenarios and three ensemble sensitivities

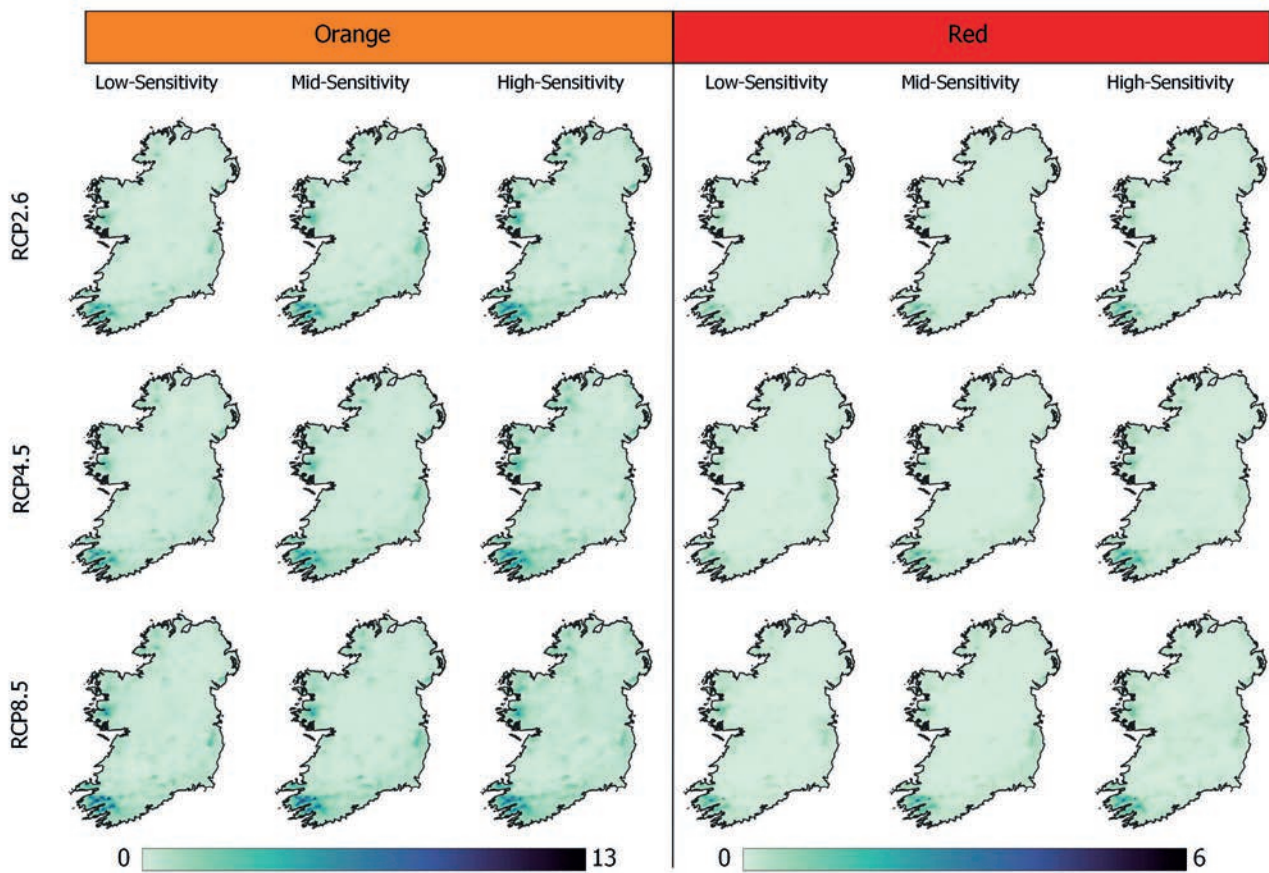


Figure 24. Projected orange and red weather warnings for daily precipitation across three RCP scenarios and three ensemble sensitivities

Step 2 – Gather spatial data for exposure and vulnerability metrics

Exposure - Total enrolment of a school captures the overall student reach, which becomes important as the scale of the aggregated grid changes. High enrolment has been used in other studies (Senapati, 2022) to reflect exposure due to the number of students who may be exposed to climate hazards and their spatial variability in response to their vulnerability to missed education. Post-primary school enrolment data is available from the All-Island Research Observatory (AIRO 2016) via data.gov.ie (Fig. 25).

Vulnerability - Deprivation is strongly linked to a disproportionate impact of missed education (Engzell et al., 2021; Burzynska and Contreras, 2020). The POBAL database (Haase and Pratschke, 2017) has deprivation values for small area polygons (SAPs) ranging from extremely disadvantaged to very disadvantaged, disadvantaged, marginally below average,

marginally above average, affluent, very affluent and extremely affluent. This was sourced from POBAL and represented our first vulnerability metric (Fig. 25). The percentage of broadband connectivity in an area is also an indicator of vulnerability (Fig. 25); if a large proportion of houses in the area do not have broadband, then this could be indicative of a connectivity issue and represent a socioeconomic disadvantage (Grubestic 2006). There is a growing body of research showing that students and schools across geographies do not have uniform access to remote learning tools, such as mobile devices and the Internet (Tomczyk et al., 2019; Johansen et al., 2021). By using pre-existing disparities such as broadband access that is not incorporated in deprivation, we may identify vulnerabilities that may exacerbate the impacts of school closures on missed educational days. The number of households in a small area polygon (SAP) and the total number of households in a SAP are available from the CSO (2018).

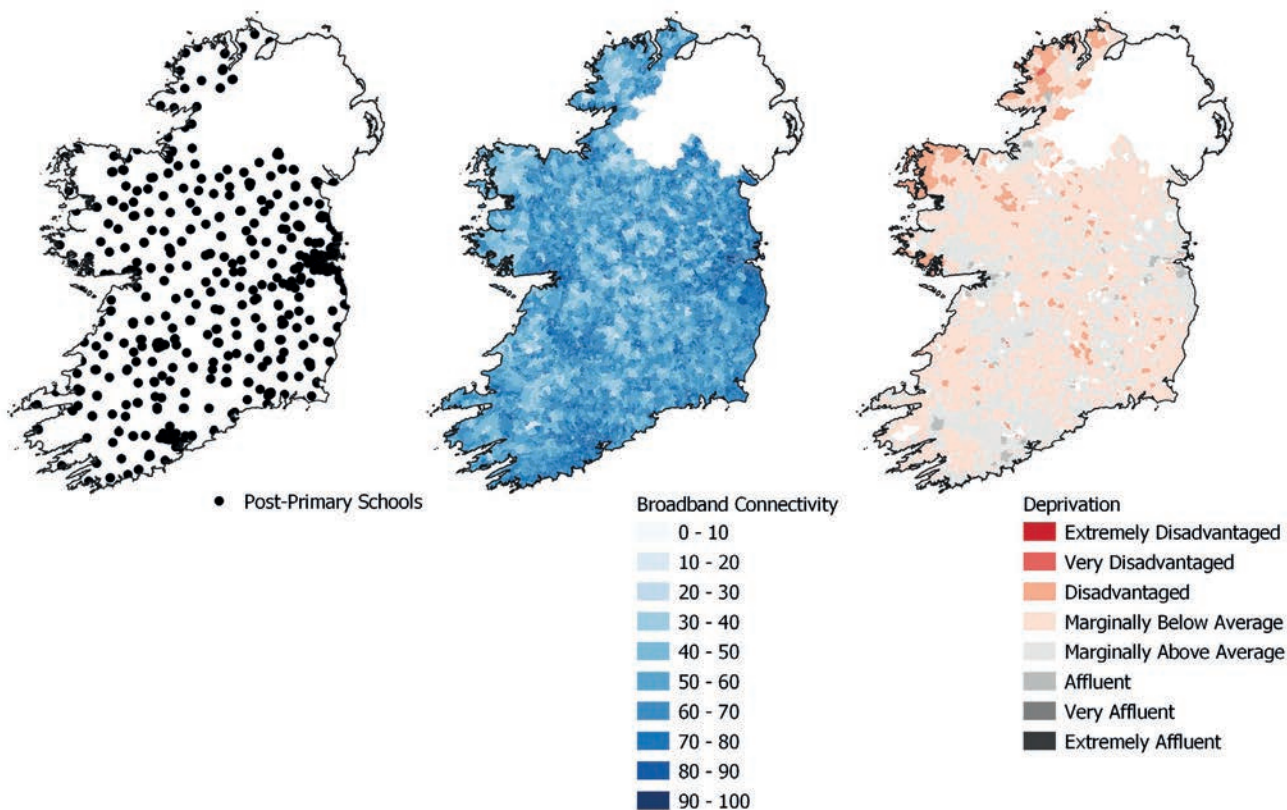


Figure 25. Spatial data for post-primary schools (AIRO 2016), broadband connectivity (CSO 2018) and POBAL deprivation (Haase and Pratschke, 2017)

Step 3 – Generate analytical grid to undertake risk assessment

For illustrative purposes, we opted to use the H5 scale of hexagonal grid as shown in Fig. 26, which is the coarsest representation. This was simply to support visualisation in this case study and support quick processing, if users are following instructions to replicate this analysis.

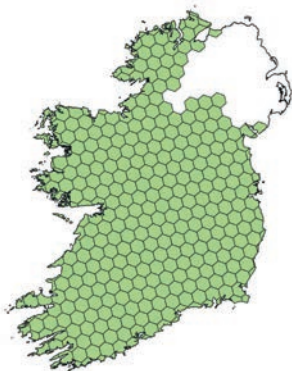


Figure 26. Example of Scale 5 in the hexagonal grid for the Republic of Ireland

Step 4 – Aggregate hazard, exposure and vulnerability data to the analytical grid

We followed our suggested protocol and used zonal statistics in QGIS to aggregate the hazard indicators to the hexagonal grid (see Fig. 27). Here, the maximum value was used, which represents the maximum number of days of extreme weather events within that grid unit. Maximum was chosen as it represents the highest value within the spatial unit and, subsequently, the highest representative hazard.

We implemented spatial joins to aggregate the vector data representing exposure and vulnerability to the hexagonal grid. For exposure, the summary statistic represented the 'sum' of enrolment in that grid as it captured the total number of students that are enrolled within the spatial unit. For deprivation and percentage of broadband, the minimum value was chosen as the summary statistic, as the lowest value would represent the highest vulnerability.

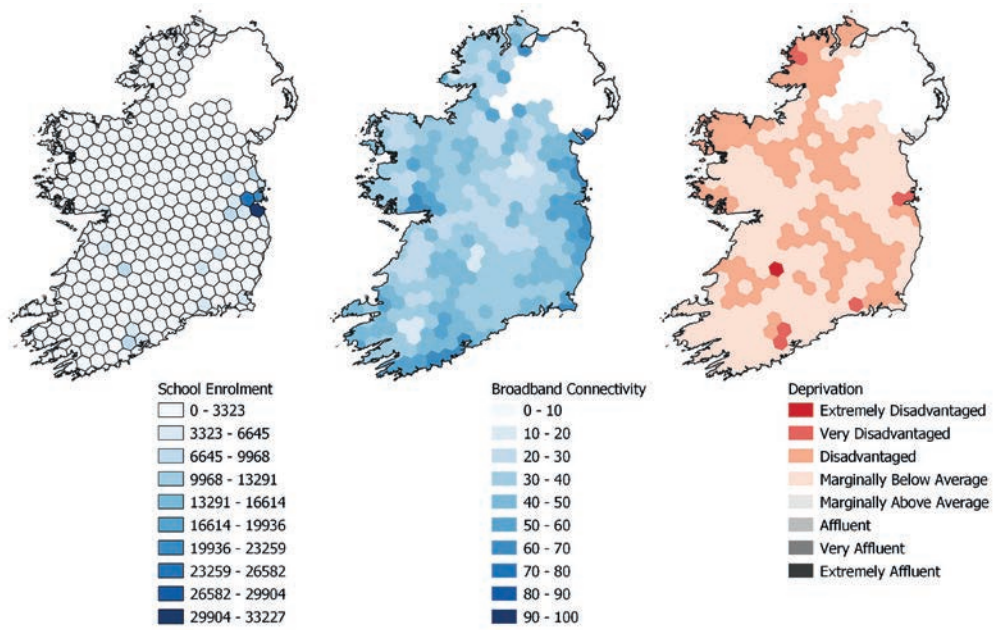


Figure 27. Aggregate hazard, exposure and vulnerability data to the analytical grid

Step 5 – Index the hazard, exposure and vulnerability values and calculate risk

The hazard indicators and exposure metric were normalised between 0-1 at the H5 grid level using the field calculator in QGIS. The two vulnerability metrics were inverted as low values represented higher vulnerability. Vulnerability was calculated as the sum of baseline vulnerability (0.333), normalised broadband (0- 0.333) and normalised deprivation (0- 0.333). The decision to provide a baseline vulnerability in this case study relates to the fact that 0 for hazard and exposure

represents recorded zero hazards recorded and zero exposure (i.e. no schools in grid square). However, vulnerability in this case can still exist, even for the least deprived areas and areas with full broadband connectivity. Therefore, to prevent the risk equation providing an inappropriate zero risk, we incorporated a baseline vulnerability of 0.333. Fig. 28 visualises precipitation hazard, exposure and vulnerability at the H5 level.

These values were then utilised in Eq. 3, to identify the current risk of missed education days based on extreme weather conditions that could represent school closures (Fig. 29).

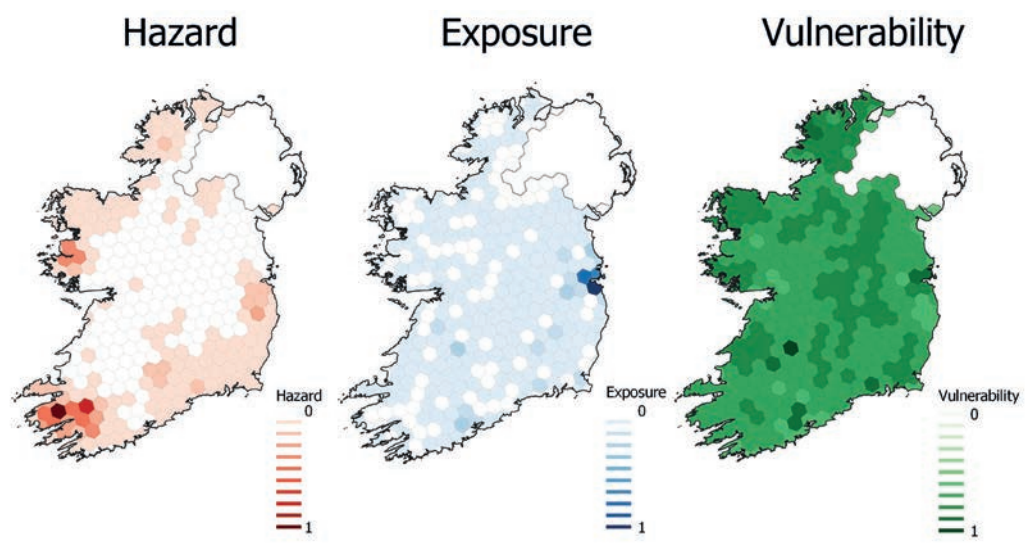


Figure 28. Indexed values of hazard, exposure and vulnerability between 0-1

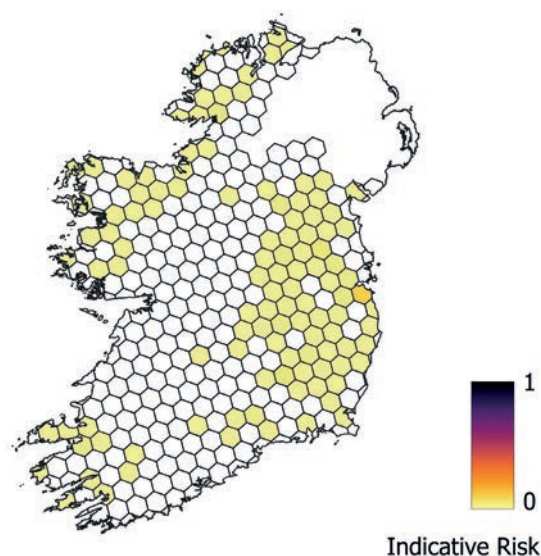


Figure 29. Indicative risk of missed education days based on current extreme weather events

Step 6 – Calculate risk across climate scenarios and time scales

To compare current risk with future risk, the GIS Semi-Quantitative Risk Assessment was repeated using the three RCP scenarios and three ensemble sensitivities to the time period 2071-2100. To simplify the analysis and the message, we kept exposure and vulnerability the same, highlighting the impact of climate change on the calculated risk values. This resulted in a risk output shown in Fig. 30. It is clear from comparing Fig. 29 and Fig. 30 that the areas of highest risk for missed education are increasing in area. In particular, the area that currently had low or no risk is increasing

substantially, across all scenarios, in the midlands, while the indicative risk is increasing around city boundaries – in particular, Cork, Waterford and Limerick, with the greatest increase in Dublin.

Finally, to compare current and future risk, we calculated the number of cells that fell within the zero (no risk), 0-0.1 and 0.1+ categories (Fig. 31). It can be seen that risk of missed education days due to extreme weather hazards are projected to increase under all scenarios, with the exception of RCP26 mid-ensemble. This is due to less extreme cold events at this RCP scenario and no extreme heat events either.

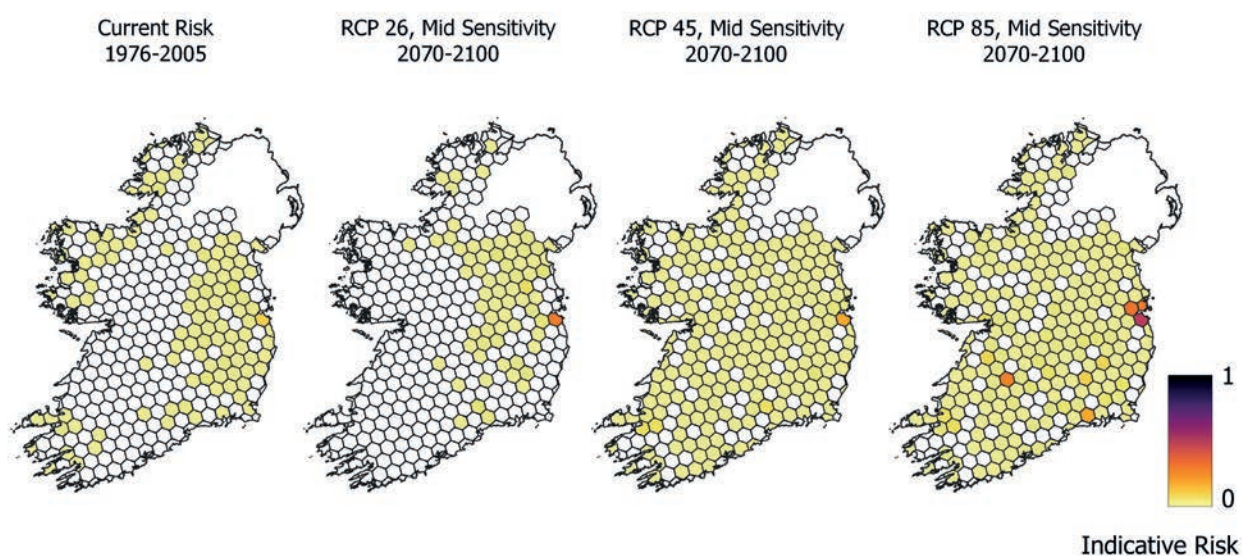


Figure 30. Indicative risk of missed education days based on future projections for extreme weather events using the RCP scenarios and mid-sensitivity ensemble

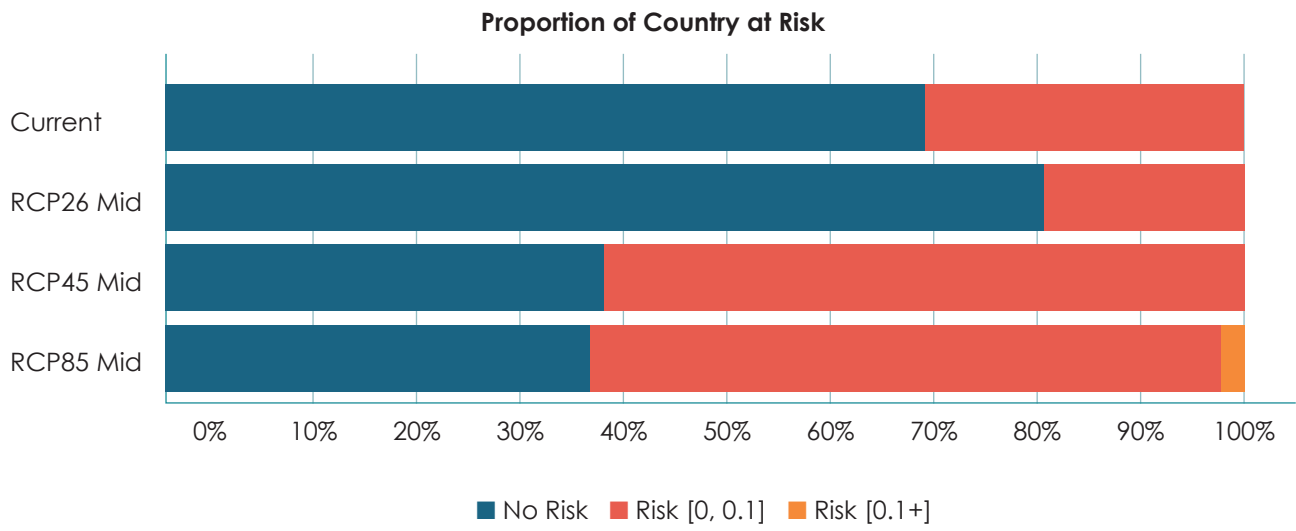


Figure 31. Proportion of study area classified No Risk [0], Risk [0,0.1] and Risk [0.1+]



12

**Fully-Quantitative
Risk-Based
Decision
Support**

12.1 Step-by-step guide

The fully-quantitative risk-based decision support step-by-step guide has been developed to help sectors, infrastructure owners and operators and other interested parties to use detailed quantitative risk analysis to help inform appropriate adaptation action. The initial steps in the framework can be used to quantify predicted climate change impacts and climate change risk, while the latter steps facilitate analysis of climate adaptation effectiveness and cost-benefit. The framework thus helps avoid common adaptation pitfalls such as opportunity costs, worst-case-thinking and inaction. It is consistent with the general framework for risk quantification proposed by IPCC, discussed in Section 9, but also extends to include consideration of climate adaptation effectiveness and cost-benefit assessment (Ryan et al., 2021). Fig. 32 presents the framework split into four key components of analysis, with typical analysis steps for various sectors and examples of data required provided for each step. It is noted that different steps present different challenges, depending on the sector type and hazard being considered.

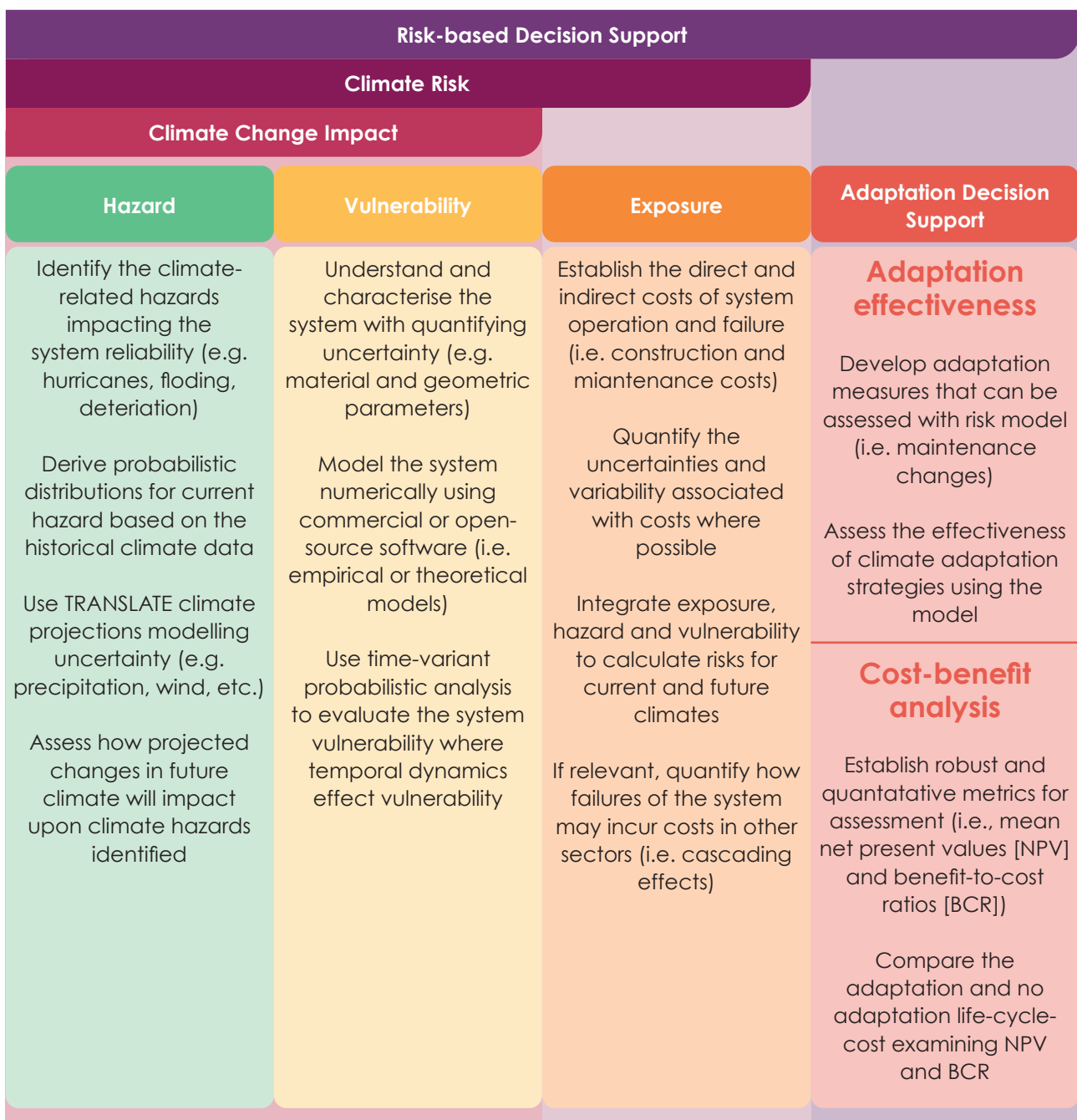


Figure 32. Framework for the fully-quantitative risk-based decision support step-by-step guide

Step 1: Modelling climate hazard

A hazard is an event with the potential to cause harm (Battles and Lilford, 2003). According to IPCC, climate hazards refers to the potential occurrence of climate-related physical events or trends that may cause damage and loss of life, injury or other health impacts, as well as damage and loss to property, infrastructure, livelihoods, service provision, ecosystems and environmental resources (IPCC, 2021). If the climate hazard being considered arises from an extreme weather event, hazard likelihood, or probability, can be associated with the frequency and magnitude of the given hazard, or with the frequency of exceedance of a given socio-economic criterion (e.g. a threshold) (Jones, 2001). Examples of climate hazards are tropical cyclones, droughts, floods, extreme wind events or conditions leading to an outbreak of disease-causing organisms (plant, animal or human), but can also be changes in annual average temperature or changes in growing season. Consideration of the hazard component is often the first step in quantitative climate risk analysis. Initially, key hazards are selected based on past experience of extreme events, stakeholder input and relevant literature. Having identified the climate hazard/hazards of concern, it is then necessary to model the extent of the existing hazard, and how the hazard will change over time due to climate change. The TRANSLATE Part A outputs can provide information on the projected change in many hazards (temperature and rainfall from TRANSLATE 1, with more to follow under TRANSLATE 2). Importantly, the large climate ensembles generated as part of TRANSLATE under low, medium and high sensitivity (see section 3.4, Fig. 1) can be used to develop probabilistic parameters for projected climate change. This allows the considerable uncertainty associated with climate change projections to be incorporated into the analysis. This is illustrated in practice in Section 12.2.3 of this report.

(1) Current hazard

In order to describe the existing climate hazard, it is necessary to select the baseline period, e.g. 1976-2005. Sources of baseline data include a wide variety of observed data, reanalysis data (a combination of observed and model-simulated data), control runs of Global Climate Model simulations and time series generated by stochastic weather generators (Pörtner et al., 2022). Some of these observed data forms for the baseline period can be downloaded from the Met Éireann official website (<https://www.met.ie/climate/available-data>). It is also possible to contact Met Éireann to obtain undisclosed meteorological records that may not be available online, i.e. meteorological records for extreme rainfall events with short durations. The types and resolutions of baseline climatological data can range from globally-gridded baseline data sets at a monthly timescale to single-site data at a daily or hourly timescale (Pörtner et al., 2022). Based on the collected climate data, the likelihood of occurrence for a fixed level of hazard, such as a peak wind speed of 10 m/s, rainfall depth of 10mm or extreme temperature threshold of 35°C, can be assessed using a statistical analysis tool. For extreme events, the user may wish to represent the climate hazard probabilistically using a specific occurrence frequency, i.e. probability distribution of maximum annual wind speed. For other hazards, such as the annual average temperature used for a material deterioration model, this parameter can be represented by a probability distribution reflecting how this variable changes from one year to the next based on the historical data for the baseline period. Regardless of the hazard, for quantitative risk assessment, modelling hazards probabilistically is a key consideration. The most common tool for this modelling is Monte Carlo Simulation. This method is explained briefly in the box below and is illustrated in the case study herein in Section 12.2.4.

Baseline period

Any climate scenario must adopt a reference baseline period from which to calculate changes in climate. This baseline data set serves to characterise the sensitivity of the exposure unit to present-day climate and usually serves as the base on which data sets that represent climate change are constructed. Among the possible criteria for selecting the baseline period, it should be representative of the present-day or recent average climate in the study region and of a sufficient duration to encompass a range of climatic variations, including several significant weather anomalies (e.g., severe droughts or cool seasons). A popular climatological baseline period is a 30-year 'normal' period, as defined by the WMO. The current WMO normal period is 1961-1990, which provides a standard reference for many impact studies (Pörtner et al., 2022).



Monte Carlo Simulation

Monte Carlo Simulation is a mathematical technique that simulates the range of possible outcomes for an uncertain event. Monte Carlo Simulations use a probability distribution for any variable that has inherent uncertainty. They recalculate the results many times, using a different set of random numbers generated from the variables' probability distributions. This process generates many probable outcomes, which become more accurate as the number of inputs grows (Harrison, 2010; Mooney, 1997). In general, this course of action is realised by commercial or open-sourced computer software, e.g., MATLAB, Python, Visual Basic, etc.



(2) Future hazard

As outlined in Part A of this report, Ireland's climate is changing and will continue to change, resulting in evolution of climate hazards over time, with the frequency and severity of many hazards increasing (e.g., Fig. 11 and Fig. 14). These changes have the potential to impact upon the operation of our critical infrastructure (Ryan and Stewart, 2019; Hawchar et al., 2020), our ecosystem (Malhi et al., 2020) and environment (Henson et al., 2017) and human health (McMichael et al., 2006). It is thus vital that we model the impact of climate change on key climate hazards.

O'Brien and Nolan (2023) have highlighted the complex nature of climate change, and the subsequent need for a robust and standardised climate projections dataset for Ireland. As outlined in Part A of this report, this need has been addressed in part through the TRANSLATE work, which develops standardised climate projections across a range of IPCC climate scenarios. These climate scenarios account for future CO₂ forcing uncertainty by considering three future emission scenarios, namely RCP 2.6, RCP 4.5 and RCP 8.5. It is noted that RCP 4.5 and RCP 8.5 are the most utilised scenarios in the literature for quantitative

risk analysis studies and our recommended climate scenarios for quantitative risk analysis. It is noted, however, that TRANSLATE 2 will build upon the TRANSLATE 1 work through post-processed model simulations based on the latest downscaled CMIP6 data and shared socioeconomic pathways (SSPs) forcing scenarios (i.e. SSP1-1.9, SSP1-2.6, SSP2-4.5, SSP3-7.0, SSP5-8.5) (IPCC, 2021).

Having selected appropriate climate scenarios, it is also important to note that the complex nature of the climate system, climate models and human factors makes it difficult to determine exactly what the impacts of change will be for a given scenario at any given location and time (Schneider and Kuntz-Duriseti, 2002). As outlined in Part A, prediction uncertainty is primarily parametric, structural and intrinsic to the climate models and, unless properly considered, has the potential to impede effective climate action. As highlighted by Lindner et al. (2014), making a conscious effort to understand uncertainties leads to:

- more informed and robust decision-making
- and better identification and management of the potential risks.

Conversely, neglecting to consider uncertainties can:

- conceal risks
- undermine risk management efforts
- and increase the chances of maladaptation.

Quantitative risk-based climate change analysis facilitates the incorporation of this unavoidable uncertainty through probabilistic modelling, using techniques such as Monte Carlo Simulation. Such approaches allow the projected change in a given hazard, or climate parameter, to be modelled as a probability distribution, representing uncertainty and variability, rather than a point estimate (e.g., normal distribution with mean value = 6% and COV = 0.2 rather than just change = 6%). This is illustrated in the case study in Section 12.2.3, where a probabilistic distribution for projected change in extreme rainfall is developed under future scenarios of RCP 4.5 and RCP 8.5. At present, the TRANSLATE project can provide projected information for temperature and precipitation based on 27 simulation ensembles for RCP 4.5 and 35 ensembles for RCP 8.5. TRANSLATE 2 will facilitate the provision of data for extra climate variables (e.g., wind, humidity) over the next two years.

Step 2: Vulnerability analysis

Before commencing a quantitative vulnerability analysis for a given system, it is necessary to establish a high-level understanding of system operation and possible climate-related weaknesses/vulnerabilities, i.e. how the system operates and how might climate change affect this operation. Having established this understanding, a mathematical model of the system can be developed which incorporates one or a number of relevant climate variables. This model could be an empirical model, developed from collected data, or a theoretical model based, for instance, on the laws of physics and mathematical representations of physical systems. The case study presented in Section 12.2.4 is an example of a theoretical vulnerability model. As discussed, the climate variable or hazard should be modelled probabilistically; however, it is generally also important to model the system itself probabilistically, taking account

of the uncertainty and variability associated with long-term performance, i.e. material properties, geometric parameters, variations in asset resilience, variability of human characteristics, deterioration, etc. It is noted that this vulnerability modelling step is normally the most challenging of the quantitative risk analysis steps, as it requires mathematical representation of complex physical systems.

In practice, the most appropriate analysis tool is the numerical modelling by computational simulation using commercial or open-source software, with the selection of empirical or theoretical models dictating this to some extent. In general, the vulnerability modelling process has four essential steps:

- Define the modelling objective and develop a conceptual model based on the physical systems or network components
- Establish the numerical model (empirical or theoretical or combination of both) that is capable of representing the operation of the system, incorporating climate/hazard variables
- Further develop the model to facilitate the incorporation of uncertainty and variability associated with the model itself and the climate projections. This can be done using the aforementioned Monte Carlo Simulation approach, recognised as the most effective method for dealing with uncertainty (Fong et al., 2020). This can be coded from first principles using coding software such as MATLAB, or in some cases achieved through commercial risk software
- The model should now represent the vulnerability of the system considered to hazard/climate parameters and can be integrated with a hazard model and an exposure model to calculate climate risk under current and projected future climates



Time-dependent vulnerability modelling

It should be noted in the context of the above steps that, for systems such as critical infrastructure networks, the vulnerability model may need to be time-dependent to account for changes over the long service lives of such infrastructure. These networks may deteriorate over time due to various natural degradation phenomena (e.g. steel corrosion, reinforced concrete corrosion, timber decay, fatigue, etc.) and may be maintained to reduce the impact of this deterioration on failure probability. Modelling these temporal dynamics in addition to the changing climate is likely to result in a far more representative vulnerability model as shown in Ryan et al. (2014, 2016).

Step 3: Exposure (consequences)

This component of the climate risk assessment represents the level of exposure to a particular hazard (i.e., how many houses are in a floodplain) and, in many cases, the consequences of failure due to the climate hazard (if flooding occurs, the cost of repair to houses). The greater the consequences of failure (i.e., cost of failure of an infrastructure asset, or impact on human health), the greater the risk will be for a given vulnerability and hazard. It may also be important to consider these costs over the life-cycle of the system being considered. This can be visualised in the context of a critical infrastructure asset, for instance. The LCC for an asset or network could be calculated as Eq.4 (but is not limited to):

$$LCC(t) = C_c + C_{IN}(T) + E_{damage}(T) \quad Eq.4$$

where C_c is the construction and materials cost, $C_{IN}(T)$ is the cost of inspections during service life T and E_{damage} is the expected cost of repair or loss during service life T . The expected cost of repair and loss can be described as:

$$E_{damage}(T) = \sum_{j=1}^{DS} \sum_{i=1}^T P_{f,i} \frac{C_{damage}}{(1+r_d)^i} \quad Eq.5$$

where $P_{f,i}$ is the probability of failure in year i calculated using time-variant reliability analysis. C_{damage} is the cost of repair, maintenance or replacement and associated indirect losses, which can include costs of cascading failures in other sectors, r_d is the discount rate and DS is the number of different limit states. User costs include monetary losses following the failure of the system,

e.g. extra costs of driving longer routes because of a flooded national road section or bridge collapse, or loss to business and industry following a disruption in energy supply or telecommunication and data services. These costs can be considerable, and, for some systems, are likely to be much greater than direct repair, replacement and maintenance costs (Ryan, 2017). It is noted that the uncertainties and variability associated with the abovementioned consequences/exposure should be quantified wherever possible as their variability and uncertainty can have a large bearing on the analysis outcomes.

Step 4: Adaptation risk-based decision support

Having quantified the climate risk to a system through integration of hazard, vulnerability and exposure models, it is straightforward to determine if climate change adaptation is needed. If the risks are small, climate change adaptation is not required. However, if they are significant across Ireland, or for a given region, climate change adaptation should be investigated. Fortunately, having developed a quantitative risk model, it is generally relatively easy to assess both the effectiveness of an adaptation strategy and its cost-benefit. This ability to implement cost-effective climate change adaptation strategies is a key factor in determining how well the systems cope with a changing climate (Ryan and Stewart, 2017). Failure to conduct this type of analysis before taking potentially costly adaptation actions could lead to significant opportunity costs, with actions typifying cost-neglect being taken after extreme events because of public pressure or other non-scientific forces (Bastidas-Arteaga and Stewart, 2019).

Firstly, the effectiveness of various climate adaptation strategies can be investigated using the risk model. For instance, if the vulnerability model developed incorporates the effect of maintenance strategies, the effectiveness of adjustments to these strategies in reducing future impacts of climate change can be investigated. This approach has been implemented in the past by one of the project Co-PIs when examining the climate adaptation strategies for Australian power distribution systems (Ryan and Stewart, 2017). Alternatively, alterations to design standards to increase climate resilience and reduce climate risk can be investigated. The effectiveness of this adaptation approach is investigated in the case study in Section 12.2.5 below for road drainage systems in Ireland.

Having established the effectiveness of a number of adaptation strategies, probabilistic cost-benefit analysis can be used to assess the financial feasibility of these adaptation actions incorporating uncertainty at all levels. The presentation of the results in this form facilitates robust and quantitative universal metrics that system managers, owners and researchers across disciplines can relate to, i.e. mean net present values (NPVs) and benefit-to-cost ratios (BCRs). As outlined by Ryan and Stewart (2017), the NPV of the system over the life cycle can be calculated as:

$$NPV(t) = LCC_{BAU}(t) - LCC_{adapt}(t) \quad Eq.6$$

where $LCC_{BAU}(t)$ and $LCC_{adapt}(t)$ are the LCCs for 'business as usual' (BAU) conditions, i.e. existing practice and under the adaptation measure, respectively, discounted to a present value. The BCR of an adaptation strategy over the life cycle can be determined by the following equation:

$$BCR = \frac{Benefit_{adapt}}{Cost_{adapt}} \quad Eq.7$$

The NPV and BCR are not mutually exclusive, but complementary. The 'benefit' of an adaptation measure ($Benefit_{adapt}$) is the reduction in damages or losses over the life cycle brought about by the adaptation strategy, and the 'cost' is the cost of implementation of the adaptation strategy ($Cost_{adapt}$). An NPV greater than 0 and a BCR

value greater than 1 indicates that an adaptation measure is cost-effective, meaning monetised risk is reduced by adaptation implementation. To assist decision-makers in the selection of adaptation strategies, more than one strategy should be investigated using probabilistic cost-benefit analysis, with the best strategy identified as the one with the maximum positive NPV.

Key component for risk-based decision support



The examination of adaptation effectiveness and cost-benefit in this step constitutes an essential component of effective risk-based decision support, complementing the risk analysis, which in isolation is limited to quantifying impacts, rather than the effectiveness and cost feasibility of adaptation.

12.2 Illustrative case study

This case study is used to illustrate how the fully-quantitative risk-based decision support step-by-step guide can be applied to an Irish sector to investigate climate change impacts and assess climate adaptation effectiveness. The case study involves the assessment of climate change impact on the Irish national road drainage systems subjected to intensive rainfall events with short durations, and the examination of the effectiveness of a climate adaptation measure employed by Transport Infrastructure Ireland (TII) from 2015 onwards. Uncertainty surrounding the potential climate change impacts on road drainage systems has led TII in recent years to apply this blanket 20% increase adaptation factor to rainfall intensity across Ireland in the design stage (DN-DNG-03022, 2015). Given the lack of research conducted in this space at the time, this factor had to be selected without scientific research or evidence base. This real-life industry challenge was the basis for the development of this case study.

It is noted that the case study is ongoing under TRANSLATE 2, with work on quantifying exposure/consequences of road flooding currently underway. This work, through collaboration with industry partners, is considering both direct

and indirect costs. Given the above ongoing research, the illustrative case study presented below demonstrates the hazard and vulnerability modelling steps of the framework, and their integration to determine projected climate change impacts. The adaptation effectiveness aspect of the risk-based decision support is also

illustrated, examining the current TII climate adaptation strategy. The steps in the risk-based decision support framework illustrated in Fig. 32, which are covered in this illustrative case study, are shown below in Fig. 33 for clarity, with steps not covered in the case study greyed out.

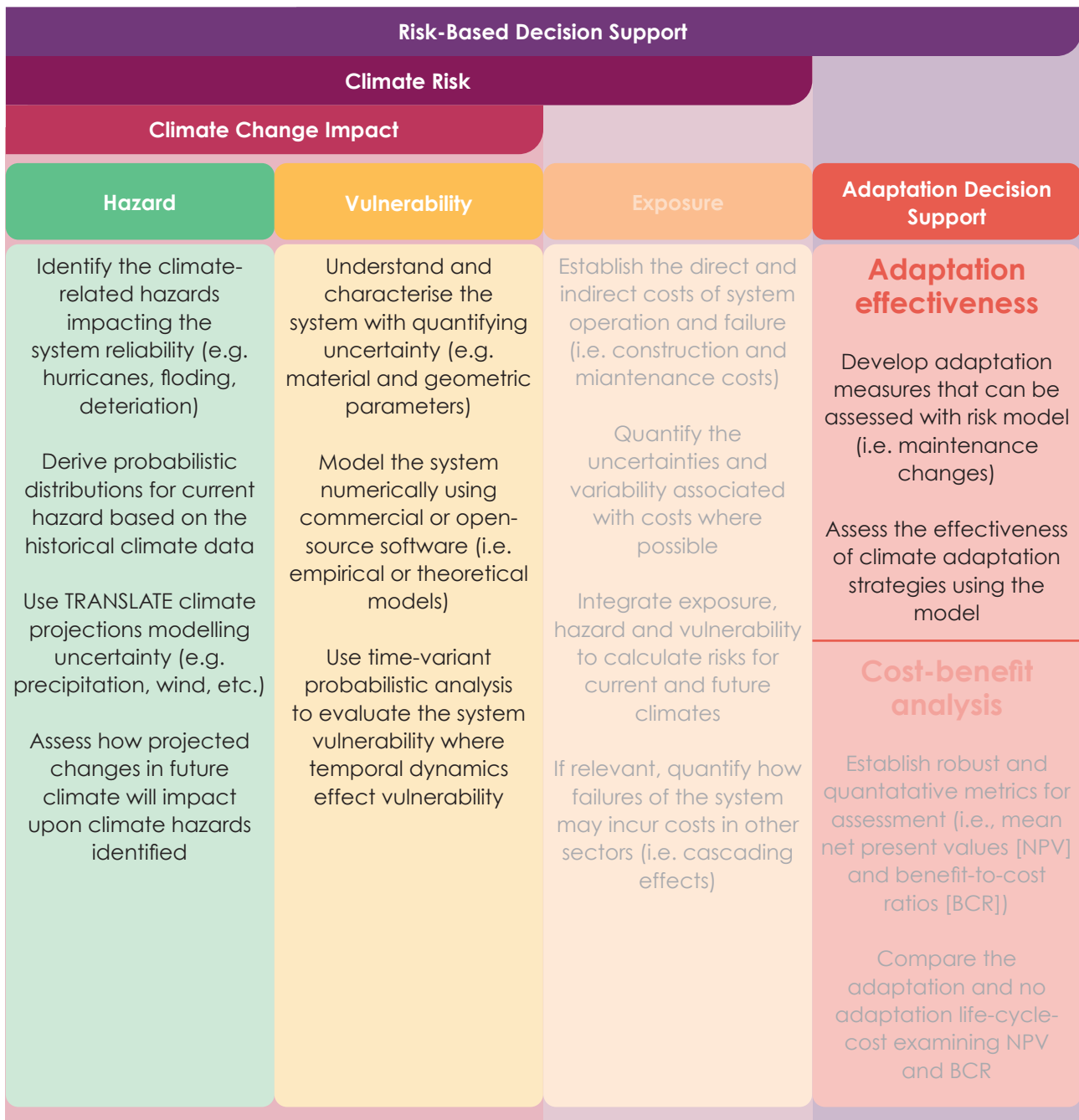


Figure 33. Fully-quantitative risk-based decision support steps illustrated in the illustrative case-study below

12.2.1 Co-creation of quantitative risk case study

The development of the fully-quantitative risk case study involved a high level of co-creation throughout, with UCC and TII forming an active research partnership. Initial meetings were conducted to explore, and then define, the planned scope of the study. Subsequently, a series of meetings were conducted with both TII and their engineering design consultants Arup, when developing the probabilistic vulnerability model of their drainage systems, as discussed in Section 12.2.4 below. These co-development design workshop meetings ensured the probabilistic drainage modelling was representative of the systems used on Ireland's motorways and national routes. The next phase in the co-creation cycle involved co-evaluation of the results. The TRANSLATE team initially presented their findings, following months of modelling and analysis, and TII provided stakeholder insights and interpretations and highlighted areas for further investigation. This feedback loop led to another iteration of the analysis and modelling work, ensuring the research outcomes had maximum relevance to the stakeholders. The discussions also highlighted aspects for future research, including assessment of regional variation of climate adaptation appropriateness and seasonal effects. Upon completion of TRANSLATE, final results were presented to TII to complete the co-creation cycle for this project. These research findings have resulted in TII beginning a process of re-examination of their design standards for drainage system. Further collaboration between UCC and TII will aid in this process, through probabilistic cost-benefit analysis of various adaptation strategies.

12.2.2 Engineering background

Meteorological observations show that Ireland's climate is changing at a scale and rate consistent with regional and global trends. As discussed in Part A of this report, the climate projections indicate a substantial increase in the frequency of extreme rainfall events in winter and autumn in the future, which will likely lead to a rise in infrastructure failures caused by flooding. An important consideration in this regard is the flooding of Irish national roads that form the key road transport arteries of the country. It is thus

crucial to conduct research into the impact of climate change on the national road drainage systems and examine the effectiveness of climate change adaptation.

For this case study, a simplistic but representative drainage system was established for national roads through consultation with TII and their current engineering design consultants, Arup. The selected road section is designed in accordance with the published TII standards (TII, 2015) for a length of road section extending 1.2km in County Cork, Ireland. The road under consideration is 8.0 metres wide, with a 7.0-metre-wide carriageway and two 0.5-metre-wide hard strips, and runs on a 1% gradient embankment before transitioning to a 0.5% gradient cutting (DoT, 2022). The catchment along the road has an impermeable footprint area of approximately 1.055 ha and the average annual rainfall depth for the site is about 1230mm based on observation of past meteorological data for the location (retrieved from Met Éireann website: <https://www.met.ie/climate/available-data>). The soil type is classified as Type 4, with a soil index of 0.45, as determined by the Flood Studies Report (DN-DNG-03068, 2015). The designed drainage systems consist of pipe networks, an attenuation pond and outfall structures at the terminal. A sketch of the systems is presented in Fig. 34.

12.2.3 Step 1: Modelling climate hazard

(1) Current hazard

Discussion with TII has highlighted that the climate hazard of concern for the drainage system in this case study is intensive rainfall events with short durations. Accordingly, the existing climate hazard model was determined from historical rainfall time series data. The generation of the existing hazard model thus requires the collection of adequate and valid rainfall records from meteorological stations in Ireland. In this case, rainfall records at the Inniscarra Station with nine metrics representing 'peak over threshold' (POT) values are adopted as the data source. To derive the intensive rainfall events, it is essential to determine the rainfall Depth-Duration-Frequency (DDF) models for the baseline period (i.e., historical period), which describe rainfall depth as a function of rainfall event duration for a given return period. Herein, the baseline period was

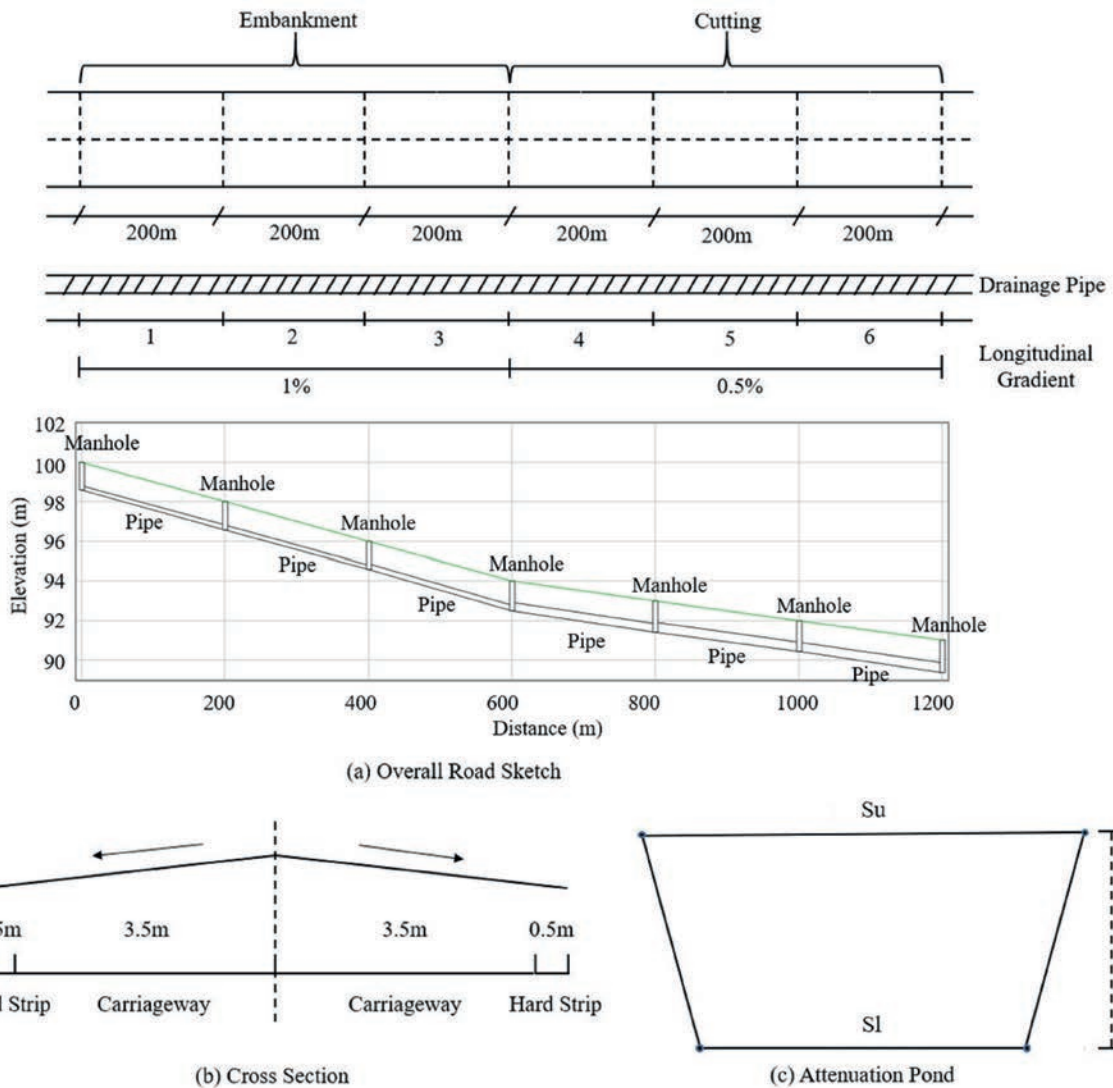


Figure 34. Schematic of the drainage system (S_u = the upper surface area of the pond; S_l = the lower surface area of the pond; H = the height of the pond).

selected as 1976-2005, due to the availability of high-resolution gridded rainfall observations for this period, which was provided by Met Éireann as discussed in Section 3.2 of Part A. Based on the Pareto Distribution, the relationship between frequency and rainfall depth for nine metrics was developed and summarised in DDF tables with six return periods (i.e., 5-year, 10-year, 15-year, 20-year, 30-year and 100-year), which can be found in Wang et al., (2024). Resulting examples of intensive rainfall events with 2-hour duration are

shown for the historical period, and under RCP 4.5 in Fig. 37.

(2) Future hazard

For future intensive rainfall events, the aggregated projected rainfall records of 23 stations located across Ireland generated in Part A were utilised as the data source to derive the DDF table for future climate scenarios (i.e. RCP 4.5 and RCP 8.5) for the 2071-2100 time period. No climate projection data was available under TRANSLATE for sub-

daily temporal resolution. Thus, historical data was used to establish the relationships between the daily intense rainfall metric 'r30in24h', and the other eight metrics i.e. 'r4in15', 'r6in30' etc. It was assumed these relationships do not change in the future. This facilitated the estimation of changes in all metrics, using the established relationships and the daily projection data, which was used to estimate changes in the 'r30in24h' metric. Further discussion on the development of this approach can be found in Wang et al., (2024).

Fig. 35 shows the projected rainfall records averaged across the 23 stations for RCP 4.5 and RCP 8.5. The curves show stable regions of rainfall depth between 10mm and 70mm, corresponding to the return period from about 12-year to 9000-year. The frequency ratios between past and future can be easily calculated within the range as the following:

$$\text{Frequency ratio} = \frac{\text{Daily rainfall occurrence frequency for the future}}{\text{Daily rainfall occurrence frequency for the historical}} \quad \text{Eq.8}$$

As discussed in the step-by-step guide, it is important to represent projected climate change probabilistically to incorporate the considerable uncertainty associated with future projections. To achieve this best-fit distribution, the calculated frequency ratios for each ensemble shown above were determined through the use of computer code developed by the TRANSLATE team. This process identified the Generalised Extreme Value Distribution as the most appropriate for representing the projected climate change uncertainty for various climate scenarios, as shown in Fig. 36. Thus, the uncertainty of future climate scenarios is realised by randomly creating samples of frequency ratios from the established probability distributions through Monte Carlo Simulation using MATLAB. The generated frequency ratios are then used to modify the frequency rainfall depth curve for the historical daily metric (i.e., r30in24h) to account for the projected climate change under the RCP4.5 and RCP 8.5 scenarios. The resulting examples of intensive rainfall time series with 2-hour durations for RCP 4.5 are shown in Fig. 37. The impact of climate change on storm intensity can be seen in this plot with, for instance, the historical 50-year storm also equal to the RCP 4.5 20-year storm.

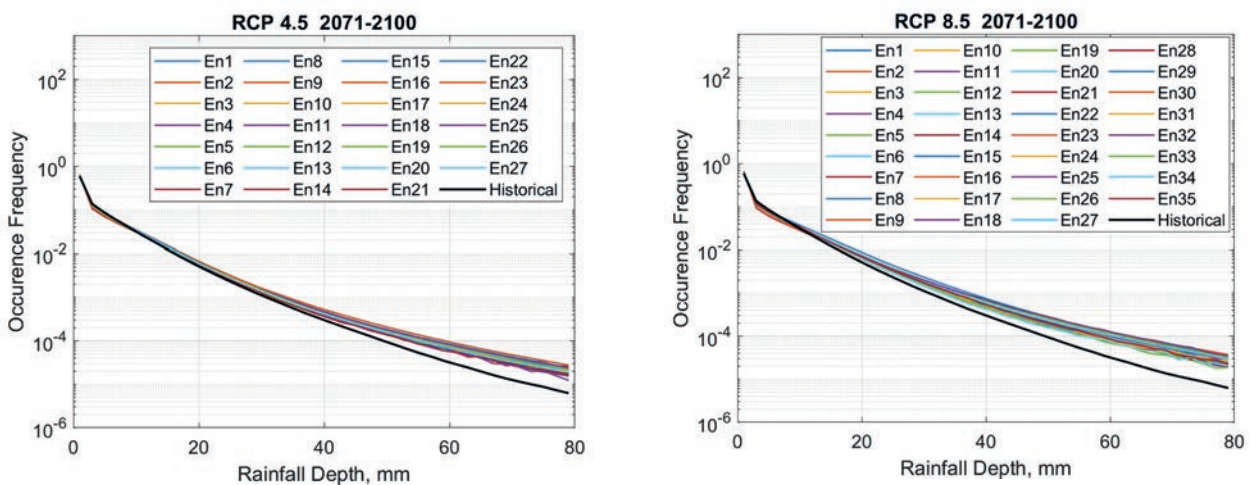


Figure 35. Climate projections of the occurrence frequency-daily rainfall depth relation

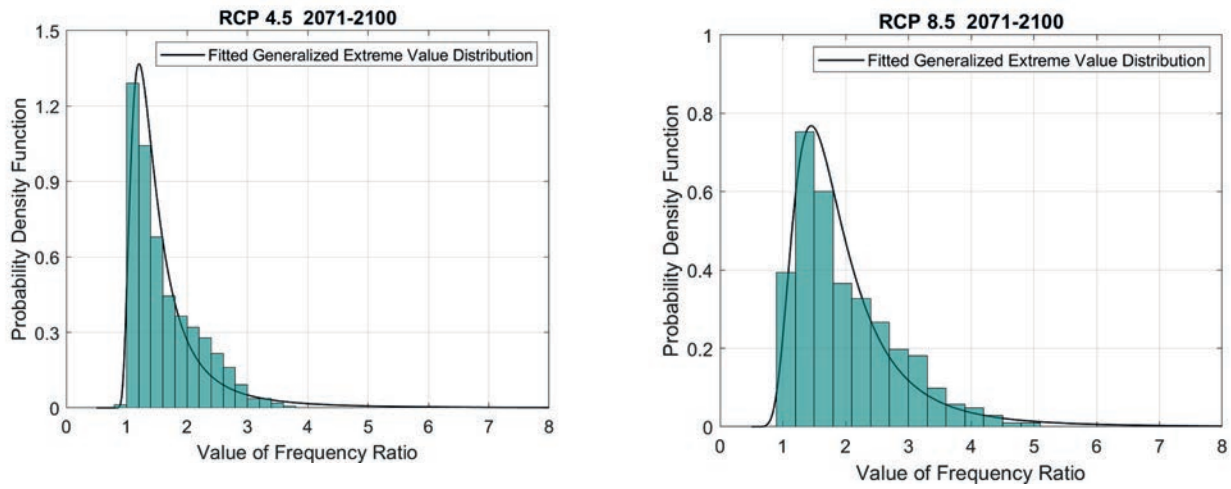


Figure 36. The best-fit distribution (GEV) for frequency ratios of daily rainfall between historical and future climates

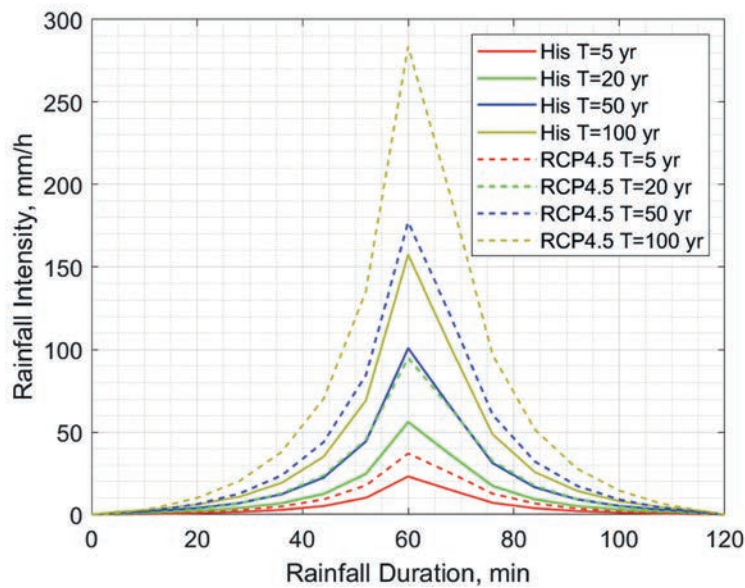


Figure 37. Intensive rainfall events with 2-hour duration and various return periods for historical climate and RCP 4.5

12.2.4 Vulnerability analysis

As mentioned in the quantitative risk step-by-step guide, the development of a vulnerability model is generally the most challenging component of this type of analysis as it involves developing representative numerical models for physical entities. For this case study, the physical drainage system was modelled using the Storm Water Management Model (SWMM), an open-source

public software developed by the United States Environmental Protection Agency for planning, analysis and design related to drainage systems (US EPA, 2023). This deterministic numerical model was expanded into a probabilistic model under TRANSLATE through the development of computer code using MATLAB (a computer programming software), to integrate climate change and model uncertainty/variability through Monte Carlo Simulation. All the required information

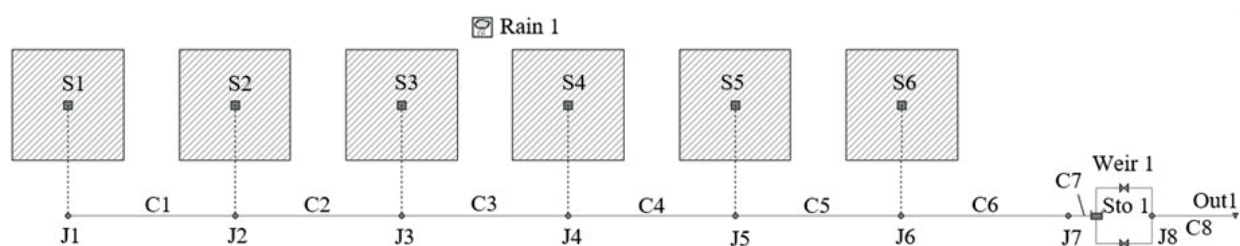


Figure 38. Vulnerability model of the drainage system

on national road drainage systems (e.g. site, topology, climate, sketch) for the numerical modelling can be found in the 'Engineering Background'. The model vulnerability model was then developed in accordance with the 4 bullet points outlined in Step 2 of the step-by-step guide. A detailed discussion of the vulnerability model development can be found in a paper by the project team Wang et al., (2024).

The established numerical model of the drainage system is shown in Fig. 38. S1-S6, J1-J6 and C1-C7 represent sub-catchments, manholes and pipe networks of the system, respectively. Sto1 refers to the attenuation pond with outfall structures, including an orifice (Orifice 1) and a weir (Weir 1). Based on the functional insights into the drainage system operation during storm events, two critical limit states were identified as follows: (i) the overflow of manholes to the road surface and (ii) the exceedance of the maximum pond level permitted under TII Standards. Thus, three aspects were quantitatively modelled in this study: a) the total system inflow, b) the occurrence probability of road flooding and c) the maximum capacity usage of the attenuation pond.

12.2.5 Climate change impact and effectiveness of climate adaptation

(1) Climate change impact

As per Fig. 33, the projected climate change impacts are determined through the integration of the hazard model and the vulnerability model. Fig. 39 to Fig. 41 illustrate the resulting impact of climate change on the three observational indicators – system inflow, probability of road flooding and maximum usage of pond capacity. Examining the mean and standard deviation

results in Fig. 39, it can be seen that the system inflow is the highest under RCP 8.5, followed by RCP 4.5, and the lowest for the historical period. The results show an increase in rainfall volume under intense rainfall events for future climates is projected to increase by approximately 37% and 55% for RCP 4.5 and RCP 8.5, respectively, when compared with the historical period. This percentage increase is quite consistent across the return periods. This projected increased inflow will result in higher pressure on the system to transmit rainwater within the limited time of an intense rainfall event. It can also be noted from Fig. 39 that the predictions of inflow volume for future climates exhibit significant standard deviation increases with the return period. This is driven by the climate change uncertainty (note historical inflows show small uncertainty), which results from the increase of ensemble divergence with rainfall depth, as shown above in Fig. 35.

Examining Fig. 40, it is clear that both the RCP 4.5 and RCP 8.5 climate scenarios result in increases in the probability of pipe flooding and subsequent road flooding. It is noted that the design return interval selected for the pipe design in the TII standards (TII-DN-DNG-03022, 2015) is 5 years. From the plot, it can be seen that the likelihood of pipe overflow and subsequent road flooring goes from 0% under the historical scenario, to 4.4% and 8.7% under the RCP 4.5 and RCP 8.5 scenarios, respectively. Similarly, for intense rainfall events with a 20-year return period, the probability of road flooding increases by 10.8% and 11.2% under RCP 4.5 and RCP 8.5, respectively. These are noteworthy increases when considered in the context of flooding implications, which include a higher likelihood of impassable major roads in Ireland and increases in road traffic

risks associated with excessive water on road surfaces (Diakakis et al., 2020; Halpin and Newell, 2022). There is thus a clear need to explore the implementation of climate adaptation measures for the pipe network. This will be discussed in detail in the next subsection.

Considering Fig. 41, it can be seen that no flooding, or exceedance of the maximum pond level permitted under TII Standards (1.0 in plot), occurs for the attenuation pond under intense rainfall events for both the historical and the future climate scenarios. This reflects the extent of conservatism in the TII design standards for pond design, which was likely implemented given the

potential for environmental damage resulting from pond overflow. It is noted, however, that the level of pond usage under future climates shows an obvious increase, with a 6%-31% increase under RCP 4.5 and a 9%-47% increase under RCP 8.5. Thus, there is a noteworthy reduction in the reserve capacity of the pond even under these short-duration events as a result of climate change. Future work will examine the potential for climate change impacts for longer-duration storms, which may have higher probabilities of exceeding the attenuation pond limit states, i.e. attenuation pond may be more susceptible to overflow for a 6-hour storm than a 2-hour storm.

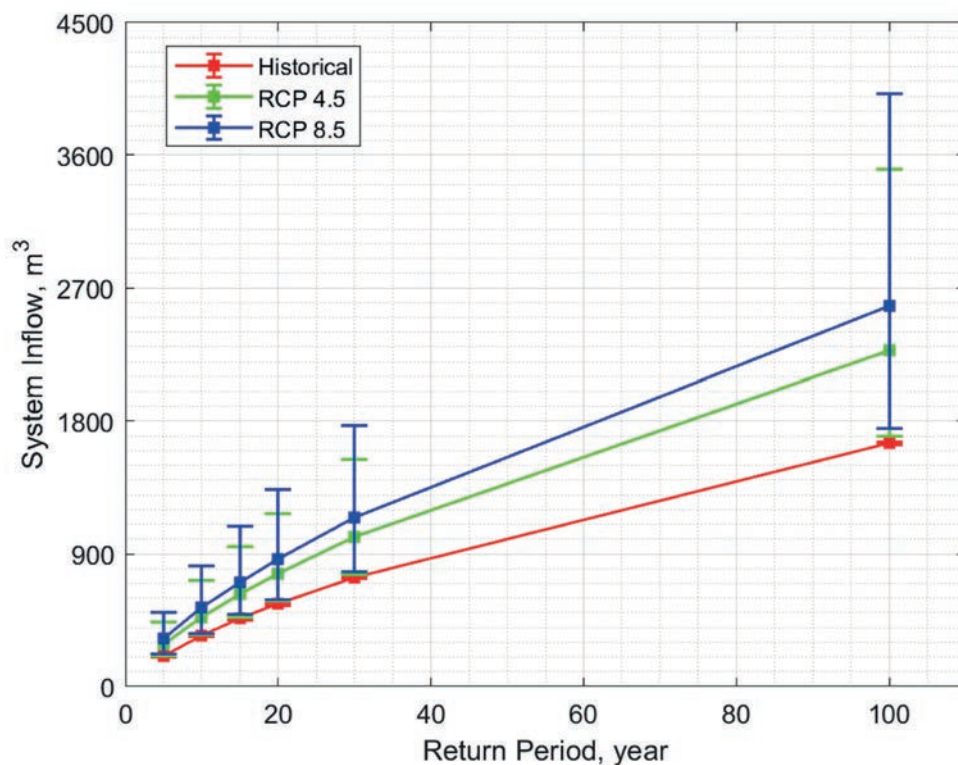


Figure 39. System inflow under storms of historical and future climates for 2071-2100 (mean value, 5th and 95th percentile shown)

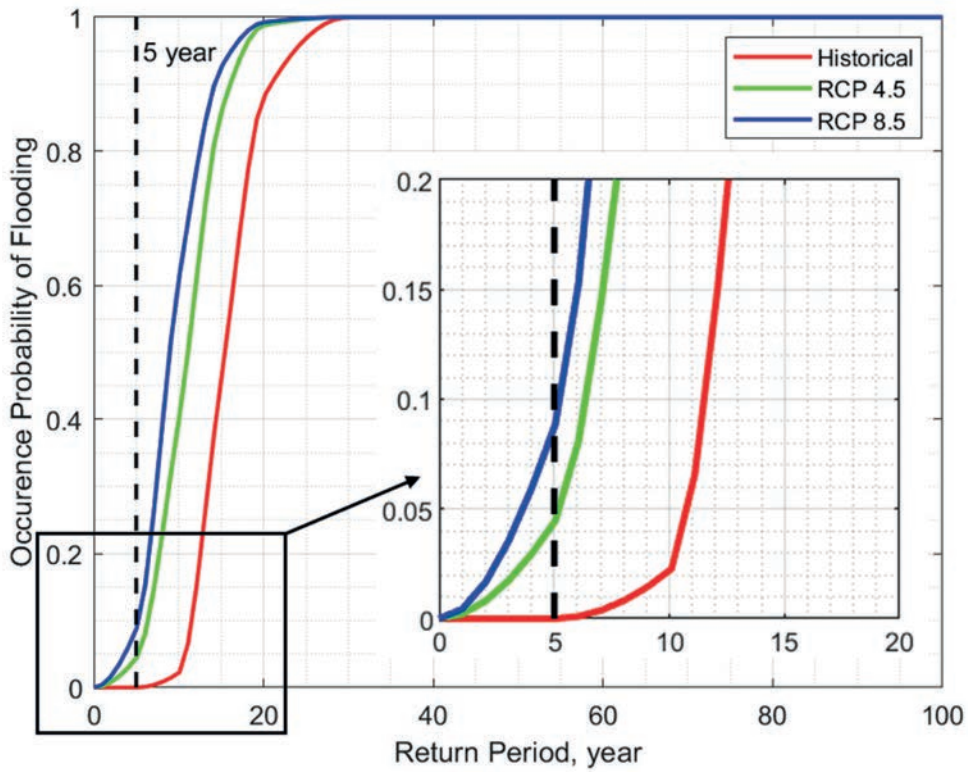


Figure 40. Flooding failure probability of the pipe network under storms of historical and future climates for 2071-2100

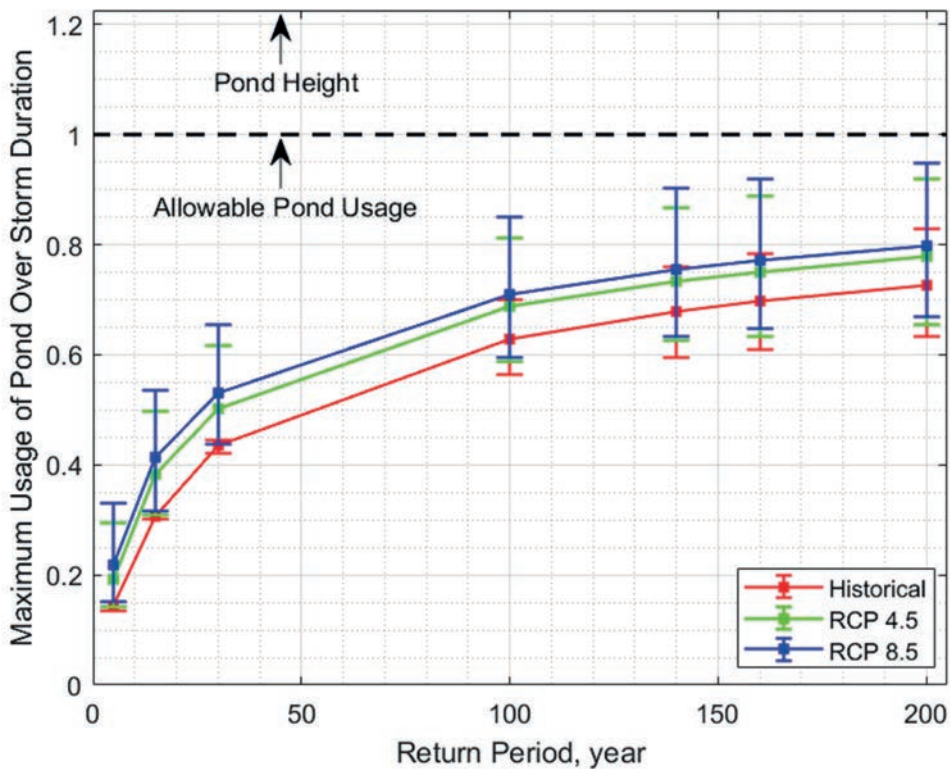


Figure 41. Maximum usage of pond capacity over storm duration under historical and future climates for 2071-2100 (mean value, 5th and 95th percentile shown)

(2) Effectiveness of climate adaptation

The above results indicate that there is significant potential for climate change to impact the safe operation of road drainage systems in Ireland. In a progressive pro-active approach, TII did take climate adaptation action in 2015, implementing a climate adaptation measure in their design standards for the national road drainage systems. This 2015 adaptation measure involved applying a 20% increase factor for the design rainfall intensity (TIIs, 2015). Thus, networks constructed prior to 2015 in Ireland are vulnerable to the impacts shown in the above section, while networks constructed since 2015 will have increased climate resilience. However, the effectiveness of the TII's climate adaptation measure under future climates has not been explored to date. This formed a key motivation for this case study, given the considerable cost associated with land and construction arising from the implementation of the 20% climate adaptation factor. The study herein thus compared the drainage system performance with and without the climate adaptation measure across the RCP 4.5 and RCP 8.5 climate scenarios to examine the effectiveness of the measure in mitigating the impacts of climate change.

Results of flooding failure probability of pipes and maximum usage of pond capacity for comparative study are displayed in Fig. 42 and Fig. 43. The occurrence probability of flooding under intense rainfall with 5-year return periods (design return period for the pipes) and 20-year return periods for the pipes drainage system, with and without adaptation, is presented in Table 3. As noted in the above subsection, without adaptation at the 5-year return period, the probability of failure goes from 0% for historical, to 4.4% and 8.7% for RCP 4.5 and RCP 8.5, respectively. With the adaptation strategy applied, the probability of failure under RCP 4.5 is 1.3%, while the corresponding figure for RCP 8.5 is 1.9%. Thus, it can be noted that, although the adaptation strategy significantly reduces climate change impact (~70% reduction), it is not fully effective

in mitigating the climate-related increases in the probability of road flooding. This can clearly be seen in Fig. 42 below by comparing the red line to the dashed blue and green lines at the 5-year return period. On a positive note, the table shows that the adaptation is almost fully effective at the 20-year return period (reduces the probability of failure to close to historical levels for RCP 4.5 and 8.5); however, the key return period is 5-year, as this is the design return period for the pipes. Thus, the analysis indicates that a more aggressive climate adaptation strategy may need to be employed by TII for the pipe design.

As noted in the above subsection, the pond did not exceed its limit state for historical or climate change scenarios for the storm duration and return periods examined herein. This thus indicates that the implementation of the adaptation strategy to the pond design may be overly conservative. However, given the strategy is in place, it is examined below in Fig. 43. As can be seen from the figure, the adaptation strategy reduced pond usage at lower return periods; however, the reduction is small for the 100-year return period (design return period for the pond). As discussed in detail in Wang et al., (2024), this analysis finding is primarily related to the fact that at this 100-year return period for the 2-hour storm, the pipe network is fully flooding, limiting the conveyance of water to the pond. Thus, overall, there may be potential to make savings on TII's pond adaptation strategy from 2015 and use some of these resources to increase the climate resilience of the pipe network. However, further research is required before action is taken, examining different storm durations and the effectiveness and cost-benefit of various adaptation strategies. The findings presented in this subsection highlight the advantages of the fully-quantitative risk-based decision support for adaptation decision-making, when compared to the semi-quantitative GIS-based approach illustrated in Section 11, which is limited to highlighting possible climate hotspots.

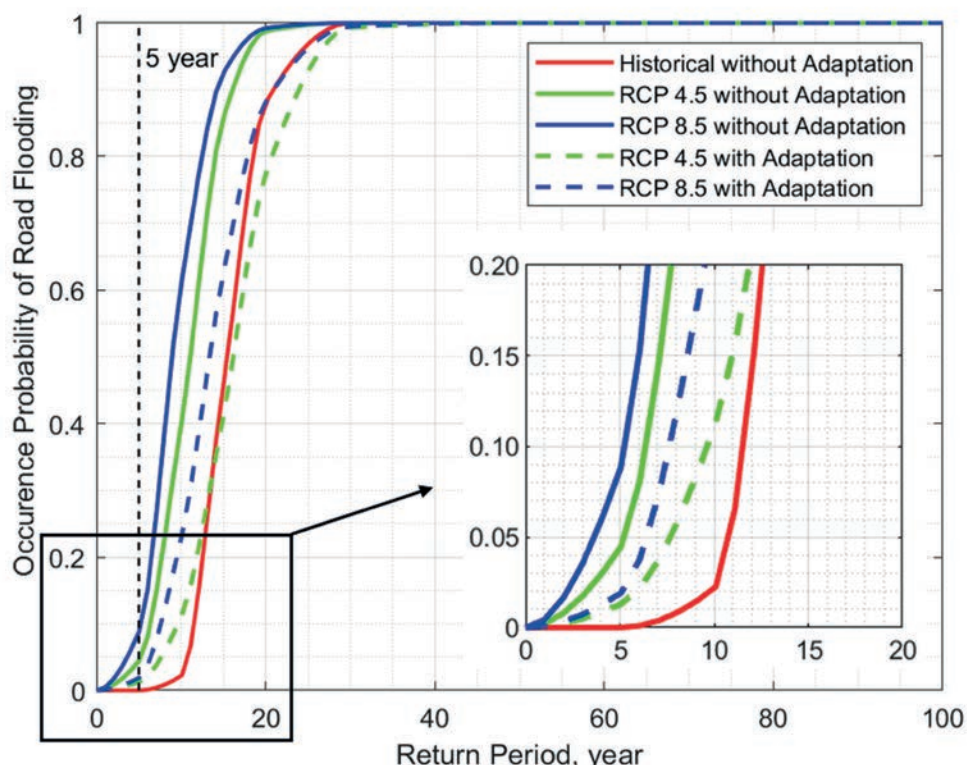


Figure 42. Flooding failure probability of pipes for drainage system with and without adaptation factor

Table 3. Flooding failure probability (%) of drainage system pipe network with and without adaptation

Climate Scenario	Flooding Failures without Adaptation		Flooding Failures with Adaptation	
	5-Year Return Period	20-Year Return Period	5-Year Return Period	20-Year Return Period
Historical	0	88	0	27.8
RCP 4.5	4.4	98.8	1.3	77.4
RCP 8.5	8.7	99.2	1.9	88.2

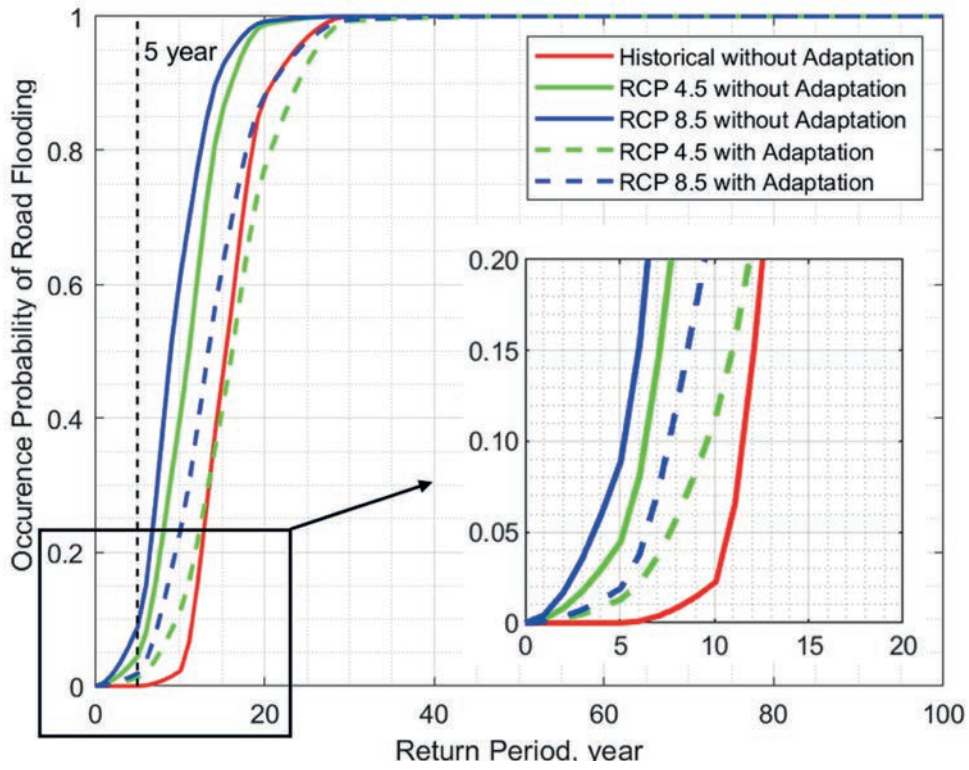


Figure 43. Maximum usage of pond capacity for drainage system with and without adaptation factor

A scenic landscape at sunset. The sky is filled with warm orange and yellow hues from the setting sun. In the middle ground, a body of water reflects the sunset. In the background, there are several houses and a small town. In the foreground, there is a rocky hillside with a stone wall and several sheep grazing.

13

Part B Discussion and Conclusions

Irish sectors, local authorities and industry stakeholders face the significant challenge of managing potential but uncertain increases in future risk to their systems. The ability to implement cost-effective climate change adaptation strategies is a key factor in determining how well the systems cope with future increases in risk (Ryan and Stewart, 2017). Failure to conduct detailed risk-based analysis before taking potentially costly adaptation actions could lead to significant opportunity costs, with actions typifying cost-neglect being taken after extreme events because of public pressure or other non-scientific forcers (Bastidas-Arteaga and Stewart, 2019). In this context, it is clear that Ireland needs both standardised climate change projection datasets and associated risk-based decision support services. Part B of this project focused on the development of these services.

The co-creation work, which commenced at the outset of TRANSLATE, and continued throughout, was a key part of the climate service development, identifying the stakeholders' need for specific hazard indicators, derived from the climate projections and vulnerability/exposure metrics. The co-creation approach was also fundamental in informing the direction and extent of the fully-quantitative risk-based decision support case study, which involved extensive collaboration with TII and Arup Consulting Engineers. For the semi-quantitative risk assessment, the co-creation highlighted that each sector has their own definition of thresholds that drive risk management. It is therefore imperative to build towards a climate services system that can allow for automation and flexibility. The development of automated computer code, datasets, automated hexagonal grid procedures, training material and a step-by-step guide for semi-quantitative GIS-based analysis was an important first step in this process. This analysis indicated that risk of missed education days due to extreme weather hazards is projected to increase in the future for most of the country, particularly in the areas around Limerick, Dublin, Wicklow and Athlone.

While the semi-quantitative risk analysis approach was shown to be very useful for highlighting potential climate risk hot-spots nationally, it tends to be limited when attempting to implement effective climate adaptation action. Consequently, as part of the TRANSLATE climate service offering, a fully-quantitative risk-based decision support guide was also developed. In keeping with the IPCC's definition of climate risk, this four-step guide focuses on integrating i) future hazard models, ii) system vulnerability models and iii) exposure/consequences to quantify future climate risks. The key fourth step is implementation of risk-based decision support through assessment of adaptation effectiveness and cost-benefit.

Again, this step-by-step risk guide was illustrated through a TRANSLATE case study, which was conducted in collaboration with Transport Infrastructure Ireland (TII). This fully-quantitative risk case study quantifies the impacts of projected climate change on national road drainage systems. It also examines the effectiveness of a climate adaptation strategy. It was found that climate change impacts on probability of road flooding under intense rainfall are projected to increase beyond the current acceptable limits set by TII standards (0% probability for 5-year intense rainfall event). The analysis also indicated that a proactive climate adaptation strategy adopted by TII standards in 2015 may require adjustment, with a need to increase climate resilience of the pipe network and the potential to make savings through adopting a less conservative adaptation approach for attenuation ponds.

Comparing the outputs from the semi-quantitative and fully-quantitative risk case studies provides vital insights to stakeholders into which approach they should use when assessing their systems. The semi-quantitative analysis is shown to be a key first step in understanding and highlighting potential climate change risks and hotspots; however, it is normally not suitable for informing climate adaptation decision-making. The fully-quantitative risk-based decision support, on the other hand, can provide detailed insight into the values of projected future risks and figures on the effectiveness and cost-benefit of proposed climate adaptation strategies.

Based on the findings of TRANSLATE, future climate services work under TRANSLATE 2 includes the following:

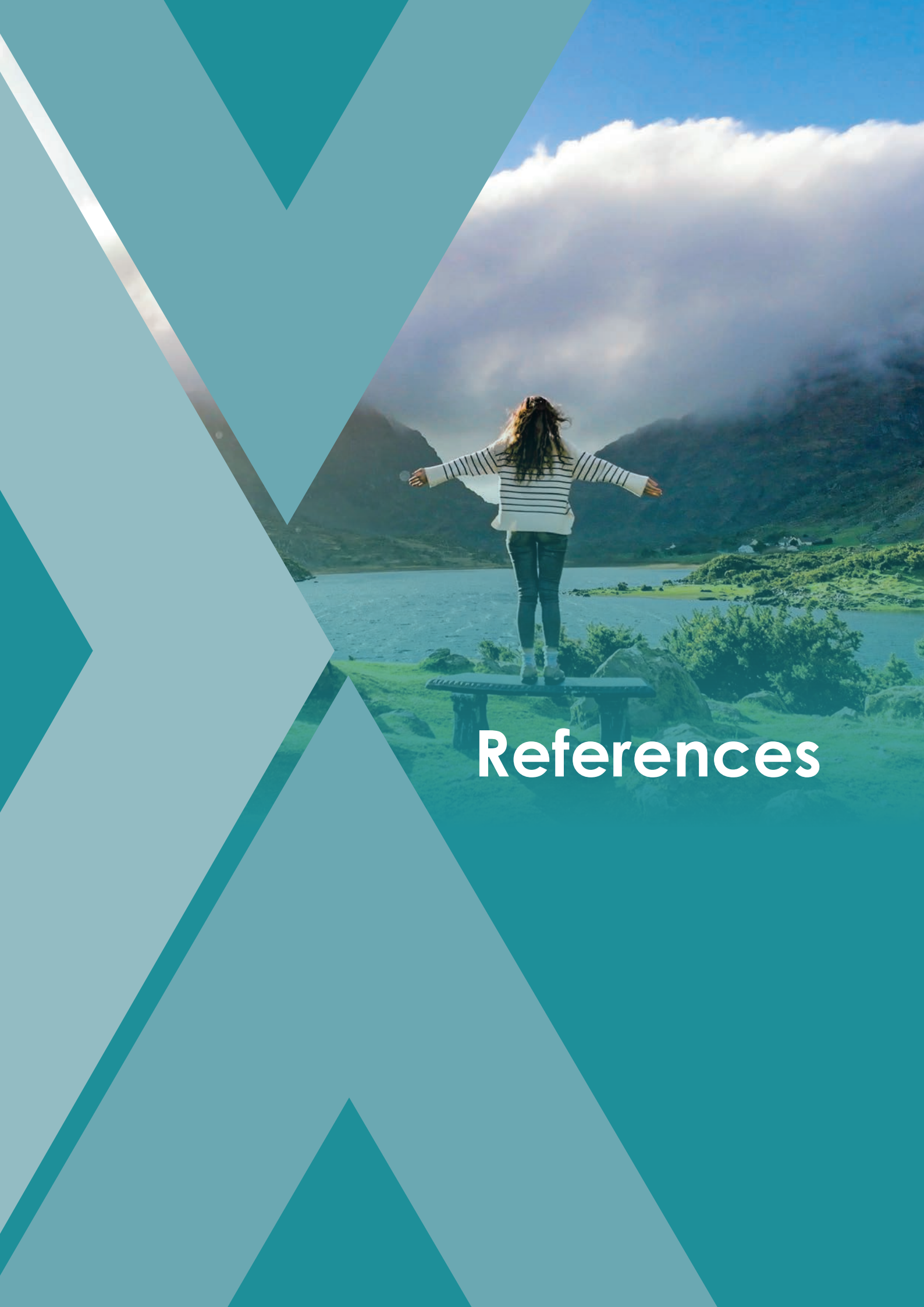
- (1) Expansion of the fully-quantitative TII case study to cover exposure/consequences and the resultant probabilistic cost-benefit analysis



of various climate adaptation strategies. The effect of regional variability on climate change impacts (i.e., east and west) and the effect of seasonal variability (i.e., summer and winter) will also be considered.

- (2)** Expansion of the fully-quantitative framework to consider cross-sectoral/cascading risks and initiation of cross-sectoral collaboration through the development of a cross-sectoral risk illustrative case study.
- (3)** Further development of the semi-quantitative services through the roll-out of the proposed framework to a range of sectors through multiple geospatial climate risk case studies.

- (4)** Development of sector-specific climate services through our ongoing stakeholder engagement strategy of co-creation and the development of a TRANSLATE pipeline architecture to automate the climate services at all user entry points that will support Met Éireann and Climate Ireland. This will integrate the risk frameworks and case studies within the national framework for climate services, as well as standardising how-to climate risk user guides and training development.



References

- Abbass, K., Qasim, M.Z., Song, H., et al., 2022. A review of the global climate change impacts, adaptation, and sustainable mitigation measures. *Environmental Science and Pollution Research*, 29(28), pp.42539-42559.
- Allen, J.T., 2018. Climate change and severe thunderstorms. In *Oxford research encyclopaedia of climate science*.
- All-Island Research Observatory (AIRO), 2016. Post Primary Schools [dataset]. Available from: https://data.gov.ie/dataset/post-primary-schools?package_type=dataset. Accessed March 1, 2022.
- Aryai, V. and Mahmoodian, M., 2017. Spatial-temporal reliability analysis of corroding cast iron water pipes. *Engineering Failure Analysis*, 82, pp.179-189.
- Battles, J.B. and Lilford, R.J., 2003. Organizing patient safety research to identify risks and hazards. *BMJ Quality and Safety*, 12(suppl 2), pp.ii2-ii7.
- Bessembinder, J., Terrado, M., Hewitt, C., Garrett, N., Kotova, L., Buonocore, M. and Groenland, R., 2019. 'Need for a common typology of climate services', *Climate Services*, 16, p.100135.
- Brasseur, G.P. and Gallardo, L., 2016. 'Climate services: Lessons learned and future prospects', *Earth's Future*, 4(3), pp.79-89.
- Burzynska, K. and Contreras, G., 2020. Gendered effects of school closures during the COVID-19 pandemic. *The Lancet*, 395(10242), p.1968.
- Cannon, A., Sobie, S., Murdock, T., 2015. Bias Correction of GCM Precipitation by Quantile Mapping: How Well do Methods Preserve Changes in Quantiles and Extremes? *J. Climate*, 28, 6938-6959. <https://journals.ametsoc.org/view/journals/clim/28/17/jcli-d-14-00754.1.xml>
- Central Statistics Office (CSO), 2018. Census 2016 Small Area Population Statistics. Available from: <https://www.cso.ie/en/census/census2016reports/census2016smallarea%20populationstatistics/>. Accessed March 1, 2022.
- CH2018 Report, 2018. CH2018 – Climate Scenarios for Switzerland, Technical Report. Eds. Fischer and Strassmann, <https://www.nccs.admin.ch/nccs/en/home/climate-change-and-impacts/swiss-climate-change-scenarios/technical-report.html> [Accessed February 9, 2022].
- CH2018, 2018. NCCS (Pub.) 2018: CH2018 – Climate Scenarios for Switzerland. National Centre for Climate Services, Zurich. <https://www.nccs.admin.ch/nccs/en/home/data-and-media-library/data/ch2018-web-atlas.html> [Accessed February 9, 2023].
- Christel, I., Hemment, D., Bojovic, D., Cucchiatti, F., Calvo, L., Stefaner, M. and Buontempo, C., 2018. Introducing design in the development of effective climate services. *Climate Services*, 9, pp.111-121.
- Ciullo, A., Martius, O., Strobl, E. and Bresch, D.N., 2021. A framework for building climate storylines based on downward counterfactuals: the case of the European Union Solidarity Fund. *Climate Risk Management*, p.100349. <https://doi.org/10.1016/j.crm.2021.100349>.
- Cox, D.T.C., Ilya M.D. Maclean, Alexandra S. Gardner, Kevin J. Gaston, 2020. Global variation in diurnal asymmetry in temperature, cloud cover, specific humidity and precipitation and its association with leaf area index. *Global Change Biology*; DOI: 10.1111/gcb.15336.
- Dawson, R.J., Thompson, D., Johns, D. et al., 2018. A systems framework for national assessment of climate risks to infrastructure. *Philosophical Transactions of the Royal Society A* 376: 20170298. <https://doi.org/10.1098/rsta.2017.0298>.
- DCCAE (Department of Communications, Climate Action and Environment), 2018a. National Adaptation Framework: Planning for a Climate Resilient Ireland. DCCAE, Dublin.
- DCCAE (Department of Communications, Climate Action and Environment), 2018c. Local Authority Adaptation Strategy Development Guidelines: December 2018. DCCAE, Dublin. Available online: <https://assets.gov.ie/76468/78653533-8792-4693-ad32-51f16e71b950.pdf> (accessed 26 January 2021).
- Design of Earthworks Drainage, Network Drainage, Attenuation and Pollution Control. DN-DNG-03066. 2015. Transport Infrastructure Ireland (TII) Publications.
- Drainage and Service Ducts Series 500. Volume 1. Specification for Road Works. March 2000. Transport Infrastructure. <https://www.tiipublications.ie/library/CC-SPW-00500-01.pdf>.
- Drainage Design for National Road Schemes-Sustainable Drainage Options. RE-CPI-07001. May 2014. Transport Infrastructure Ireland (TII) Publications.

Drainage Systems for National Roads. DN-DNG-03022. March 2015. Transport Infrastructure Ireland (TII) Publications.

DTAS (Department of Transport, Tourism and Sport), 2017. Adaptation Planning: Developing Resilience to Climate Change in the Irish Transport Sector. DTAS, Dublin.

Engzell, P., Frey, A. and Verhagen, M.D., 2021. Learning loss due to school closures during the COVID-19 pandemic. *Proceedings of the National Academy of Sciences*, 118(17), p.e2022376118.

Esnard, A.M., Lai, B.S., Wyczalkowski, C., Malmin, N. and Shah, H.J., 2018. School vulnerability to disaster: examination of school closure, demographic, and exposure factors in Hurricane Ike's wind swath. *Natural Hazards*, 90, pp.513-535.

EURO-CORDEX Data repository: <https://www.euro-cordex.net/060378/index.php.en>

European Commission, 2015. A European research and innovation roadmap for climate services. Available at: <https://data.europa.eu/doi/10.2777/750202> (Accessed 13/04/2022).

Findlater, K., Webber, S., Kandlikar, M. and Donner, S., 2021. 'Climate services promise better decisions but mainly focus on better data', *Nature Climate Change*, 11(9), pp.731-737.

Flood, S., Paterson, S., O'Connor, E., O'Dwyer, B., Whyte, H., Le Tissier, M. and Gault, J., 2020. National Risk Assessment of Impacts of Climate Change: Bridging the Gap to Adaptation Action. Environmental Protection Agency, Johnstown Castle, Ireland.

Fong, S.J., Li, G., Dey, N., et al., 2020. Composite Monte Carlo decision making under high uncertainty of novel coronavirus epidemic using hybridized deep learning and fuzzy rule induction. *Applied soft computing*, 93, p.106282.

Gallina, V., Torresan, S., Critto, A., Sperotto, A., Glade, T. and Marcomini, A., 2016. A review of multi-risk methodologies for natural hazards: Consequences and challenges for a climate change impact assessment. *Journal of environmental management*, 168, pp.123-132.

Grubestic, T.H., 2006. A spatial taxonomy of broadband regions in the United States. *Information Economics and Policy*, 18(4), pp.423-448.

Guo, J., Wang, X., Fan, Y., Liang, X., Jia, H., and Liu, L., 2023. How extreme events in China would be affected by global warming—Insights from a bias-corrected CMIP6 ensemble. *Earth's Future*, 11, e2022EF003347. <https://doi.org/10.1029/2022EF003347>

Haase, T., and Pratschke, J. 2017 The 2016 Pobal HP Deprivation Index for Small Areas (SA). Available at: <https://www.pobal.ie/app/uploads/2018/06/The-2016-Pobal-HP-Deprivation-Index-Introduction-07.pdf>

Harrison, R.L., 2010, January. Introduction to Monte Carlo Simulation. In AIP conference proceedings (Vol. 1204, No. 1, pp. 17-21). American Institute of Physics.

Hawchar, L., Naughton, O., Nolan, P., Stewart, M.G. and Ryan, P.C., 2020. A GIS-based framework for high-level climate change risk assessment of critical infrastructure. *Climate Risk Management*, 29, p.100235.

Hawkins, E. and Sutton, R., 2009. The potential to narrow uncertainty in regional climate predictions. *Bull. Am. Meteorol. Soc.*, 90, 1095–1107, <https://doi.org/10.1175/2009BAMS2607.1>

Henson, S.A., Beaulieu, C., Ilyina, T., John, J.G., Long, M., Séférian, R., Tjiputra, J. and Sarmiento, J.L., 2017. Rapid emergence of climate change in environmental drivers of marine ecosystems. *Nature Communications*, 8(1), p.14682.

Hewitt, C., S. Mason, and D. Walland, 2012. 'The Global Framework for Climate Services', *Climate Change*, 2, pp.831–832.

Hewitt, C.D., Allis, E., Mason, S.J., Muth, M., Pulwarty, R., Shumake-Guillemot, J., Bucher, A., Brunet, M., Fischer, A.M., Hama, A.M. and Kolli, R.K., 2020. 'Making society climate resilient: International progress under the global framework for climate services' *Bulletin of the American Meteorological Society*, 101(2), pp.E237-E252.

Higham, D.J. and Higham, N.J., 2016. MATLAB guide. Society for Industrial and Applied Mathematics.

Hollis, D., McCarthy, M., Kendon, M., Legg, T., Simpson, I., 2018. HadUK-Grid gridded and regional average climate observations for the UK. Centre for Environmental Data Analysis. UK Met. Office. <http://catalogue.ceda.ac.uk/uuid/4dc8450d889a491ebb20e724debe2dfb> [Accessed February 9, 2023].



Holloway, P., 2023. Understanding GIS through Sustainable Development Goals: Case Studies using QGIS. CRC Press Taylor Francis.

IPCC, 2014. Climate Change 2014: Impacts, Adaptation and Vulnerability. Contribution of Working Group II to the Fifth Assessment Report of the Intergovernmental Panel on Climate Change. Cambridge and New York: Cambridge University Press.

IPCC Climate Change 2021: The Physical Science Basis. Contribution of Working Group I to the Sixth Assessment Report of the Intergovernmental Panel on Climate Change. Cambridge University Press, Cambridge, United Kingdom and New York, NY, USA, In press.

Johansen, J., Noll, J., and Johansen, C., 2021. InfoInternet for education in the Global South: A study of applications enabled by free information-only internet access in technologically disadvantaged areas. *African Journal of Science, Technology, Innovation and Development*, pp. 1-13

Jones, R.N., 2001. An environmental risk assessment/management framework for climate change impact assessments. *Natural hazards*, 23(2-3), pp.197-230.

Kenobi, K., Read, W., Bowgen, K., MacGregor, Talyor, R., Camaro, W., Hodges, C., Dennis, P., and Holloway, P., 2023. Lasso penalisation identifies consistent trends over time in landscape and climate factors influencing the wintering distribution of the Eurasian Curlew. Preprint.

Kiely, G., Leahy, P., Ludlow, F., Stefanini, B., Reilly, E., Monk, M. and Harris, J., 2010. Extreme weather, climate and natural disasters in Ireland.

Lehner, F., Deser, C., Maher, N., Marotzke, J., Fischer, E. M., Brunner, L., Knutti, R., and Hawkins, E., 2020. Partitioning climate projection uncertainty with multiple large ensembles and CMIP5/6, *Earth Syst. Dynam.*, 11, 491–508, <https://doi.org/10.5194/esd-11-491-2020>.

Lenderink, G., van den Hurk, B., Klein Tank, A., van Oldenborgh, G. , van Meijgaard, E., de Vries, H., Beersma, J., 2015. Preparing local climate change scenarios for the Netherlands using resampling of climate model output. *Environmental Research Letters*, 9(11). <https://doi.org/10.1088/1748-9326/9/11/115008>.

Lindner, M., Fitzgerald, J.B., Zimmermann, N.E., Reyer, C., Delzon, S., van Der Maaten, E., Schelhaas, M.J., Lasch, P., Eggers, J., van Der Maaten-Theunissen, M. and Suckow, F., 2014. Climate change and European forests: what do we know, what are the uncertainties, and what are the implications for forest management? *Journal of environmental management*, 146, pp.69-83.

Majda, A.J. and Kramer, P.R., 1999. Simplified models for turbulent diffusion: theory, numerical modelling, and physical phenomena. *Physics Reports*, 314(4-5), pp.237-574.

Malhi, Y., Franklin, J., Seddon, N., Solan, M., Turner, M.G., Field, C.B. and Knowlton, N., 2020. Climate change and ecosystems: Threats, opportunities and solutions. *Philosophical Transactions of the Royal Society B*, 375(1794), p.20190104.

McMichael, A.J., Woodruff, R.E. and Hales, S. Climate change and human health: present and future risks. *The Lancet*. 2006 Mar 11;367(9513):859-69.

Melchers, R.E. and Beck, A.T., 2018. Structural reliability analysis and prediction. John Wiley & Sons.

Mooney, C.Z., 1997. Monte Carlo Simulation (No. 116). Sage.

Murphy, J.M., Harris, G.R., Sexton, D.M.H., Kendon, E.J., Bett, P.E., Clark, R.T., Eagle, K.E., Fosse, G., Fung, F., Lowe, J.A., McDonald, R.E., McInnes, R.N., McSweeney, C.F., Mitchell, J.F.B., Rostron, J.W., Thornton, H.E., Tucker, S., Yamazaki, K., 2018. UKCP18 Land Projections: Science Report. <https://www.metoffice.gov.uk/pub/data/weather/uk/ukcp18/science-reports/UKCP18-Land-report.pdf> [Accessed February 9, 2023].

Nilsen, I.B., Hanssen-Bauer, I., Dyrddal, A.V., Hisdal, H., Lawrence, D., Haddeland, I., Wong, W.K., 2022. From Climate Model Output to Actionable Climate Information in Norway. *Front. Clim.*, Vol. 4, <https://doi.org/10.3389/fclim.2022.866563>.

Nolan, P., and J. Flanagan, 2020. High-resolution Climate Projections for Ireland – A Multi-model Ensemble Approach. EPA Research 339. 81pp. <https://www.epa.ie/publications/research/climate-change/research-339-high-resolution-climate-projections-for-ireland-.php>

- Nolan, P. (2024). Updated High-resolution Climate Projections for Ireland. Environmental Protection Agency, Ireland (in Press).
- O'Brien, E., and P. Nolan. TRANSLATE: standardised climate projections for Ireland. *Front. Clim.* 5, 4 May 2023. <https://doi.org/10.3389/fclim.2023.1166828>
- Ordnance Survey Ireland (OSi) 2016. Roads – OSi National 250k Map of Ireland. Available at https://data-osi.opendata.arcgis.com/datasets/1434c3b-05da742cdb47e00040edc9dd5_24/explore?location=53.281779%2C-8.238600%2C7.72. Accessed on March 1 2022.
- Pendergrass, A.G., Knutti, R., Lehner, F., et al., 2017. Precipitation variability increases in a warmer climate. *Sci Rep* 7, 17966. <https://doi.org/10.1038/s41598-017-17966-y>.
- Pörtner, H.O., Roberts, D.C., Adams, H., Adler, C., Aldunce, P., Ali, E., Begum, R.A., Betts, R., Kerr, R.B., Biesbroek, R. and Birkmann, J., 2022. *Climate change 2022: Impacts, adaptation and vulnerability* (p. 3056). Geneva, Switzerland.
- Rinaldi, S., Peerenboom, J. and Kelly, T., 2001. Identifying, understanding and analyzing critical infrastructure interdependencies. *IEEE Control Systems* 21(6): 11-25.
- Ryan, P. C., Hawchar, L., Naughton, O., and Stewart, M. G., 2021. CIViC: Critical Infrastructure Vulnerability to Climate Change. Environmental Protection Agency (EPA) Ireland. Retrieved from https://www.epa.ie/publications/research/climate-change/Research_Report_369.pdf.
- Ryan, P.C. and Stewart, M.G., 2019. Timber Power Pole Network Management in a Changing Climate. In *Climate Adaptation Engineering* (pp. 127-163). Butterworth-Heinemann.
- Ryan, P.C., and Stewart, M.G. (2017) Cost-benefit Analysis of Climate Change Adaptation for Power Pole Networks. *Climatic Change* 143:519–533 (August 2017).
- Ryan, P.C., Stewart, M.G., Spencer, N. and Li, Y. (2014). Reliability Assessment of Power Pole Infrastructure Incorporating Deterioration and Network Maintenance. *Reliability Engineering and System Safety* 132:(December 2014).
- Ryan, P.C., Stewart, M.G., Spencer, N. and Li, Y. (2016). Probabilistic Analysis of Climate Change Impacts on Timber Power Pole Networks. *International Journal of Electrical Power and Energy Systems* 78:513-523 (June 2016).
- Sahr, K., White, D. and Kimerling, A.J., 2003. Geodesic Discrete Global Grid Systems. Available at: <http://webpages.sou.edu/~sahrk/sqspc/pubs/gdgs03.pdf>
- Schneider, S.H. and Kuntz-Duriseti, K., 2002. Uncertainty and climate change policy. *Climate change policy: a survey*, pp.53-87.
- Senapati, S., 2022. Vulnerability and risk in the context of flood-related disasters: A district-level study of Bihar, India. *International Journal of Disaster Risk Reduction*, 82, p.103368.
- Skelton, M., Fischer, A.M., Liniger, M.A. and Bresch, D.N., 2019. 'Who is 'the user' of climate services? Unpacking the use of national climate scenarios in Switzerland beyond sectors, numeracy and the research–practice binary', *Climate Services*, 15, p.100113.
- Tamayo, J., Rodriguez-Camino, E., Hernanz, A., Covalleda, S., 2022. Downscaled climate change scenarios for Central America. *Adv. Sci. Res.*, 19, 105-115, <https://doi.org/10.5194/asr-19-105-2022>.
- The Royal Society (UK), National Academy of Sciences (USA), 2020. *Climate Change: Evidence and Causes, Update 2020*. https://royalsociety.org/~media/royal_society_content/policy/projects/climate-evidence-causes/climate-change-evidence-causes.pdf.
- Thornton, P.K., Ericksen, P.J., Herrero, M. and Challinor, A.J., 2014. Climate variability and vulnerability to climate change: a review. *Global change biology*, 20(11), pp.3313-3328.
- Tomczyk, □. and Sunday Oyelere, S., 2019. ICT for learning and inclusion in Latin America and Europe. Case Study from Countries: Bolivia, Brazil, Cuba, Dominican Republic, Ecuador, Finland, Poland, Turkey, Uruguay. Cracow: Pedagogical University of Cracow
- Van den Hurk, B., Siegmund, P., Klein Tank, A. (Eds), 2014. KNMI'14: Climate Change Scenarios for the 21st Century – A Netherlands Perspective. KNMI scientific report WF 2014-01. <https://cdn.knmi.nl/knmi/pdf/bibliotheek/knmiplibWR/WR2014-01.pdf>

Vautard, R., Gobiet, A., Sobolowski, S., Kjellstrom, E., Stegehuis, A., Watkiss, P., ..., Jacob, D., 2014. The European climate under a 2 °C global warming. *Environ. Res. Lett.*, 9(034006). <https://iopscience.iop.org/article/10.1088/1748-9326/9/3/034006/pdf>.

Walsh, S., 2016: Long-term rainfall averages for Ireland, 1981-2010, Met Éireann, Dublin, Climatological Note No. 15. <http://hdl.handle.net/2262/76135>.

Walsh, S., 2017: Long-term temperature averages for Ireland, 1981-2010, Met Éireann, Dublin, Climatological Note No. 16. <http://hdl.handle.net/2262/79901>.

Wang, J., O'Brien, E., Holloway, P., Nolan, P., Stewart, M. G., Ryan, P.C., 2024. Climate Change Impact and Adaptation Assessment for Road Drainage Systems. *Journal of Environmental Management*, Volume 364, 2024, 121209, ISSN 0301-4797, <https://doi.org/10.1016/j.jenvman.2024.121209>.

Wennersten, R., Sun, Q. and Li, H., 2015. The future potential for Carbon Capture and Storage in climate change mitigation – an overview from perspectives of technology, economy and risk. *Journal of Cleaner Production*, 103, pp.724-736.

Zscheischler, J., Westra, S., Van Den Hurk, B.J., Seneviratne, S.I., Ward, P.J., Pitman, A., AghaKouchak, A., Bresch, D.N., Leonard, M., Wahl, T. and Zhang, X., 2018. Future climate risk from compound events. *Nature Climate Change*, 8(6), pp.469-477.



Met Éireann's Weather and Climate Research Programme

Science Serving Society

Met Éireann, Ireland's National Meteorological Service maintained by the State under the Convention of the World Meteorological Organisation, monitors, analyses and predicts Ireland's weather and climate. We do this to provide Irish decision-makers with world-class weather, climate, and flood services to protect life and property, and to promote wider societal and economic wellbeing.

Research funding is a key component of Met Éireann's strategy and is central to Met Éireann's Weather and Climate Research Programme.

Met Éireann's Weather and Climate Research Programme underpins the expertise and knowledge needed to enable the delivery and

continuous improvement of national predictive capability in the areas of weather, climate and hydrology and to ensure that, particularly in the climate context, research outputs provide the evidence and tools necessary to inform government policy and action.

Met Éireann's Weather and Climate Research Programme's mission is to contribute to the development of national research capacity and to address key scientific questions in response to the challenges and opportunities facing Ireland from an extreme weather and changing climate's perspective.

Met Éireann welcomes research in the spirit of diversity, inclusivity, cooperation, co-creation, collaboration, open data and multidisciplinary.

